INVESTIGATING GALVANIC CORROSION IN LOW-ALKALINITY WATER: THE
EFFECTS OF PH, HIGH DOSE CORROSION INHIBITORS, AND DISSOLVED
INORGANIC CARBON

by

Amy Meredith McClintock

Submitted in partial fulfilment of the requirements
for the degree of Master of Applied Science

at

Dalhousie University
Halifax, Nova Scotia
July 2013

TABLE OF CONTENTS

LIST OF TABLES

LIST OF FIGURES

ABSTRACT

Galvanically connected lead and copper materials in premise plumbing has shown to accelerate lead corrosion compared to lead pipe alone and can be a persistent lead release mechanism in a drinking water distribution system. pH and alkalinity adjustment and/or corrosion inhibitors are commonly used for controlling lead and copper release. The objective of this study was to evaluate galvanic corrosion potential under various pH and corrosion control conditions, and under varying buffering capacity through alkalinity addition. Bench-scale dump-and-fill beaker experiments evaluated galvanic corrosion from a lead and copper couple under stagnant conditions. Two corrosion inhibitors, orthophosphate (OP) and zinc orthophosphate (ZOP), were dosed at 10 or 20 mg PO_4/L against variable pH, chlorine doses, and dissolved inorganic carbon (DIC) concentrations. As well, a new in-situ ellipsometry method was evaluated for its ability to measure nanoscale drinking water films for corrosion control applications.

Key findings from this study were that pH plays a larger role in corrosion control when alkalinity is low (DIC<3 mg $CaCO_3$/L), and under certain conditions, high-dose corrosion inhibitor can exacerbate lead release. In particular, after 1-day stagnation, increasing pH from 7.4 to 9.2 in low alkalinity water reduced average lead release by 430 μg/L compared to 210 μg/L with ZOP addition. However, when DIC was increased to either 7 or 17 mg $CaCO_3$/L, higher pH did not significantly reduce lead release. The combination of ZOP dose of 20 mg PO_4/L and pH 9.2 resulted in the lowest lead release compared to no-corrosion inhibitor or pH adjustment alone, whereas an OP dose of 20 mg PO_4/L exacerbated lead release compared to no corrosion inhibitor in some cases. On the other hand, an OP dose of 10 mg PO_4/L mitigated lead release compared to no corrosion inhibitor. High lead release with 20 mg PO_4/L as orthophosphate may be attributed to microbial corrosion. In-situ ellipsometry was used to evaluate lead oxide films on lead plates as well as the effects of chlorine on protein adhesion to a copper coupon to simulate bacteria adhesion to copper pipe. Analysis showed that lead films are slightly absorbing and require extensive analysis to determine film thickness and protein thickness on copper was found to be independent of chlorine dose. At this stage, ellipsometry for water treatment applications requires more troubleshooting.

This study demonstrated that lead and copper release due to galvanic couples in drinking water systems could be exacerbated with certain high-dose corrosion control strategies. The potential for exacerbating lead release with high-doses of corrosion inhibitor emphasizes the need for testing and optimizing site-specific corrosion control strategies. Additional microbial tests should be conducted when evaluating galvanic corrosion to help elucidate the role of bacteria in lead and copper corrosion, and techniques such as ellipsometry may be beneficial in understanding scale and biofilm adhesion to copper and lead materials.

LIST OF SYMBOLS AND ABBREVIATIONS USED

Al	Aluminum
$(CaOH)_2$	Lime
ANOVA	Analysis of variance
C	Carbon
Ca	Calcium
$CaCO_3$	Calcium carbonate
CF_{Pb}	Lead concentration factor
Cl^-	Chloride
Cl_2	Chlorine
CO_3^{2-}	Carbonate
CSMR	Chloride to sulfate mass ratio
Cu	Copper
DIC	Dissolved inorganic carbon
DOC	Dissolved organic carbon
e^-	Electron
EDS	Electron dispersive spectroscopy
E_H-pH	Pourbaix
EMA	Effective medium approximation
EMF	Electromotive force
H_2O	Water
HCO_3^-	Bicarbonate
HOCl	Hypochlorous acid
ICP-ms	Inductively coupled plasma mass spectrometry
ID	Inner diameter
JDKWSP	J.D. Kline Water Supply Plant
KH_2PO_4	Potassium phosphate monobasic
$KMnO_4$	Potassium permanganate
L_f	Biofilm thickness, nm
LSL	Lead service line

MAC	Maximum allowable concentration
MSE	Mean square error
NAD	Nitric acid digestion
$NaHCO_3$	Sodium bicarbonate
NaOH	Sodium hydroxide/soda ash
O	Oxygen
OH^-	Hydroxyl
ORP	Oxidation reduction potential
P	Phosphorus
$Pb(OH)_2$	Lead(II) hydroxide
Pb	Lead
$Pb_3(PO_4)_2$	Lead(II) phosphate
$Pb_5(PO_4)_3Cl$	Chloropyromorphite
$PbCO_3$	Lead(II) carbonate
PbO_2	Pb(IV) oxide
PBS	Phosphate buffered solution
$PbSO_4$	Pb(II) sulfate
PO_4^{3-}	Phosphate
SEM	Scanning electron microscope
SO_4^{2-}	Sulfate
THM	Trihalomethane
TOC	Total organic carbon
wt%	Weight percent
XRD	X-ray diffraction
ZOP	Zinc orthophosphate
Δ	Optical constant delta
Ψ	Optical constant psi

ACKNOWLEDGEMENTS

I would like to acknowledge my supervisor, Dr. Graham Gagnon, who let me find my way and who has supported my research and personal goals over the last 3 years. I am very thankful for the opportunities you have provided me at Dal and in St. John's that have and will continue to play a major role in my professional development.

To Sarah Jane Payne, my lab partner and friend, your support and advice both academically and personally have been invaluable to me. Rock on, Cowboy!

I would like to thank Heather Daurie for her guidance in the lab and for always answering my questions with a smile on her face. I would also like to acknowledge my laboratory assistants, Margaret Grierson and Matthew King, for their hard work and enthusiasm. It was a pleasure working with you all.

To my committee members, Dr. Liu and Dr. Dahn, thank you for your time and participation in my thesis development. As well, I would like to thank Dr. Dahn for allowing me to conduct experiments in his lab, and to Mark McArthur, for patiently showing an engineer the ellipsometry ropes and willingly lending a helping hand.

I would like to thank Tarra Chartrand for keeping paperwork and deadlines in check. The 'small things' made the biggest difference on stressful days, so, thank you!

To my family, who have showed ceaseless support and encouragement over the last 3 years: I finally did it! Thanks for always standing by me.

And last but certainly not least, I would like to acknowledge my labmates and friends: You are a constant reminder that engineering is fun, and friendship will get you through the longest of lab days.

CHAPTER 1   INTRODUCTION

1.1   Project Rationale

Corrosion control is a major operational challenge and cost for drinking water utilities. Corrosion within the distribution system can lead to a loss of hydraulic capacity and component replacements (Koch et al., 2001) as well as contribute to elevated levels of metals, such as lead and copper, in drinking water (Cartier et al., 2012a). Although lead is rarely naturally present in source waters, it can enter the distribution system through the corrosion of lead bearing materials such as lead service lines (LSL), lead pipe fittings, flux, brass, and solder.

Prior to 1975, lead was commonly used for service lines and plumbing materials because it was soft and inexpensive, and was believed to resist corrosion by readily forming a protective scale on the interior of pipes (Craig and Anderson, 1995). However, lead was banned for use in plumbing material in Canada in 1975 and in solder in 1986 due to the detrimental health effects related to the leaching of lead into drinking water. Current regulations require that plumbing materials be 'lead free', however, 'lead free' pipes and pipe fittings may contain up to 8% lead (SDWA, 1996). In 2011, the United States enacted the "Reduction of Lead in Drinking Water Act" that redefines 'lead free' as not containing more than 0.2% lead by weight and will come into effect January of 2014. However, no such law has been passed in Canada and 8% by weight lead in plumbing materials is generally accepted. Although older buildings are most likely to contain lead bearing materials, new buildings constructed with 'lead free' plumbing may also contribute to lead in drinking water (Elfland et al., 2010).

Research has shown that service lines and premise plumbing contribute a greater proportion of dissolved and particulate lead in drinking water than does distribution system infrastructure (Johnson et al., 1993). Service lines branching off of distribution mains and premise plumbing are fundamentally different from the main distribution system in terms of pipe materials, higher temperature ranges, longer stagnation times, and higher pipe surface area to water volume ratio which all contribute to increased corrosion

of metals in plumbing (NRC, 2006). The connection of dissimilar metals, mainly copper and lead that are commonly found in service lines and premise plumbing, allow for galvanic corrosion. This commonly occurs in service lines, where the public portion (from the distribution main to the property line) is replaced with copper and connected to the existing lead service line on the property owner's side. This galvanic connection has shown to increase lead corrosion compared to undisturbed lead service lines (Triantafyllidou and Edwards, 2011; Wang et al., 2012). For example, Cartier et al. (2012a) found that replacing upstream lead pipe with copper pipe did not reduce the lead concentration in water compared to lead pipe alone due to galvanic and deposition corrosion.

To minimize the effects of corrosion on distribution and premise plumbing, two corrosion control strategies are commonly used: (1) pH adjustment, and/or (2) passivation. Raising water pH to above 8 typically promotes a calcium based protective scale to form on the interior of most metal pipes (Schock, 1990). However, this approach is limited to source waters with high buffering capacities to maintain a stable pH. In many source waters, such as those found in the Atlantic regions, the alkalinity is low and this approach is not feasible.

The second strategy, passivation, is facilitated using chemical corrosion inhibitors. Phosphate passivation is effective in mitigating corrosion by creating a metal-phosphate barrier between the copper or lead surface and the bulk water. A 2001 survey of medium and large U.S. water utilities identified that the majority of all surface water utilities surveyed dosed phosphate inhibitors (as opposed to pH adjustment alone) for corrosion control (McNeill and Edwards, 2002). Orthophosphates with and without zinc are among the most common corrosion inhibitors used in the water industry (Hill and Gianni, 2011), however, the role of zinc in lead and copper corrosion control is not well understood. Recent work has found that zinc orthophosphate can reduce pitting corrosion tendencies of copper (Lattyak, 2007), however, Schneider et al. (2007) found that zinc did not play a significant role in lead corrosion control. The type of corrosion inhibitor in conjunction with the water chemistry and quality make corrosion control a utility–specific issue.

2

In practice, the majority of medium and large U.S. utilities surveyed dosed corrosion inhibitors between 1 and 2 mg PO_4/L (MacNeill and Edwards, 2002). Often, low dosages are selected based on phosphorus costs that are increasing as phosphorus reserves are depleting in quantity and quality (Smil, 2000) and to reduce the potential of phosphorus loads on wastewater treatment processes and the receiving water bodies. Recent studies, however, have found that high doses of orthophosphate (7 and 75 mg PO_4/L) mitigated copper corrosion (Goh et al., 2008; Lewandowski et al., 2010). These studies did not investigate the effects of high-dose phosphate on galvanic corrosion, which is most commonly found in premise plumbing. Although corrosion inhibitors are dosed at low concentrations in practice, it is not known whether high doses of phosphate may be beneficial in mitigating lead release when a galvanic connection exists.

Understanding film passivation is critical to improving corrosion control. Film thickness, uniformity, and porosity are important characteristics in passivation effectiveness to reduce corrosion (Hill and Cantor, 2011). Lewandowski et al. (2010) observed that metals surfaces undergo considerable nanoscale changes in surface composition and morphology due to corrosion within a few hours of exposure to water. Passivation scale analysis typically occurs post experiment and no method has been developed to characterize passivation in real-time. In-situ ellipsometry is a novel optical tool that can measure transparent and absorbing film properties and thicknesses in real-time within a liquid environment. Ellipsometry could provide novel information with respect to the properties, thickness, and stability of films formed on metals which could contribute towards our understanding of film passivation and therefore corrosion control.

1.2   Research objectives

The main objective of this study was to compare galvanic corrosion potential under various pH conditions, corrosion control conditions, and under varying buffering capacities through alkalinity addition. To achieve this, a series of bench-scale studies were designed to address the following:

Objective 1. Compare the effects of pH adjustment, high-dose corrosion inhibitor, and buffering capacity on galvanic corrosion:

i) Compare lead and copper release over the short- and long-term for various corrosion control strategies.

ii) Characterize corrosion by-products formed under various corrosion control strategies to better understand film passivation.

Objective 2. Develop an in-situ ellipsometry method for quantifying passivation film formation at the nanometer scale in real-time to better understand passivation corrosion control.

1.3   Organization of Thesis

A summary of each chapter is described below.

Chapter 2 presents a literature review of galvanic corrosion, premise plumbing conditions, water quality impacts on galvanic corrosion, corrosion control strategies, and background on the optical tool ellipsometry.

Chapter 3 describes the materials and methods used in 3 experimental designs in Chapter 4. Electrochemical cell and ellipsometry set-ups are described, experimental designs are presented, as well as influent water preparation, analytical sampling techniques, and statistical methods are described in this chapter.

Chapter 4 presents the results of three experimental designs described in Chapter 3. Results are discussed, including a comparison between corrosion control strategies used in the two experimental designs.

Chapter 5 summarizes the research objectives and provides a summary of findings from Chapter 4. Conclusions are presented followed by recommendations for future pilot- and full-scale galvanic corrosion studies.

CHAPTER 2   LITERATURE REVIEW

2.1   Characteristics of Premise Plumbing

The series of pipework within a distribution system consists of service lines that distribute water from the distribution mains to premise plumbing in the property being served.   Premise plumbing constitutes the portion of the distribution system that is located within the building on the end-users property and differs from the distribution system in many ways. These main differences are summarized in Table 2.1.

Unlike the distribution system, premise plumbing uses unique materials such as copper, plastics, brass, lead, and galvanized iron with dissimilar metals often in contact. Premise plumbing uses smaller inner diameter (ID) piping and has more surface area to unit length than the other portions of the distribution system. As a result, higher concentrations of metals can occur in premise plumbing than elsewhere in the system. As well, water age varies in consumer plumbing as water can sit stagnant in pipework for extended periods if the building is irregularly occupied. It is not uncommon for sections of plumbing within a building to have varying water ages and temperatures if certain sections are infrequently used. A generally accepted rule of thumb is that corrosion rates will double for every 10°C increase in water temperature (Droste, 1997).

Water velocity and disinfection residual are different compared to the remainder of the system. Water velocity is typically faster in premise plumbing than in the distribution system and consists of intermittent start-and-stop flow patterns. The high velocity start-and-stop flow can disturb corrosion scales. Cartier et al. (2012a) found that particulate lead scales are more likely to be released at moderate to high flow rates (8-32 L/min) but not low flow (1.3 L/min) in 1.3 cm inner diameter pipes. As well, disinfection residual is typically below the objective disinfectant residual of the utility because of extended stagnation times, warmer temperatures, and plumbing materials (such as copper) that react with chlorine. Edwards et al. (2005) observed a three-log increase in bacteria during stagnation in premise plumbing due to bacterial regrowth. As well, biofilms have shown to be present and active even in water types with consistently high levels of chlorine

(White et al., 2011). The potential for bacterial regrowth within the distribution system has public health implications, as well as corrosion control considerations.

Table 2.1 – Comparison between premise plumbing and the main distribution system (Edwards et al., 2003)

Plumbing Characteristic	Distribution System	Premise Plumbing
Materials	Cement, ductile iron, plastic, cast iron	Copper, plastics, brass, lead, galvanized iron
Surface area to volume	0.26 cm^2/mL	2.1 cm^2/mL
Stagnation	Infrequent, except in dead-ends	Frequent, variable length
Temperature (°C)	0-30	0-100
Variable Velocity (m/s)	0.6-1.8	≤10 with continuous & start-and-stop flow
Disinfection residual	Present	Frequently absent, dependent on stagnation time
Responsible party	Utility	Individual customer

2.2   Principles of Galvanic Corrosion between Lead and Copper

In order for galvanic corrosion to occur, all components of a galvanic cell must be present (Schock, 1990): an anode, a cathode, a connection between the anode and cathode for electron transport, and an electrolyte that will conduct ions between the anode and cathode. Since metals are not homogeneous, anodic and cathodic sites can occur on lead pipe alone causing corrosion, however galvanic corrosion occurs when two dissimilar metals with different electrochemical potentials are in contact. The tendency for a metal to corrode in a galvanic cell is determined by its position on the galvanic series: the higher the electrochemical potential, the more cathodic the metal. In the case of copper (+0.334 V) and lead (-0.126 V), copper has a higher electrochemical potential and will act as the cathode when in a galvanic cell with lead; lead will act as the anode and will corrode. Corrosion occurs via a series of reduction and oxidation reactions at the anode

and cathode, respectively. Each reaction at the anode and cathode are called 'half-cell' reactions. For every oxidation reaction at the anode and dissolution of the metal, electrons migrate towards the cathode where they are consumed in reduction reactions at the cathode. Within the electrolyte, cations will migrate towards the anode and anions will migrate towards the cathode to maintain an electrically neutral solution (electroneutrality). The reactions that take place at the lead anode and copper cathode are described below and shown in Figure 2.1.

2.2.1 Reactions at the Anode and Cathode

For every pair of electrons removed from lead by the electromotive force (EMF) of copper, one lead molecule can be corroded (forming pits) and potentially released to water. The half-cell reaction at the anode is shown in Equation 1.

$$Pb^0 \rightarrow 2e^- + Pb^{2+}$$
<div align="right">Equation 1</div>

The Pb^{2+} can then diffuse into the water or participate in secondary reactions with other ions in the electrolyte to produce lead(II) hydroxides and lead(II) carbonates. For example, OH^- typically combines with the oxidized lead ions to form surface deposits, such as $Pb(OH)_2$. These secondary reactions are shown in Equations 2, 3, and 4, below.

$$Pb^{2+} + CO_3^{2-} \longrightarrow PbCO_3(s)$$
<div align="right">Equation 2</div>

$$Pb^{2+} + 2OH^- \rightarrow Pb(OH)_2(s)$$
<div align="right">Equation 3</div>

$$2Pb^{2+} + \frac{1}{2}O_2 + 4OH^- \longrightarrow 2PbOOH(s) + H_2O$$
<div align="right">Equation 4</div>
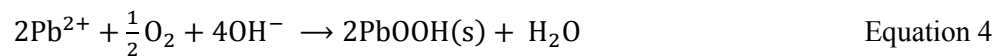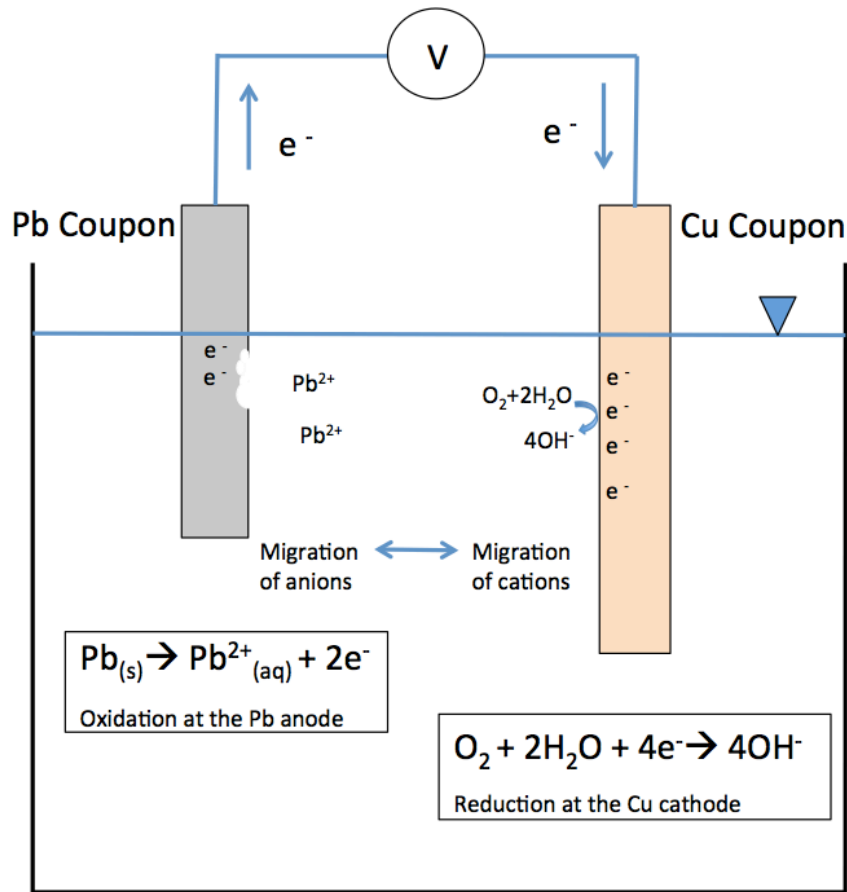
Figure 2.1 – The galvanic cell between a lead (anode) coupon and copper (cathode) coupon. Lead oxidation and oxygen reduction occur at the anode and cathode, respectively.

Many possible cathodic reactions may occur at the cathode, however, due to the abundance of oxygen in natural waters, oxygen reduction is the most likely reaction. The half-cell reaction at the cathode is shown in Equation 5, whereby oxygen and water are reduced to form hydroxyl (OH⁻) ions.
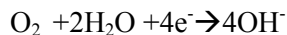
$$O_2 + 2H_2O + 4e^- \rightarrow 4OH^- \qquad\qquad \text{Equation 5}$$

The reaction shown in Equation 5 causes an increase in pH at the cathode, and promotes the conversion of bicarbonate to carbonate and calcium carbonate to precipitate (Equations 6 and 7):

$$OH^- + HCO_3^- \rightarrow CO_3^{2-} + H_2O \qquad\qquad \text{Equation 6}$$

$$Ca^{2+} + CO_3^{2-} \rightleftharpoons CaCO_3(s) \qquad\qquad \text{Equation 7}$$
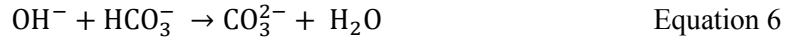
2.2.2 Accelerated Corrosion due to Galvanic Couple

Uniform corrosion of a single metal can occur due to impurities or differences in the metal crystal structure that cause potential difference within the metal (Schock, 1990). Concentration of oxidants and reductants within the solution can also cause differences in potential over the metal surface. Anodic and cathodic sites can occur uniformly over the metal resulting in uniform rather than localized corrosion. In this instance, oxidation and reduction reactions occur relatively closely on the pure lead pipe surface (Dudi, 2004). Lead ions released at the anodic site can form a number of complexes, but unlike in a galvanic cell, all complexation reactions either increase or do no not affect pH (Dudi, 2004). However, when lead and copper pipe are connected, anodic and cathodic reactions occur separately, and the reaction of lead with water produces H^+ ions that will decrease pH whereas reactions at the cathode will increase pH. Therefore, unlike the case for lead pipe alone, the reactions that occur at the anode in a lead and copper galvanic cell decrease pH and further perpetuate lead release. Edwards and Triantafyllidou (2007) observed that pH at the anode decreased from initial pH of 7.7 to as low as 3.7 and 4.4 in water dosed with either orthophosphate or zinc orthophosphate, respectively. A pH decrease of 2 units can occur after as little as 1-hour stagnation (Nguyen et al., 2010). For this reason, an increase in lead release has been observed when a galvanic connection existed compared to lead pipe alone (Triantafyllidou and Edwards, 2011; Wang et al., 2012). As well, low alkalinity water is particularly vulnerable to galvanic corrosion

because the low buffering capacity in low alkalinity water can exacerbate the pH drop at the anode and increase corrosion (Nguyen et al., 2010).

2.3   Other Forms of Corrosion

2.3.1 Concentration Cell Corrosion and Tuberculation

Concentration cell corrosion alongside galvanic and uniform corrosion can contribute towards lead and copper release in premise plumbing. Varying concentrations of corrosion reaction species along a metal, such as dissolved oxygen and hydrogen ions, can affect the potential difference between the sites (Schock, 1990). Since oxygen participates in reduction reactions at the cathode, the metal surface with higher oxygen concentration will be the cathode and the area with lower oxygen will be the anode. For example, oxygen concentration cells can occur when scales or biofilm adhere to the metal surface and oxygen is depleted below these deposits. Concentration cell corrosion typically causes localized pitting corrosion below the deposited scale or film and turbucles (nodule-like scale growths) accumulate above the pit (Schock, 1990).

2.3.2 Microbial Corrosion in Premise Plumbing

Aside from the public health risks associated with bacterial regrowth, bacterial corrosion may also contribute to copper and lead concentrations in premise plumbing. Microorganisms can promote corrosion in one of two ways (Schock, 1990): (1) By creating oxygen concentration cells on the metal when biofilm adhere to the pipe surface, and (2) catalyzing corrosion reactions, though these reactions are not well understood. Aerobic and/or anaerobic microbial corrosion processes can occur within the distribution system, though the latter is typical in polluted environments and when oxygen is limited (Gu, 2009). Under aerobic conditions, microorganisms utilize the electron acceptor oxygen for growth; once a biofilm establishes on a metal surface, oxygen is depleted below the biofilm and an oxygen concentration cell is created (Figure 2.2). The initial

biofilm adhesion mechanism is still not well understood, and presents a challenge for controlling biofilm and microbial corrosion (Gu, 2009).

Another challenge is that bacteria have shown to be resistant to premise plumbing metals, such as copper and lead. For example, *Escherichia coli* possess genes which are resistant to copper (Grass and Rending, 2001) and biofilm isolated from a distribution system LSL identified a group of bacteria that have previously been found to exist in heavy metal environments including lead (White et al., 2011).

Studies have shown that biofilms can contribute to the release of copper by-products and have shown to increase pitting corrosion of copper (Reyes et al., 2008). Biofilms have also been characterized on the surface of corroded lead drinking water surface lines (White et al., 2011). Other studies have shown that bacterial members in cast iron pipe tubercles were the same as the community in stagnant water (Chen et al., 2013). Though the presence of biofilm on lead and copper plumbing materials has been found, it is much more difficult to definitively attribute lead and copper release in a distribution system to microbial corrosion as water quality plays a major role in corrosion control. Therefore, the role of biofilm in drinking water lead and copper corrosion is still not well understood.
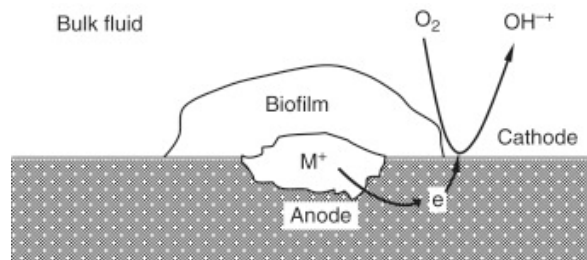
Figure 2.2 – Schematic of an oxygen concentration cell that can occur due to biofilm adhesion to a metal surface. Oxygen concentration is low below the biofilm (anode) and electrons migrate towards the oxygenated cathodic site whereby oxygen reduction occurs (Gu, 2009).

2.4   Impacts of Water Quality on Galvanic Corrosion

2.4.1 Conductivity

Conductivity (μS/cm) represents the ability of water to conduct a current. In a galvanic cell, the release of Pb^{2+} at the anode induces a positive net charge in the solution near the anode and the flow of electrons towards the cathode induces a negative charge at the copper cathode surface. Therefore, the charge carried by the electrons from the anode to the cathode must be accompanied by a transport of ions between the two cells to maintain electroneutrality. Without electroneutrality, galvanic corrosion would no longer proceed. The main ions that contribute to conductivity in natural waters are chloride, sulfate, bicarbonate, hydroxide, and phosphate (Nguyen et al., 2011a). A concentration gradient of chloride, phosphate, and sulfate occurs between the anode and cathode with concentrations of negative ions higher at the anode and positive ions (i.e., sodium) higher at the cathode (Nguyen et al., 2010).

Although all ions contribute towards electrolyte conductivity, the transport and presence of ions at the lead anode, particularly sulfate, carbonate/bicarbonate, and phosphate, is also important for lead passivation. Although bicarbonate is generally believed to protect lead by forming lead carbonate complexes as well as increase the buffering capacity of the water, Nguyen et al. (2011a) found that increasing bicarbonate concentration, and therefore conductivity, can exacerbate lead release when initial conductivity is low. Therefore, conductivity can contribute towards lead release, even anions that typically form lead passivation scales.

2.4.2 Chloride to Sulfate Mass Ratio (CSMR)

Chloride and sulfate anions both migrate towards the lead anode and form complexes with Pb^{2+}. Even in acidic conditions, chloride typically forms $PbCl^{+}$, a soluble lead complex, whereas sulfate forms $PbSO_{4(s)}$ that can passivate lead pipe (Nguyen et al., 2011a; Revie and Uhlig, 2008). Studies have shown that corrosion rate increases when CSMR is high (Edwards and Triantafallydou, 2007; Nguyen et al., 2011b). Nguyen et al.

(2011a) have developed a critical CSMR value of 0.77; when CSMR is 0.77, chloride and sulfate are transported at equal rates to the lead anode. Water is considered more corrosive when CSMR exceeds 0.77 as more chloride than sulfate is reaching the anode surface and likely forming soluble lead complexes. Other authors have found that despite having similar CSMR values (0.5), test conditions with higher concentrations of chloride and sulfate released significantly more lead than conditions with lower concentration of chloride and sulfate (Willison and Boyer, 2012). A shift in CSMR was found to have greater impact on lead release when CSMR was low and increasing CSMR above 1 may not necessarily increase adverse effects on lead, though the water is still corrosive (Edwards and Triantafyllidou, 2007; Nguyen et al., 2011b).

2.4.3 Oxidation Reduction Potential and the Role of Oxidants

Oxidation reduction potential (ORP) is a measure of the relative oxidizing and reducing power of a solution. A solution with high ORP is a solution with a high content of oxidizing species that readily gain electrons from other species through reduction reactions. ORP governs the metal speciation and mineral formation in water. An E_H-pH (Pourbaix) diagram for the lead-water-carbonate system is shown in Figure 2.3. E_H-pH diagrams demonstrate the relationship between E_H (ORP) and pH and metal speciation and mineral formation (Hill and Gianni, 2011). Although E_H-pH diagrams cannot predict water corrosiveness, they can be used to identify the thermodynamically stable metal complexes that are most likely to be present under given ORP and pH conditions.

2.4.4 The Effect of Oxygen and Chlorine on Lead Release

The oxidation half-cell reactions that occur at the anode are coupled with the reduction of an oxidizing agent at the cathode. Common oxidants in drinking water are dissolved oxygen and chlorine species. Since oxygen reduction is the most common cathodic reaction in the galvanic cell, corrosion rate is typically limited by the rate at which oxidants, such as dissolved oxygen, are transported to the cathode surface (Snoeyink and Wagner, 1996). Higher water temperature (such as temperatures in premise plumbing)

will increase the diffusion coefficient of oxygen and decrease viscosity, both of which increase the rate at which oxygen is transported to the cathode surface (Snoeyink and Wagner, 1996). As well, lead concentrations have been observed to increase in pipes containing higher water flow rates (1.9 m/s) compared to low flows (0.07 m/s) (Cartier et al., 2012a). The explanation for this phenomenon has been increased dissolved oxygen content reaching the cathode with higher flow rates (Cartier et al., 2012a) and shearing of particulate-based lead with accelerated flow (Zidou, 2009).

Chlorine can also participate in half-cell reactions at the cathode. As shown in Equation 8, hypochlorous acid can be reduced to form chloride and water and can be a significant half-cell reaction in drinking water (Schock, 1990).

$$HOCl + H^+ + 2\,e^- \leftrightarrows Cl^- + H_2O \qquad\qquad \text{Equation 8}$$
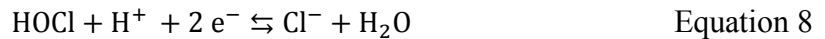
Despite having the potential to participate in half-cell reactions, chlorine addition has shown to mitigate lead release (Cantor et al., 2003; Xie and Giammar, 2011). The addition of chlorine increases ORP (Vasquez et al., 2006), and when ORP increases to approximately 1 V in the pH range of natural water (as shown in Figure 2.3), the formation of Pb(IV) oxides is promoted over the more soluble Pb(II) oxides (Hill and Gianni, 2011). Studies have shown that chlorine in sufficient dosages will oxidize Pb(II) scales to Pb(IV) scales such as PbO_2 (Liu et al., 2008; Nadagouda et al., 2011). Cantor et al. (2003) found that a dose as low as 0.2 mg/L free chlorine reduced lead corrosion but caused increased corrosion of copper and iron.
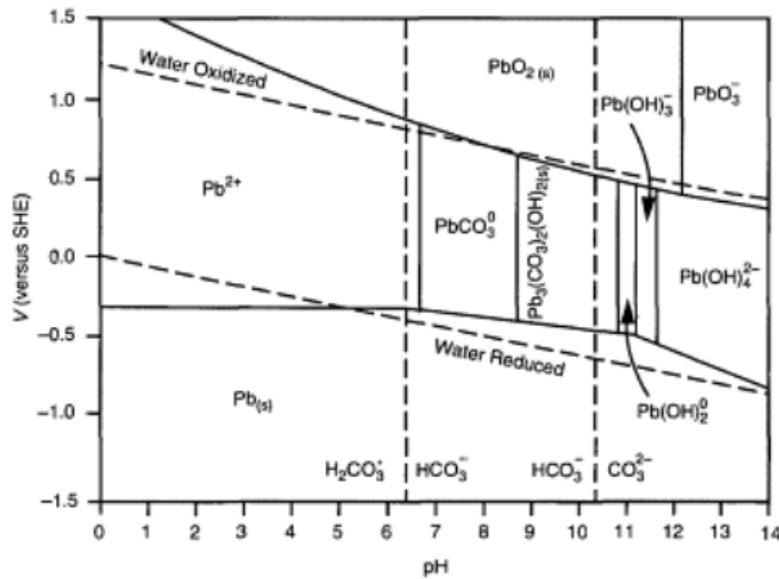
Figure 2.3 – E_H-pH (Pourbaix) diagram for the Pb-H_2O-CO_3 system. Dissolved lead species activities = 0.05 mg/L, DIC=40 mg $CaCO_3$/L (4×10^{-4} mol/L) (Schock et al., 1996)

2.5 Buffering Capacity and Water Stability

Buffering capacity in water refers to a solution's ability to resist pH changes as acids or bases are added to or formed within the system (Sawyer et al., 2003). Alkalinity is the measure of buffering capacity of all salts of weak acids. Carbon dioxide and its related species (bicarbonate, carbonate, and hydroxide) are the most significant source of alkalinity in natural waters (shown in Equation 9), however, when bases other than carbonates are present in significant quantities, they can also consume protons and will contribute towards alkalinity (Schock, 1990)

$$\text{Total Alkalinity} = [HCO_3^{2-}] + 2[CO_3^{2-}] + [OH^-] - [H^+] + [\text{Bases}] \quad \text{Equation 9}$$

Water stability is governed by pH, alkalinity, carbon dioxide (CO_2) and ionic strength, among other parameters (Schock, 1990). Though $CaCO_3$ deposition is used to determine water stability and is a passivation approach for corrosion control, Snoeyink and Wagner (1996) state that $CaCO_3$ scales are not a reliable passivation film and should not be used

16

for corrosion control. Therefore, alternative corrosion control strategies are often required for sufficient corrosion control in distribution systems.

2.6   Corrosion Control Strategies

2.6.1 pH and Alkalinity Adjustment

The role of pH in corrosion control is the following (Schock et al., 1990):

(1) At low pH, there is a higher concentration of H^+ that can readily accept electrons given up by a metal when it corrodes.

(2) Film formation and solubility is greatly affected by water pH.

(3) Pipe materials are more soluble when pH is lower.

Most chemicals added to water to increase pH will simultaneously increase alkalinity. In practice, the typical chemicals added for pH adjustment are lime $(CaOH)_2$, caustic soda (NaOH), and sodium bicarbonate $(NaHCO_3)$ and can increase alkalinity between 0.6 and 1.3 mg $CaCO_3/L$ for every 1 mg/L dose (Schock et al., 1996).

When no corrosion inhibitor is dosed, research has shown that average lead concentrations are significantly higher when alkalinity is less than 30 mg $CaCO_3/L$ compared to when alkalinity was between 30 and 74 mg $CaCO_3/L$ (Dodrill and Edwards, 1995). Utility experience has shown that increasing pH to above 8 had the most significant impact on corrosion in drinking water (Douglas et al., 2004). North American utilities have found pH adjustment to pH>8.5 with alkalinity adjustment >30 mg $CaCO_3/L$ without corrosion inhibitor to be effective in controlling copper and lead corrosion (Douglas et al., 2004; Karalekas et al., 1983).

2.6.2 Orthophosphate Corrosion Inhibitors

2.6.2.1 Orthophosphate and Zinc Orthophosphate

Corrosion by-products are formed when metals ions released at the anode form compounds with ions, such as phosphate, in the water. When a corrosion by-product compound exceeds its saturation concentration in water, excess compound precipitates on the pipe wall and forms a protective solid film. Effective corrosion control occurs when the solubility of the lead-phosphate film is low, preventing it from reverting to its soluble form that requires continuous corrosion inhibitor dosing (Hill and Gianni, 2011). Based on solubility models, the optimal pH for orthophosphate film formation is between 6.5 and 7.5 for copper surfaces (Schock et al., 1995) and between 7 and 8 on lead surfaces (Schock, 1989).

Many studies have found that the addition of orthophosphate decreases lead release (Edwards and McNeill, 2002; Cartier et al., 2012b). In some cases, orthophosphate dosing can result in greater than 70% reduction in lead release (Edwards and McNeill, 2002). Orthophosphate has shown to be more effective than pH adjustment to 8.4 in reducing lead release (Cartier et al. 2012b), and 20-90% less lead was released for utilities using phosphate inhibitors when alkalinity was less than 30 mg $CaCO_3$/L compared to utilities not dosing corrosion inhibitors (Dodrill and Edwards, 1995). Orthophosphate has the largest impact on reducing dissolved lead, however is less effective in reducing particulate lead release (Xie and Giammer, 2011). Edwards and McNeill (2002) found soluble lead concentrations were always lower in the presence of orthophosphate than in an equivalent system without corrosion inhibitor. In another study, particulate lead constituted less than 10% of the total lead in water conditions without phosphate, whereas particulate lead accounted for 49% of the total lead in water with phosphate (Xie and Giammar, 2011).

Theoretically, when zinc is dosed with orthophosphate, zinc forms complexes with carbonates and passivates cathodic sites (Hill and Gianni, 2011). Churchill et al. (2000) found that zinc orthophosphate (dosed at 3 mg PO_4/L) was more effective at reducing

lead and copper to below the control levels in standing water samples compared to pH-alkalinity treatment. Pinto et al. (1997) found that orthophosphate performed better than zinc orthophosphate with respect to mitigating lead release, and other studies have shown no statistical difference in lead release between orthophosphate corrosion inhibitors with and without zinc (Schneider et al., 2007). Though zinc orthophosphate may not be as effective as orthophosphate in reducing lead release, the addition of zinc may have benefits with respect to copper release. The addition of zinc may improve the phosphate deposition on copper and reduce the copper pitting corrosion and inhibit nonuniform corrosion (Lattyak, 2007; Scheffer, 2006). In contrast, phosphate corrosion inhibitors have shown to adversely affect copper release in water with high pH (>8.4) and alkalinity less than 30 mg $CaCO_3$/L (Dodrill and Edwards, 1995).

2.6.2.2 Corrosion Inhibitor Dose

A 2001 survey of U.S. utilities and their corrosion inhibitor practices identified that the majority of utilities dosing phosphate inhibitor dose between 1 and 2 mg PO_4/L (McNeill and Edwards, 2002). Recent research has tested the effects of high-dose corrosion inhibitor on copper corrosion (Nguyen et al., 2011a; Goh et al., 2008). The benefits of high-dose phosphate have been demonstrated with respect to copper corrosion: Goh et al. (2008) tested various PO_4 concentrations and found that the optimal dose of orthophosphate to reduce copper corrosion was 76 mg PO_4/L. Copper corrosion rate was also impeded when orthophosphate was dosed at 7 mg PO_4/L (Lewandowski et al., 2010). Neither of these studies evaluated the effects of high-dose phosphate on galvanic corrosion between lead and copper, however.

Few studies exist whereby the effects of high-dose corrosion inhibitor on lead release were measured. Orthophosphate concentrations as high as 3 mg PO_4/L (Churchill et al., 2000; Xie and Giammer, 2011), and 9.3 mg PO_4/L (Nguyen et al., 2011a) have been published in the literature. Zinc orthophosphate doses of 3 mg PO_4/L was effective in reducing lead and copper concentrations to below regulatory levels (Churchill et al., 2000) whereas at higher doses, Nguyen et al. (2011a) found that a dose of 9.3 mg PO_4/L

had a tendency to increase lead concentration in bulk water when sulfate concentration was low (<10 mg SO_4/L). The authors attribute the negative effects of high orthophosphate dose to the increase in conductivity that occurred when high-doses of PO_4 were added. The limited research on high-dose inhibitor on lead corrosion but the demonstrated benefits of high-dose corrosion inhibitor on copper corrosion merit more investigation in low-alkalinity water.

2.7   Corrosion By-Products

Lead pipe scales can be complex and may contain up to four different layers (Nadagouda et al., 2011). Corrosion scales can also accumulate other elements such as arsenic, vanadium, tin, copper, and chromium (Kim and Herrera, 2010). In general, lead compounds identified on lead pipes are lead(II) oxides and lead(II) carbonates (Wang et al., 2012). Lead(IV) oxides can also be present when a sufficient dose of chlorine is added: Chlorine concentrations as low as 3.5 mg/L (Xie and Giammar, 2011) and 2 mg/L (Liu et al., 2008)   resulted in oxidation of lead(II) (hydrocerussite and cerussite) to lead(IV), whereas Wang et al. (2012) did not identify any lead(IV) oxides in water with pH 9.5 and low free chlorine concentration of 0.4 mg/L. As well, dosing orthophosphate has shown to inhibit the formation of lead(IV) oxides (Lytle et al., 2009). Reddish colour scales have been identified as characteristic of lead(IV) oxides (Lytle et al., 2009; Xie and Giammar, 2011) whereas lead(II) carbonates, such as hydrocerussite, are a white solid (Xie and Giammar, 2011).

Water pH and alkalinity can affect the structure of films on lead pipe surfaces. Kim and Herrera (2010) found that lead(II) carbonates dominate in high alkalinity water whereas more hydroxide rich solids would form in water with high pH and low alkalinity. At lower pH (i.e. 6-7, with DIC=100 mg/L as C) the formation of different shapes, such as nanorods, microrods, and dendritic structures, were favoured with and without orthophosphate inhibitor whereas increasing pH to 8 and above with orthophosphate

20

inhibitor started the formation of spheres and a uniform layer of phosphate/$PbCO_3$ coating (Nadagouda et al., 2008).

2.8   Spectroscopic Ellipsometry

The properties, thickness, and stability of anodic passivation films formed on lead are important to better understand galvanic corrosion and improving corrosion control. Generally, passivation film analysis consists of elemental and/or compositional analysis such as electron dispersive spectroscopy (EDS) and X-ray diffraction (XRD), though other techniques such as atomic force microscopy do allow for surface structure analysis. The disadvantage of these techniques is that they require direct analysis of a sample; once the sample has been analyzed, it has either been disturbed (such as scales removed for direct analysis) or been exposed to air and cannot be re-tested.

Spectroscopic ellipsometry is an optical tool that is commonly used in the semi conductor industry to measure the optical constants and thickness of dielectric and semiconductor films. Spectroscopic ellipsometry can also be used to measure the thickness and optical constants of thin absorbing metals, such as metals (Hilfiker et al., 2008). The potential for ellipsometry as a new research tool to understand corrosion film growth and formation in the drinking water distribution system has never been evaluated.

Spectroscopic ellipsometry has advantages over the other surface analysis techniques previously mentioned: 1. Ability to make in-situ (in a liquid environment) film thickness measurements non-invasively, without intervention between adsorption and measuring steps, 2. A relatively fast data acquisition rate (in the order of 10 s per point), and 3. Ability to measure film thickness in the order of Angstrons (10^{-10} m). Therefore, in-situ ellipsometric measurements could be a useful tool to provide insight into the film growth of anodic oxide films.

2.8.1 Basic Principles of Ellipsometry

The ellipsometer does not directly measure layer thickness or optical properties of a film but measures changes in the polarization state of a beam of light once it interacts with a surface. The polarization state of a light beam refers to the path its Electric field traces as it propagates through space and time. Upon contact with a sample, the polarization of light is affected by the physical sample parameters.

The general method of spectroscopic ellipsometry can be described as follows (shown in Figure 2.4): linearly polarized light at a range of wavelengths (300-1000 nm) is emitted by a source and reflects off a sample. Contact with the sample changes the light from linearly polarized to elliptically polarized light. Subtle changes in the reflected light's electric and magnetic fields are detected by a photodetector. Each measurement records two values, the amplitude ratio (Ψ) and the phase difference (Δ) that are related to the reflectance ratio of *p*- and *s*- polarized light in the following way (Equation 10):

$$\rho = \tan(\Psi)e^{i\Delta} = \frac{R_p}{R_s} = \text{Reflectance ratio} \qquad\qquad \text{Equation 10}$$

where ρ is the ratio of Fresnel reflection coefficients for the s- and p-polarizations of light (R_p and R_s, respectively). The polarization state is used to determine three sample properties including index of refraction (n), extinction coefficient (k), and film thickness. The index of refraction, n, is the ratio of the speed of light in a vacuum to the speed of light through the medium, and k represents how far a light beam of given wavelength will transmit into a film prior to becoming fully absorbed. Once the polarization state has been measured, regression analysis using CompleteEASE® software is conducted to determine the unknown sample properties n, k, and thickness, that best generate a theoretical response to match the experimental data (Hilfiker et al., 2008). This procedure is called 'fitting' the data. When data fitting, the mean square error (MSE) is a parameter that represents the difference between a model and the experimental data; generally, a lower MSE suggests the model fits the experimental data well.
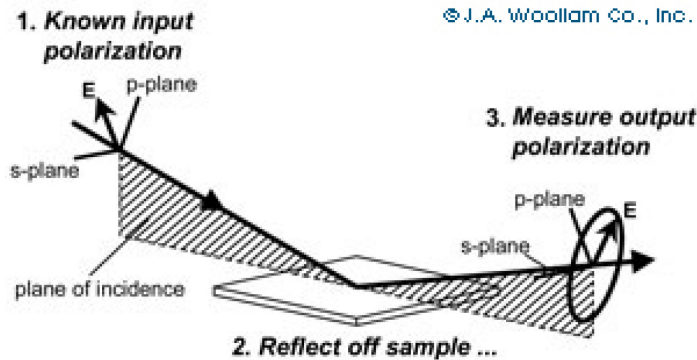
Figure 2.4 – Polarization state of light reflecting off of a sample during an ellipsometric measurement (Woollam, 2013).

2.8.2 Transparent and Absorbing Films

At every wavelength, Ψ and Δ are measured, however, potentially three film properties are unknown (n, k, and thickness). In general, transparent films are less complicated to model because the extinction coefficient, k, of a transparent film is equal to zero and does not need to be determined by regression analysis. A common transparent film modeled in literature is protein (Byrne et al., 2009; McArthur et al., 2010). Recently, in-situ ellipsometry has been used to quantify adsorbed protein onto metal surfaces such as copper and aluminum (McArthur et al., 2010). Metals, on the other hand, absorb at all wavelengths (Hilfiker et al., 2008). Absorbing films are more complex films to model than transparent films since k is also unknown at each wavelength. While Ψ and Δ are measured at every wavelength (2λ), three sample unknowns exist for an absorbing film: n, k, and film thickness ($2\lambda + 1$).

Certain strategies have been proposed to improve modeling of absorbing films. For example, measuring Ψ and Δ at multiple angles can increase the number of measured values per wavelength, however this strategy will only be beneficial if new information is generated at the additional angle (Hilfiker et al., 2008). Often with absorbing films, despite measuring sufficient ellipsometry data points, the solution is not unique, meaning multiple film thicknesses result in a similar quality fit (low MSE). Since absorbing films

23

are more complex to model, there are strategies to simplify the analysis. For example, depositing a film so thick it is opaque will prevent light from penetrating the layer and film thickness is no longer an unknown. In addition, films can be absorbing and transparent at different wavelengths; one approach is to measure film thickness in the transparent region where only one other unknown, n, must also be determined (Hilfiker et al. 2008). Then, with known thickness, $n(\lambda)$ and $k(\lambda)$ can be determined in the absorbing region.

Anodic oxide film thickness measurements have not been performed on lead or copper in the literature, and most anodic oxide film studies were conducted over 10 years ago. Ohtsuka et al. (1985) studied the anodic oxide film thickness of titanium in phosphate solution, whereas other studies have measured anodic oxide films on iron (Sato et al., 1971), and aluminum (De Laet et al., 1992) for example. One challenge is that metal films are absorbing at all wavelengths and to the author's knowledge, spectroscopic ellipsometry has never been applied in drinking water applications.

CHAPTER 3   MATERIALS AND METHODS

3.1   Pockwock Lake Source Water

Water used for all experiments was from the J. D. Kline Water Supply Plant (JDWSP) in Halifax, Nova Scotia, which draws surface water from Pockwock Lake. Pockwock Lake raw water is generally described as low pH, low in turbidity, low in alkalinity, and low in organic content.

JDKWSP is a direct filtration plant consisting of pre-screening, oxidation of iron and manganese with potassium permanganate ($KMnO_4$), pre-chlorination, coagulation with aluminum sulfate, flocculation, direct filtration through dual-media sand and anthracite filters, and chlorination. The pH and alkalinity of raw water are changed twice during the treatment process with either lime or CO_2 addition. Firstly, lime is added prior to the oxidation phase to increase pH to between 9.6 and 10 to optimize the oxidation of iron and manganese. The addition of lime also increases the water alkalinity from less than 1 mg $CaCO_3$/L to between 18 and 20 mg $CaCO_3$/L. After oxidation but prior to coagulation, CO_2 is dosed to decrease pH to 5.5 - 6. The following finishing chemicals are added post direct filtration but prior to distribution:

1) Chlorine for disinfection at a dose that will achieve a residual of 1.0 mg/L in the distribution system,

2) Sodium hydroxide to increase pH to 7.4, and

3) Zinc/ortho polyphosphate is dosed at 0.5 mg PO_4/L for corrosion control.

The water used for all experiments was collected post filtration but prior to chemical addition and will herein be referred to as filtered water. A summary of filtered water quality characteristics can be found in Table 3.1. Filtered water pH was below 6 and alkalinity was always less than 3 mg $CaCO_3$/L. Filtered water CSMR was 0.84 and is considered corrosive as it exceeds the threshold value of 0.77 proposed by Nguyen et al. (2011a).

Table 3.1 – Summary of filtered water characteristics

Analyte	Range	Average
pH	5.92-6.7	6.2
Alkalinity (mg $CaCO_3$/L)	1.8-2.9	2.5
Turbidity (NTU)	N.A.*	0.06
TOC (mg/L)	N.A.	1.9
Cl^- (mg/L)	6.2-8.1	7.4
SO_4^{2-} (mg/L)	7.2-9.7	8.6
PO_4 (mg/L)	0.2-0.4	0.3
CSMR	0.83-0.86	0.84
Conductivity (μS/cm)	N.A.	89
Pb (μg/L)	0.002-0.035	0.04
Cu (μg/L)	2.9-3.0	3.0

*N.A.=Not available

3.2 Electrochemical Experimental Set-up and Design

3.2.1 Lead and Copper Galvanic Cell Set-Up

Experiments were designed to simulate a lead and copper galvanic cell in premise plumbing. Identical 250 mL Erlenmeyer flasks (Fisher Scientific) were filled with 200 mL of filtered test water (measured with a volumetric flask). Each flask housed a copper coupon (76.2 mm x 12.7 mm x 1.68 mm) and lead coupon (38.1 mm x 12.7 mm x 1.74 mm) made of sheet metal (Ames Metal Products Co., IL, USA). The metal coupons were connected with copper alligator clips on each coupon with copper primary wire running between the two alligator clips (Certified® 14 AWG/CAF). No metals other than lead and copper were introduced into the system. The copper alligator clips were fastened to the Erlenmeyer flask opening such that approximately 50% of the electrode surface area was submerged in the test water.

Water stagnated within the flasks for either 1, 2, or 4 days. Water was changed using a static dump-and-fill procedure three times per week (every Tuesday, Wednesday, and

Friday). The longest stagnation time of 4 days was chosen to simulate a worst-case scenario of stagnant water in premise plumbing over a holiday or long weekend; this is consistent with other researchers who have conducted dump-and fill experiments to simulate premise plumbing conditions (Edwards and Triantafyllidou, 2007; Nguyen et al., 2011a).

Flasks were rinsed with deionized water prior to re-filling after each 'dump' to prevent metal carry-over from the previous 'fill' cycle. A water quality analysis was conducted on dump-and-fill water samples. Water quality parameters measured included:

1) Current (μA) (measured in-flask upon filling and prior to dumping);

2) Phosphate, chloride, and sulfate concentrations (mg/L);

3) pH;

4) Copper and lead concentrations (μg/L);

5) Conductivity (μS/cm);

6) Turbidity (NTU).

3.2.2 Electrochemical Experimental Designs

Electrochemical flask experiments were factorial experimental designs. Factorial designs determine which experimental factors (independent variables) produce a significant effect, and provide an estimation of the magnitude of that effect (Berthouex and Brown, 2002). Factorial designs estimate the main effects of each experimental factor, but also the interactions between factors (Berthouex and Brown, 2002). In addition, a large number of variables can be tested in comparatively few experimental runs.

Two experimental designs were conducted in this study. The factors evaluated were (1) fill water pH, (2) chlorine dose, (3) corrosion inhibitor type and dose, and (4) dissolved

inorganic carbon concentration. Parameter levels tested were chosen to mimic corrosion control conditions at the JDKWSP with a few exceptions. Although 0.5 mg PO_4/L of an ortho/polyphosphate blend is dosed at JDKWSP, higher doses of the corrosion inhibitors orthophosphate (OP) or zinc orthophosphate (ZOP) were chosen for this study to determine the effects of high-dose corrosion inhibitor on metals release. A chlorine concentration of 1 mg/L was dosed since this is the target chlorine residual in the distribution system at the JDKWSP. A low pH level of 7.4 was chosen because JDKWSP adjusts finished water to pH 7.4 prior to distribution and a high pH level of 9.2 was chosen as increasing pH to above 9 in low alkalinity water increases water stability.

Both experimental designs are described in the sections below. A total of 26 water conditions were tested between the two experiments and a diagram indicating the various DIC, pH, and corrosion inhibitor types and doses tested is shown in Figure 3.1. A summary table of all the water conditions is shown in Table 3.4

3.2.2.1 Effects of ZOP, pH, and Chlorine on Metals Release at Low DIC

The corrosion and passivation of copper and lead surfaces as influenced by ZOP, initial pH, and chlorine (Cl_2) were investigated with a factorial design. A three factor two-level (low and high levels) factorial experiment was conducted. A total of eight experimental conditions resulted from the combination of the three parameters and levels:

(1) ZOP dose of 0 and 20 mg PO_4/L;

(2) Initial pH of 7.4 or 9.2;

(3) Cl_2 dose of 0 or 1 mg/L.

The experimental water conditions are summarized in Table 3.2. DIC of all water conditions was not manipulated and all water conditions had DIC concentrations below 3.5 mg $CaCO_3$/L. These water conditions will be referred to as DIC(3) and had comparatively lower DIC than all water conditions described in Section 3.2.2.2.

The experimental design ran for 16 weeks and each condition was tested in duplicate. After the dump-and-fill experimentation, a surface analysis was conducted on lead and copper coupons to identify corrosion products that formed. Surface analysis techniques included scanning electron microscope (SEM) and electron dispersive spectroscopy (EDS).

Table 3.2 – Low- and high- parameter levels for the electrochemical experimental design testing ZOP dose, Cl_2 dose and initial pH.

	Low	High
ZOP (mg PO_4/L)	0	20
Cl_2 (mg/L)	0	1
Initial pH	7.4	9.2

3.2.2.2 Effects of OP, pH and DIC on Metals Release

The corrosion and passivation of copper and lead surfaces as influenced by orthophosphate, initial pH, and dissolved inorganic carbon levels were investigated with a factorial design analysis. DIC was chosen as a factor for this test for the following reasons: (1) Increasing DIC concentration could increase pH stability, and (2) increased concentrations of DIC was found to prevent the initiation of localized corrosion (Lytle and Schock, 2008). OP dose and pH were evaluated at three levels, and DIC was evaluated at 2 levels. Eighteen experimental conditions resulted with the following factors and levels:

(1) OP dose of 0, 10, or 20 mg PO_4/L;

(2) Initial pH of 7.4, pH 8.3, or pH 9.2; and

(3) Average initial DIC equal to 7 or 17 mg $CaCO_3$/L.

Due to the large number of experimental conditions, conditions were not tested in duplicate. A summary of the factors and levels in this experimental design can be found in Table 3.3.

The experimental design ran for 12 weeks. Similar to the first electrochemical experiment, coupon surface analysis was conducted post-experiment to identify surface corrosion products. SEM and EDS analysis was conducted on lead and copper coupons and XRD was conducted on lead coupons only.

Table 3.3 – Low, medium, and high parameter levels for the electrochemical experimental design testing OP dose, initial pH, and DIC concentration.

	Low	Med	High
OP (mg PO_4/L)	0	10	20
Initial pH	7.4	8.3	9.2
DIC (mg $CaCO_3$/L)	7		17

Corrosion Inhibitor Type:

No Corrosion Inhibitor

Orthophosphate

Zinc Orthophosphate

Dose:

0 mg PO_4/L

10 OR 20 mg PO_4/L

20 mg PO_4/L

pH:

pH 7.4   pH 8.3   pH 9.2

pH 7.4   pH 8.3   pH 9.2

pH 7.4   pH 9.2

Chlorine:

+/- Cl2   +/- Cl2

+/- Cl2   +/- Cl2
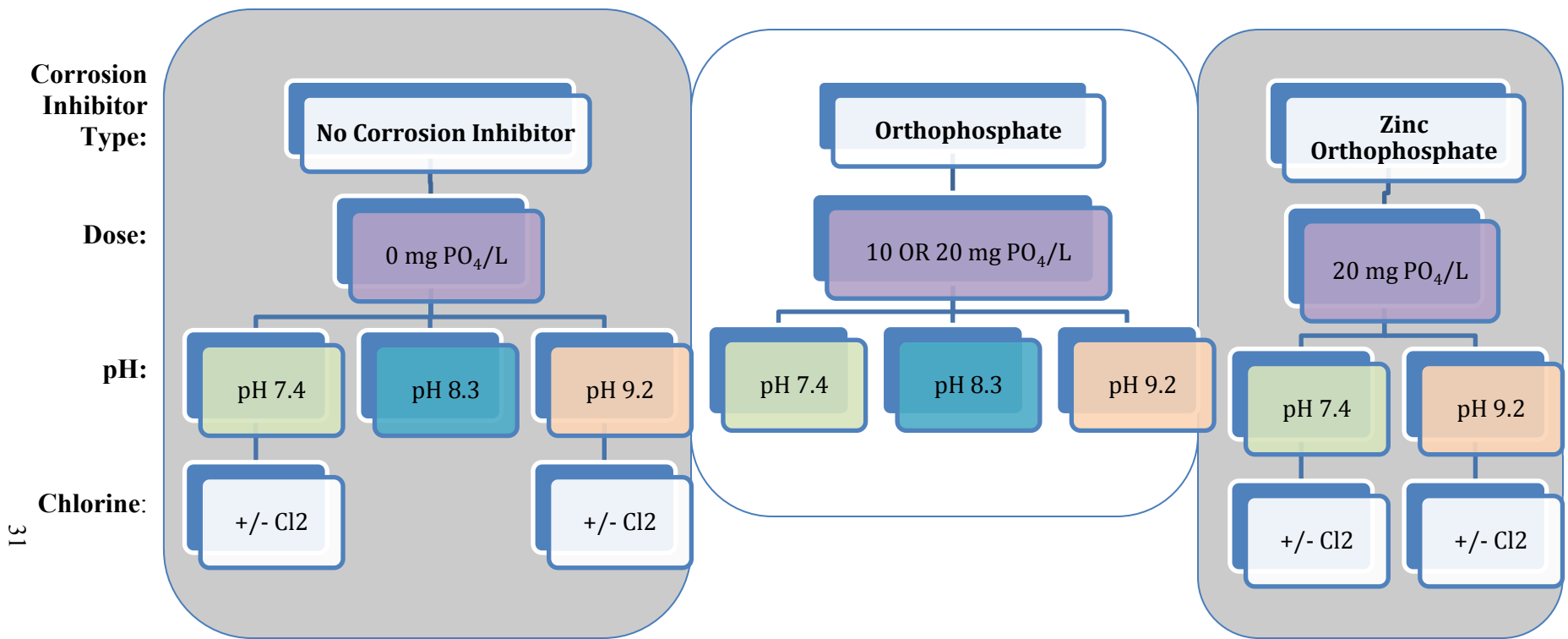
Figure 3.1 – Summary map of the various water conditions tested according to corrosion inhibitor type, dose, pH, and chlorine dose. Note that the 3 DIC levels tested in this study are not indicated on this map. OP was tested at 10 or 20 mg PO_4/L whereas ZOP was only tested at 20 mg PO_4/L.

Table 3.4 – Summary table of the 26 water conditions according to corrosion inhibitor type, dose, DIC, Cl$_2$ dose, and pH. Each 'x' in the table represents a water condition that was tested in the study.

No Corrosion Inhibitor	x	x	x	x			x	x					x	x	x	x		
Orthophosphate (10 mg PO$_4$/L)		x	x				x	x						x	x			
Orthophosphate (20 mg PO$_4$/L)		x	x				x	x						x	x			
Zinc Orthophosphate (20 mg PO$_4$/L)	x			x									x			x		
DIC (mg/L)	3	7	17	3	7	17	3	7	17	3	7	17	3	7	17	3	7	17
Cl$_2$ (mg/L)	0			1			0			1			0			1		
pH	7.4						8.3						9.2					

3.3   Stock Solution Preparation

Influent 'fill' water was prepared by adding chemical stock solutions to JDKWSP filtered water. Since phosphate and alkalinity addition affected bulk water pH, chemical addition occurred in the following order: (1) phosphate (either ZOP or OP), (2) sodium bicarbonate for DIC adjustment, if applicable, (3) sodium hydroxide (NaOH) for pH adjustment, and (4) chlorine. The maximum chlorine dose of 1 mg/L did not significantly affect pH and could be added post pH adjustment with NaOH. All chemicals used for stock solutions were laboratory grade, and all stock solutions were made with deionized water obtained from a Milli-Q Academic water purification system (Millipore, MA, USA).

3.3.1 Phosphate Stock Solutions

Zinc Orthophosphate (ZOP): A stock solution of ZOP was prepared by adding ZOP (Carus 3180, Carus Chemical Company, IL, USA) to deionized water. Ingredients in the ZOP product included proprietary concentrations of zinc chloride, zinc phosphate, phosphoric acid, and other non-hazardous ingredients. ZOP stock solutions were prepared once a week and 3 mL of ZOP was added to 1 L of deionized water, stored in large amber jugs and kept at 4°C. Flasks were dosed with 20 mg PO_4/L and zinc concentration was approximate 26 mg/L (Zinc:PO_4 ratio of 1:1.3). Batches of ZOP were made each day flasks were filled, and consisted of diluting ZOP stock solution into JDKWSP filtered water.

Orthophosphate (OP): A stock solution of OP was prepared by diluting 1.0 g of potassium phosphate monobasic (KH_2PO_4) (Fischer Scientific, MA, USA) into 1.0 L of deionized water. Batches of 10 and 20 mg/L OP were prepared by diluting the orthophosphate stock solution into JDKWSP filtered water. 10 and 20 mg/L OP batches were prepared once a week, stored in 1 L amber jugs and kept at 4°C.

3.3.2 Chlorine Stock Solution

A chlorine stock solution was prepared by adding sodium hypochlorite (NaClO) (Fischer Scientific, MA, USA) to deionized water. Chlorine stock was prepared once a week and the stock concentration was confirmed prior to use. Chlorine stock solution was dosed to achieve a Cl_2 concentration of 1 mg/L in the designated flasks.

3.3.3 Sodium Bicarbonate Stock Solution

A 0.1 eq/L sodium bicarbonate (NaHCO$_3$) stock solution was prepared by dissolving 8.4 g of NaHCO$_3$ (Fisher Scientific, M.A., USA) into 1.0 L of deionized water. Stock solution was stored in a plastic bottle and kept at 4°C.

3.3.4 pH Adjustment

Various molarities of NaOH were added to water conditions that required increasing pH to reach the target initial pH of 7.4, 8.3, or 9.2. However, addition of sodium bicarbonate often increased pH to above the target pH and acidification was required. To lower pH, H_2SO_4 was added which resulted in a decrease in CSMR. This may have had beneficial effects on corrosion control. As such, CSMR was monitored over the course of the experiment.

3.4   Ellipsometry Set-Up and Design

3.4.1 In-Situ Flow Cell Set-Up

A custom-made flow cell was used to make *in-situ* ellipsometric measurements along a sample (shown in Figure 3.2). The flow cell was made of 147 mm long fused quartz tube (8 mm ID) (Technical Glass Products Inc., OH, USA), which sat in a groove in a machined block of aluminum (25.4 mm x 108.0 mm x 12.7 mm). The quartz tube was

secured to the aluminum block with metal tie-downs. A recessed aluminum insert was machined to fit within the quartz tube and to hold an 89 mm long glass sample (described in the following paragraph). Once the sample was inserted, two stainless-steel spring clamps held down the sample to the aluminum insert. As well, stainless steel tube fittings (Swagelok, Co., OH, USA) provided an air-tight connection between the quartz tube and the influent and effluent water lines. The cell was mounted onto a custom-machined aluminum ellipsometer mounting stage that is capable of moving in the x, y, and z directions. Measurements were taken along the sample's centerline to ensure equal incident and reflected beam path lengths.
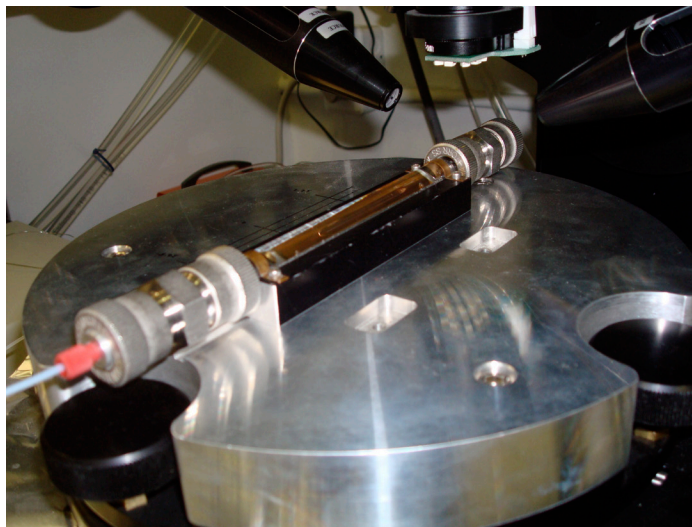
Figure 3.2 – The flow-cell used to perform in-situ ellipsometry measurements.

3.4.2 Sample Preparation

Copper and lead films were deposited onto 89 mm x 6.4 mm glass substrates by magnetron sputtering with a VT-3 system (Corona Vacuum Coaters, B.C., Canada). Firstly, glass substrates were cleaned (ultrasonic cleaning in acetone, ethanol, and nano-pure water for 15 minutes each), and a thin chromium tie-layer was sputtered onto the

glass substrate to improve the adhesion of the metallic films to the glass during submersion in solution. Samples were stored in airtight containers prior to use.

3.4.3 Protein Solution Preparation And Dosing

The plasma protein albumin (bovine serum albumin, Sigma, USA) was used to simulate the proteins involved in microbial attachment to metals. A 1.0 mg/mL albumin solution was prepared in phosphate buffered saline (PBS) at pH 7.4. Protein solution as well as PBS alone and distilled water for rinsing were pumped through the flow cell at 2.5 mL/min using Series I diaphragm pump (Lab Alliance, PA, USA). A diaphragm pump was chosen to reduce shearing that could potentially damage the protein in solution.

3.4.4 In-Situ Adsorption Measurements

Adsorption measurements were performed using a M-2000 Spectrocopic Ellipsometer with an automated motion stage (J.A. Woollam, Co., NE, USA). Ellipsometric measurements were performed with focusing optics (beam spot diameter approximately 150 μm) at incidence angles of 65, 70, and 75° over a wavelength range of 200-1000 nm in steps of 2 nm at each point. Supplied software, CompleteEASE® (J.A. Woollam, Co., NE, USA), was used to align the sample for maximum signal intensity, create sample scan patterns, and measure the ellipsometric parameters psi (Ψ) and delta (Δ) along the designed scan pattern.

First, the optical constants of the plate prior to exposure to water were determined by measuring Ψ and Δ in a baseline scan and fitting with a B-spline. This was to best model the optical constants of the metal surface prior to film growth. These optical constants were then used in the model to fit data post exposure. Measurements were taken at 20 points along the length of the sputtered plate.

3.5   Analytical Procedures

3.5.1 General Water Quality Parameters

Conductivity, temperature, pH, and ORP were measured using an Accumet Excel XL60 dual channel probe (Fisher Scientific, MA, USA.) according to the manufacturer's instructions. Probes were calibrated daily using standard buffer solutions from Fisher Scientific. Turbidity was measured using a HACH 2100N laboratory turbidimeter (HACH, CO, USA.) Samples were inverted at least three times before measuring. Free chlorine was measured using a DR 4000 UV-Spectrophotometer (HACH, CO, USA.) according to method DPD 8021. Alkalinity was measured using a titration method according to Method 2320B (APHA, 1995)

3.5.2 Current

The galvanic current between the copper and lead coupons within the electrochemical flasks was measured using a True RM Industrial Multimeter EX530 (Extech Instruments Corporation, MA, USA.)

3.5.3 Organic and Inorganic Carbon

Total organic carbon (TOC), dissolved organic carbon (DOC), and dissolved inorganic carbon (DIC) was analyzed using a Shimadzu TOC-VCSH TOC Analyzer (Shimadzu Corporation, Kyoto, Japan) with a minimum detection limit of 0.6 mg/L. Samples were poured into a 50 mL head-space free glass vial. DOC samples were first filtered through a 0.45 μm polysulphone filter paper (GE Water & Process Technologies, PA, USA.) that had been pre-rinsed with 500 mL of deionized water. Concentrated phosphoric acid was added to TOC and DOC samples to decrease pH to below 2, however no acid was added to DIC samples. Sample vials were capped and stored at 4°C until analysis.

3.5.4 Anions

Chloride (Cl^-), phosphate (PO_4^{2-}), and sulfate (SO_4^{3-}) were measured using a 761 Compact Ion Chromatogram with 788 filtration sample processor (Metrohm, Herisau, Switzerland) according to USEPA method 300.1. Standards of 2, 5, 10, 20, and 30 mg/L Cl^-, PO_4^{2-}, and SO_4^{3-} were prepared and measured on the instrument once a week. The method detection limit for Cl^-, PO_4^{2-}, and SO_4^{3-} were, 0.6 mg/L, 0.7 mg/L, and 0.5 mg/L, respectively.

3.5.5 Metals

Influent and bulk water samples were analyzed for metals using inductively coupled plasma mass spectrometry (ICP-ms) (Thermo Fisher X-Series 2 ICP-ms, MA, USA.). The limit of detection was 0.7 μg/L and 0.4 μg/L for copper and lead, respectively. Metals samples were analyzed according to Standard Methods 3030 (APHA, 2012) which states that samples with turbidity greater than 1 NTU should undergo nitric acid digestion (NAD) prior to analysis by ICP-ms. According to the method, all metals samples are acidified to pH less than 2 to dissolve all particulate metals such that they can be measured by ICP-ms. Water samples with high turbidity have been associated with high particulate metals concentrations and NAD is a technique used to break down large particulates into dissolved form such that they can be measured by ICP-ms (APHA, 2012).

Up to three metals concentrations were measured for each water sample: dissolved, total, and NAD lead and copper concentrations. Dissolved metals refer to the concentration of metals after passing the sample through a 0.45 μm filter, whereas total metals refers to the concentration of metals without filtration and represents the dissolved as well as particulate metals. NAD metals refers to metal concentration after NAD digestion and includes the dissolved and particulate portion of metals, and may increase metals concentration compared to total metals.

Dissolved metals samples were filtered through a 0.45 μm cellulose nitrate membrane filter (Whatman, Dassel, Germany), acidified with nitric acid to below pH 2 and stored at 4 °C until analysis by ICP-ms. To determine total metals concentrations, bulk water samples were acidified with nitric acid to below pH 2 and stored at 4° C until analysis by ICP-ms (direct analysis). NAD metals concentrations were determined via the following procedure:

1) 10 mL of sample was poured into a disposable digestion sample tube and 0.5 mL of nitric acid was added,

2) Samples were heated to 105° C for 2 hours and water was allowed to evaporate,

(3) Samples were removed from the batch heater and allowed to cool slightly. Deionized water was poured into the sample to return the total sample volume to 10 mL (replenish the evaporated water volume), and

(4) Samples were stored at 4° C until analysis by ICP-ms.

As a general rule, metals concentration after NAD should be equivalent or higher than the metals concentration without NAD (total metals), and total metals concentration will be equivalent or higher than dissolved metals concentration (i.e. Dissolved metals ≤ Total metals ≤ NAD metals).

3.5.6 Electrode Corrosion Scale Surface Analysis

Virgin as well as corroded lead and copper coupons from each treatment condition were analyzed for corrosion products. SEM with EDS anlayisis using a Hitachi S-4700 FEG SEM determined the morphology and elemental composition of the corrosion products. The elemental percent composition was determined by averaging percent composition of at least 3 spots on each electrode, or an area scan was performed. XRD analysis was conducted to identify crystalline and solid phases present in the lead corrosion scales of some lead coupons. A D500 Diffractometer x-ray system was used (Siemens, USA) and

was equipped with diffracted beam Soller Slits and a graphite monochrometer. The beam path was configured with 0.3° divergence and anti-scatter slits and a 0.15° receiving slit. Copper K-alpha radiation was used for these measurements. Samples were scanned in step mode with a 0.05° step size and a 6 second integration time. MATCH! software and a powder diffraction files database was used for pattern analysis. Search/match criteria were restricted to the elements already identified in the EDS analysis. Sample sizes were not large enough to estimate the relative proportions of each compound in a sample. As a result, XRD analysis was used to identify the presence of particular corrosion products.

3.6   Data Analysis for Electrochemical Experiments

Minitab® software (Minitab® 2010, 16.2.2, PA, USA) was used to conduct all statistical analysis.   The statistical tests conducted included one-way analysis of variance (ANOVA), paired t-tests, and factorial design analysis. One-way ANOVA tests were conducted in conjunction with Tukey's Method - one-way ANOVA was conducted to identify in any of the population means differed, and Tukey's method compared each pair of means to form groups whose means were not significantly different (using a family error rate to control the rate of type 1 error). Paired observations, such as lead concentration before and after NAD, were analyzed with one-tailed paired t-tests. Lastly, the factorial design analysis function in Minitab® was used to identify significant factors from the factorial design experiments. Responses for factorial design analysis were (1) lead concentration and (2) copper concentration. Only data collected during steady state was used for factorial analysis, and metals data was categorized according to stagnation time.   Since metals release had stabilized during steady state, lead and copper concentration in each bulk water sample after a stagnation time was considered a replicate. All statistical tests were conducted at the 95% confidence level ($\alpha=0.05$).

CHAPTER 4   RESULTS AND DISCUSSION

4.1   Water Condition Notation

Five parameters were tested at various levels and combinations and included the following:

1. Phosphate type: ZOP or OP
2. Phosphate dose (0, 10, or 20 mg PO_4/L),
3. Initial water pH (7.4, 8.3, or 9.2),
4. DIC (3, 7, 17 mg/L), and
5. Cl_2 dose (0 or 1 mg/L).

The following notation will be used to identify each water condition: corrosion inhibitor type (corrosion inhibitor dose in mg PO_4/L)/initial pH/DIC in mg $CaCO_3$ per L/Cl_2. For example, **ZOP(10)/pH(7.4)/DIC(3)/Cl$_2$** denotes the water condition with a ZOP dose of 10 mg PO_4/L, initial pH 7.4, 3 mg/L DIC, and 1 mg/L Cl_2, whereas **pH(9.2)/DIC(3)** represents the water condition without corrosion inhibitor, initial pH 9.2, DIC of 3 mg $CaCO_3$/L and no chlorine addition.

4.2   Relationship Between Turbidity and Particulate Lead

Standard Method 3030 (APHA, 2012) states that drinking water samples with turbidity greater than 1 NTU should undergo heated NAD prior to analysis by ICP-ms whereas samples with turbidity less than 1 NTU may be analyzed directly. Regardless of turbidity, a minimum of 13 bulk water samples from each of the 26 water conditions were analyzed for lead by both methods: (1) direct analysis without NAD, and (2) NAD prior to analysis by ICP-ms.

Average bulk water turbidity ranged from 0.12 to 10.9 NTU (data shown in Table A.1 in Appendix A). Bulk water turbidity was above 1 NTU in 11 water types and below 1

NTU in 15 water types. Turbidity was always less than 1 NTU in water conditions that did not dose corrosion inhibitor (10 water conditions). Average bulk water turbidity was occasionally below 1 NTU when OP was dosed at 10 or 20 mg PO$_4$/L and ranged from 0.62 to 3.41 NTU. The highest bulk water turbidity occurred in the 4 water conditions that dosed ZOP at 20 mg PO$_4$/L; average turbidity ranged from 4.9 to 10.9 NTU.

One-sided paired t-tests ('NAD lead concentration' minus 'Direct analysis lead concentration') were conducted to identify if a significant increase in lead concentration occurred after NAD. Twenty of the 26 water conditions exhibited a significant increase in lead concentration after NAD (α=0.05). Of these 20 water conditions, 12 had average sample turbidity below 1 NTU. Water types with turbidity less than 1 NTU that exhibited significant increases in lead concentration is likely because lead particulates settled in the turbidity sample bottle during analysis and did not contribute towards measured turbidity as was observed by other authors (Triantafyllidou et al., 2007). Only three water conditions with average bulk water turbidity below 1 NTU did not result in increased lead concentration after NAD; these water conditions all contained OP. Of the 11 water conditions with average turbidity above 1 NTU, eight observed significant increases in lead concentration with NAD (α=0.05). Lead concentration significantly increased in all water conditions with ZOP addition (sample turbidity>1 NTU) after NAD indicating that particulate lead was not completely dissolved without NAD in all ZOP water conditions.

In water conditions where lead significantly increased with NAD, the amount by which lead increased after NAD varied by water type. The 95% lower bound of the average difference between NAD and direct analysis samples represents the minimum increase in lead concentration after NAD with 95% confidence. The 95% lower bound of the average difference ranged from 2 to 60 μg/L; in other words, NAD increased lead concentration by a minimum of 2 to 60 μg/L (α=0.05). The highest 95% lower bound increase in lead concentration with NAD was in water condition pH7.4/DIC(3). As well, NAD increased lead concentration by at least 10 μg/L in 12 of the 20 water conditions that exhibited significant lead increases (α=0.05). These results demonstrate the potential for NAD to significantly increase lead concentration by as much as 10 μg/L, the maximum allowable

concentration (MAC) for lead in drinking, even in water conditions with corrosion inhibitor (Health Canada, 2012).

Other authors have conducted similar analyses on water samples. Deshommes et al. (2010) tested 76 water samples from homes with lead service lines with turbidity>1 NTU. The authors found no significant difference between lead concentrations with and without NAD (p>1). The current study, however, indicates that significant particulate lead can be present when turbidity is greater or less than 1 NTU. This study likely had significant particulate lead in the majority of water samples because galvanic corrosion has shown to increase particulate lead (Wang et al., 2012) and the metal materials used in this study were new and passivation scale was likely not as resilient as those in lead service lines from older homes. Therefore, it is valuable to characterize lead concentrations by both direct analysis and NAD to identify if significant portions of particulate lead exist, regardless of turbidity.

The results from this analysis show that it is not exclusively samples with turbidity above 1 NTU that exhibit increased lead concentrations after NAD. These findings suggest that the recommendation by Standard Methods 3030 to only require NAD for samples with turbidity above 1 NTU may not adequately measure particulate lead concentrations in some water samples. By digesting only the samples with turbidity above 1 NTU, the particulate portion of lead in samples with turbidity less than 1 NTU may not be represented, and potential parameter exceedences could be missed. Based on this study, NAD lead concentrations were used in all analysis for all water conditions, regardless of bulk water turbidity.

4.3   Metals Release Over Time

Other authors conducting dump-and-fill experiments with aged lead pipes acclimated the pipes for 8 weeks (Wang et al., 2012) and 8 months (Cartier et al., 2013; Xie and Giammar, 2011). Residuals from the average represent the difference between the observed Pb concentration on a given day and the average Pb release over the

experimental duration for a single water type. When the residual is 0, the observed Pb concentration is equal to the overall average Pb concentration. A plot of residuals over time for two representative water types is shown in Figure 4.1. Vertical deviations from 0 are highest at the beginning of the experiment and residuals from the average were sometimes greater than 7000 in the first 7 days of experimentation. According to Figure 4.1, steady state metals release was achieved after approximately 7 days, however a conservative acclimation period of 30 days was used to ensure steady-state lead release had occurred. In comparison to other studies, a shorter acclimation period was required in the current study due to the difference in lead materials and the smaller lead surface area exposed to water in the current experiment.
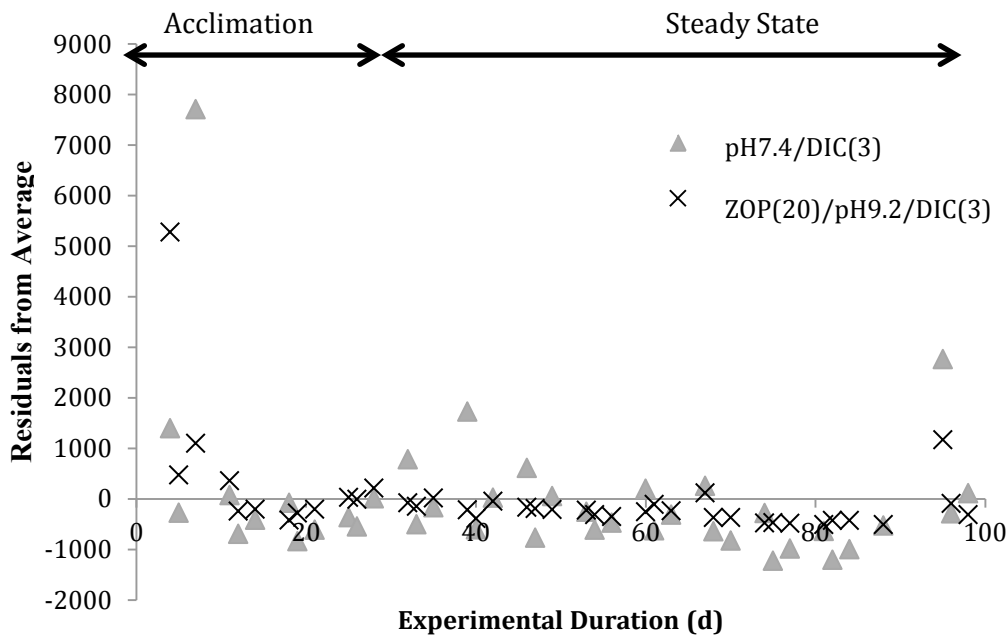
Figure 4.1 – Plot of the residual from the average over time for two representative water conditions. High lead release events towards experimental day 100 were identified as outliers and removed from the data set prior to data analysis.

Two distinct phases of metals release were identified for data analysis (Figure 4.1):

Acclimation (30 days, short term): For all water conditions, the highest lead levels were observed during the first 30 days of experimentation. Higher lead release during this period coincides with higher current measurements (discussed in Section 4.4.2). Higher current and therefore lead concentration is likely due to lead release prior to the development of a passivation film, leading to sloughing of metal complexes into the bulk water.

Steady State (49-68 days long-term): Systems had stabilized and consistent metals release was observed. High lead concentration events were observed in some bulk water samples, mainly in initial pH 7.4 conditions without corrosion inhibitor. These spikes can be attributed to lead particles sloughing off the coupon surface during the dump-and-fill procedure. Triantafyllidou and Edwards (2011) categorized lead release due to galvanic corrosion as independent of other lead release mechanisms including normal dissolution, deposition corrosion, and particle detachment (sloughing). In the current data set, metals release events that were 1.5 times the interquartile ranges were considered due to particle detachment rather than galvanic corrosion and were removed from the data set for factorial analysis. Outlier events in particular water types will be addressed, however.

4.4   Influent Water Quality of the 26 Water Conditions

Influent water quality of the 26 water conditions is shown in Table 4.1.

4.4.1 Fill Water CSMR

Influent water CSMR varied between experimental conditions. Water types with ZOP(20) had the highest average CSMR values and ranged from 4.12-4.35. Average CSMR for water conditions with OP(10) and OP(20) ranged from 0.70 to 0.97. Without corrosion inhibitor at all DIC levels, average CSMR values ranged from 0.55 to 1.95, and

Table 4.1 – Influent water quality during steady state of the 26 water conditions tested in the study

Water Condition	CSMR	Conductivity (µS/cm)	Current (µA)	DIC (mg CaCO$_3$/L)	Alkalinity (mg CaCO$_3$/L)
pH7.4/DIC(3)	1.16	71.3	6.4	2.12	8.1
pH7.4/DIC(3)/Cl$_2$	1.95	71.3	12.4	2.12	15.2
ZOP(20)/pH7.4/DIC(3)	4.12	180.1	11.8	1.25	13.7
ZOP(20)/pH7.4/DIC(3)/Cl$_2$	4.35	180.1	13.6	1.25	13.7
pH9.2/DIC(3)	1.16	94.0	6.0	2.74	14.0
pH9.2/DIC(3)/Cl$_2$	1.46	94.0	11.6	2.74	12.6
ZOP(20)/pH9.2/DIC(3)	4.23	188.7	8.7	2.26	25.8
ZOP(20)/pH9.2/DIC(3)/Cl$_2$	4.32	188.7	8.2	2.08	25.8
pH7.4/DIC(7)	0.79	125.3	9.5	7.2	31.3
pH7.4/DIC(17)	0.55	223.2	8.2	19.0	73.9
pH8.3/DIC(7)	0.78	140.0	8.9	8.3	36.0
pH8.3/DIC(17)	0.87	252.7	17.0	21.7	87.8
pH9.2/DIC(7)	0.87	132.9	7.2	8.3	34.6
pH9.2/DIC(17)	0.96	247.8	16.7	21.4	91.1
OP(10)/pH7.4/DIC(7)	0.95	133.6	10.4	7.0	30.9
OP(10)/pH7.4/DIC(17)	0.70	249.4	7.8	17.6	74.5
OP(10)/pH8.3/DIC(7)	0.79	178.6	11.6	6.7	30.5
OP(10)/pH8.3/DIC(17)	0.97	250.7	8.7	18.7	82.4
OP(10)/pH9.2/DIC(7)	0.80	140.7	10.1	6.0	27.3
OP(10)/pH9.2/DIC(17)	0.92	226.0	12.2	18.5	79.4
OP(20)/pH7.4/DIC(7)	0.96	147.5	15.4	5.3	25.3
OP(20)/pH7.4/DIC(17)	0.77	266.0	14.5	19.1	82.4
OP(20)/pH8.3/DIC(7)	0.91	154.5	13.5	6.2	31.8
OP(20)/pH8.3/DIC(17)	0.88	277.2	14.7	18.6	84.1
OP(20)/pH9.2/DIC(7)	0.71	156.8	13.7	5.9	31.1
OP(20)/pH9.2/DIC(17)	0.94	241.8	16.1	18.7	82.4

CSMR was always higher in water conditions with either DIC of either 7 or 17 mg CaCO$_3$/L.

This is likely because of H$_2$SO$_4$ addition in higher DIC water conditions to reduce pH after bicarbonate addition increase the sulfate concentration and decreased CSMR. In all but three water conditions, average CSMR was greater than the threshold value of 0.77 and were considered corrosive (Nguyen et al., 2011a). Though CSMR ranged from 0.55-4.35, CSMR was not correlated to lead release. Other research has shown that further increasing CSMR above 1 does not necessarily increase adverse effects on lead release (Nguyen et al., 2011b).

4.4.2 Fill Water Current

Large galvanic currents were measured when the copper and lead coupons were initially connected during acclimation followed by a decrease in current upon filling the flasks during steady state. Generally, current was highest in water conditions with either 7 or 17 mg CaCO$_3$/L and lowest currents were observed in water conditions with DIC of 3 mg CaCO$_3$/L. Maximum current ranged from 37 μA to 109 μA in water condition conditions with either 7 or 17 mg CaCO$_3$/L. During steady state, average current ranged from 7 to 17 μA in these water conditions (Table 4.1). In contrast, in water conditions with DIC(3), maximum current over the experimental duration did not exceed 32 μA. Current was highest in the two water conditions with ZOP(20) addition at pH 7.4, and average current during steady state was always less than 14 μA.

In addition, elevated current upon filing the flasks at the beginning of the experiment coincides with higher lead release (shown in Figure 4.2). In general, current decreased between filling and dumping the bulk water (after 1, 2, and 4 days stagnation). The greatest decreases in current over stagnation time were observed prior to reaching steady state: in one water condition, current decreased by as much as 54 μA over a 2-day stagnation time. Within one week, galvanic currents decreased by a factor of 4 to 26 times. Other studies have shown that galvanic current decreased on average by 29% when lead pipe was upstream of copper pipe over the 214 day experiment, with galvanic

47
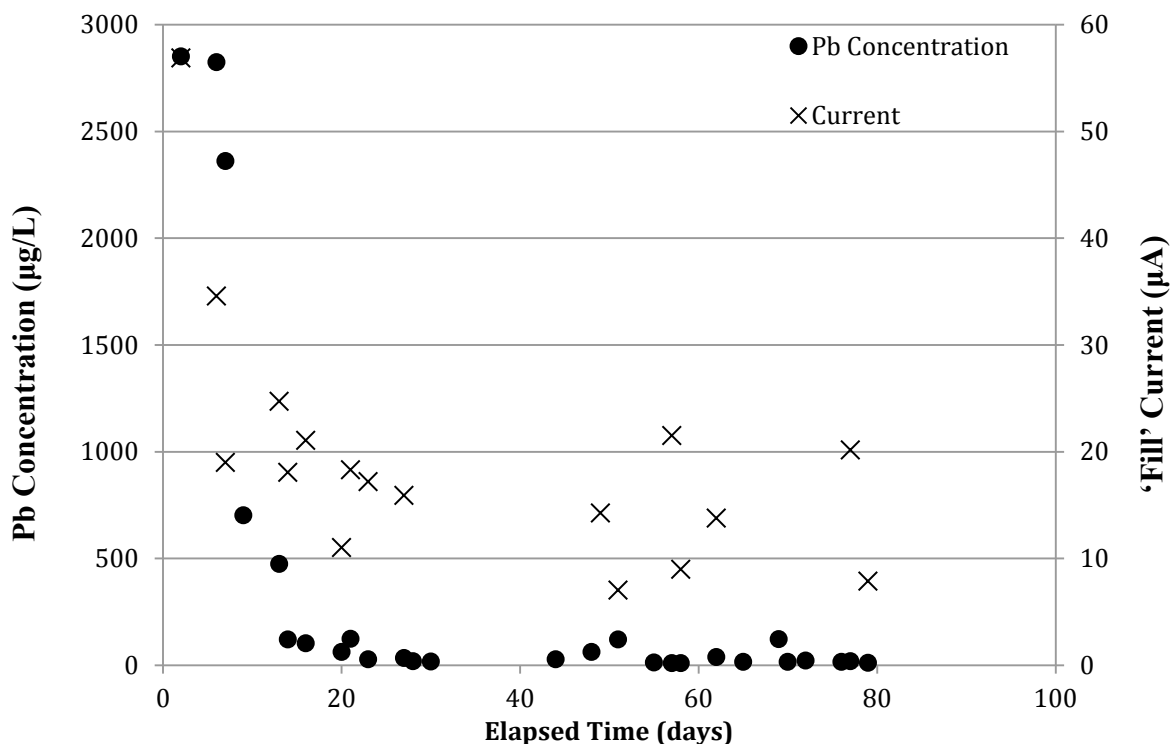
Figure 4.2 – Pb concentration and current over the experimental duration for water type OP(10)/pH7.4/DIC(7). Higher initial current corresponds with higher lead release.

currents of 18 μA at the end of the experiment in water conditions with ZOP addition (Cartier et al., 2012a).

The lowest and highest average fill currents were in water conditions without corrosion inhibitor, with DIC(3) and DIC(17), respectively. The five lowest average currents upon filling the flasks were in water conditions without corrosion inhibitor and low DIC(3) but different initial pH conditions, and the water conditions with the two highest average fill currents were also water conditions without corrosion inhibitor but at high DIC (fill currents were significantly different between these two groups). This suggests that DIC concentration played a major role in sustaining galvanic current, particularly in water conditions without corrosion inhibitor. As well, adding 1 mg/L Cl_2 to water conditions with 3 mg/L DIC increased average fill current. Average fill current significantly increased between 3.1 and 5.2 μA when chlorine was dosed ($\alpha=0.05$) except in water

condition ZOP(20)/pH(9.2)/DIC(3) where average fill current did not significantly increase with addition of 1 mg/L Cl_2.

All water conditions with DIC(3) observed significant decreases in current with stagnation time (p<0.002) and dump current was always at least 0.9 μA lower than fill current (α=0.05). When DIC was 7 or 17 mg $CaCO_3$/L, current did have a tendency to decrease with stagnation though a smaller difference between initial and dump current was observed and current decrease over time was only significant in 5 of the 18 water types. This could be because higher DIC concentration increased the water conductivity and was able to sustain galvanic current even after longer stagnations times compared to low DIC concentrations.

4.4.3 Fill Water Conductivity

Average fill conductivity ranged from 69 to 335 μS/cm in the 26 water conditions. Water conductivity was most heavily influenced by DIC whereas phosphate addition did not significantly impact conductivity. For example, water conditions without corrosion inhibitor with DIC of 17 mg/L had higher conductivity than water conditions with ZOP and OP with DIC of 3 or 7 mg/L, respectively. As well, increasing OP dose from 10 to 20 mg PO_4/L did not significantly increase bulk water conductivity in water conditions with DIC of 7 mg/L or 17 mg $CaCO_3$/L. As well, all water conditions with DIC(7) had significantly lower bulk water conductivity than water conditions with DIC(17). Therefore, increasing bicarbonate dose had the largest influence on increasing water conductivity in this study.

Water conditions in order of lowest conductivity to highest conductivity are shown below. Bulk water pH did not significantly impact conductivity, but rather, conductivity was governed by DIC concentration. The addition of corrosion inhibitors also increased conductivity.

DIC(3) < DIC(7) < OP(10)/DIC(7) < ZOP(20)/DIC(3) < DIC(17) < OP(20)/DIC(17)

4.5   Lead Release During the Acclimation Stage

4.5.1 No Corrosion Inhibitor

The highest lead concentrations were observed during the acclimation phase in water conditions without corrosion inhibitor. The highest average lead concentrations occurred in water conditions with initial pH 7.4 and low DIC (either 3 or 7 mg $CaCO_3$/L). When DIC was increased to 17 mg $CaCO_3$/L, average lead release during acclimation decreased. When DIC was below 3 mg $CaCO_3$/L, low pH of 7.4 resulted in the highest lead release event and highest average lead release during the acclimation stage. Condition pH7.4/DIC(3) also had the largest standard deviation and coefficient of variation indicating frequent sloughing events.

The combination of higher DIC and higher pH had the largest impact on reducing average lead release and fewer outlier lead release events occurred when initial pH was increased from 7.4 to either 8.3 or 9.2. When DIC was 3 mg/L or less and pH was 7.4, lead concentrations ranged from 790 μg/L to 9339 μg/L (average 2078 μg/L), whereas lead concentrations ranged from 259 to 2665 μg/L in water conditions when pH was increased to 9.2. When DIC was increased to 7 mg/L, lead concentration ranged from 160 to 3358 μg/L during acclimation (6000 μg/L lower than the maximum lead release event when DIC was 3 mg/L), and when DIC was further increased to 17 mg $CaCO_3$/L, maximum lead concentration ranged from 86 to 1294 μg/L and had the lowest outlier lead event of any DIC group. At all three DIC concentrations, the highest average lead release was in water conditions with initial pH 7.4 whereas the combination of high DIC and high initial pH had the greatest impact on mitigating lead release during acclimation; in water condition pH9.2/DIC(17), lead concentration never exceeded 320 μg/L during acclimation. Therefore, without corrosion inhibitor, higher DIC and higher pH reduced average lead release during the acclimation period, and prevented high lead release events. In all cases, however, lead concentration exceeded the Health Canada guideline of 10 μg/L during acclimation, demonstrating the potential for public health risks when copper and lead are initially connected.

4.5.2 Zinc Orthophosphate Corrosion Inhibitor (DIC 3 mg/L)

ZOP was dosed at 20 mg PO_4/L and was only tested with DIC of 3 mg $CaCO_3$/L. At initial pH 7.4, the addition of ZOP reduced average lead release. However, due to the large amount of variation during this stage, average lead release was not significantly different between any water condition with and without ZOP at 3 mg/L DIC. Though the range of lead concentrations observed during acclimation was similar between initial pH 7.4 and pH 9.2 and ranged between 170 μg/L and 5800 μg/L, the low pH condition, ZOP(20)/pH7.4/DIC(3), had higher average lead concentration than the corresponding water condition with pH 9.2.

All water conditions with ZOP experienced at least one event where lead concentration in bulk water exceeded 1000 μg/L. The highest measured lead concentration in bulk water with ZOP addition was 5892 μg/L in water condition ZOP(20)/pH9.2/DIC(3)/Cl_2 and was more than 3000 μg/L less than the maximum lead concentration observed without corrosion inhibitor. Overall, the addition of ZOP reduced outlier lead release events compared to no corrosion inhibitor at 3 mg/L DIC, though no water condition succeeded in reducing lead release to below the Health Canada guideline of 10 μg/L during the acclimation stage.

4.5.3 Orthophosphate Corrosion Inhibitor

OP corrosion inhibitor was dosed at either 10 or 20 mg PO_4/L and DIC was either 7 or 17 mg $CaCO_3$/L. The lowest average lead concentration during acclimation was observed in pH 9.2 and high DIC water condition, OP(10)/pH9.2/DIC(17). The highest lead concentration event occurred in the corresponding water condition but with lower DIC, OP(10)/pH9.2/DIC(7), and was 13,200 μg/L. This was the highest lead concentration observed in any water type during the acclimation phase. All but two water conditions with OP observed at least one lead release event above 1000 μg/L during the acclimation stage; Lead concentration in water conditions OP(20)/pH8.3/DIC(17) and OP(20)/pH9.2/DIC(17) never exceeded 530 μg/L during the acclimation phase. Overall, all water conditions at lower DIC (3 or 7 mg/L) with corrosion inhibitor addition (either

ZOP or OP) observed at least one event with lead concentration at least 1000 μg/L, whereas only water conditions with high DIC and high initial pH and corrosion inhibitor never exceeded 530 μg/L. Therefore, the addition of corrosion inhibitor in high DIC(17) and high pH (either 8.3 or 9.2) was the most effective strategy to reduce outlier lead events, though no water conditions reduced lead release to below the health Canada guideline.

4.6   Effect of Stagnation Time on Lead Concentration During Steady State

ANOVA tests with Tukey's Statistical Method were performed to identify if average lead concentration in bulk water significantly increased with longer stagnation time during the steady state phase. In general, average lead concentration increased with longer stagnation time, however in most cases, lead concentration was not significantly different between stagnation times.

Average lead release was not significantly different between 1- and 2-day stagnation time in any water condition, and average lead released was higher after 4-day stagnation time only in water conditions without corrosion inhibitor at 3 mg/L DIC. In contrast, mean lead concentrations in bulk water conditions without corrosion inhibitor and medium (7 mg $CaCO_3$/L) and high (17 mg $CaCO_3$/L) DIC were not statistically different after 1, 2, and 4-day stagnation time (α=0.05). As well, the addition of both corrosion inhibitors resulted in insignificant differences in lead release with longer stagnation times at all DIC levels. Therefore, increasing DIC without corrosion inhibitor as well as dosing both ZOP and OP addition had beneficial impacts on mitigating lead release as stagnation time increased.

4.7   The Effect of pH, Cl_2, and ZOP on Lead Release at Low DIC (3 mg $CaCO_3$/L)

The current section describes the results from the factorial design described in Table 3.2: initial pH either 7.4 or 9.2, ZOP dose either 0 or 20 mg PO_4/L, and Cl_2 dose of either 0 or 1 mg/L. All water conditions had DIC less than 3 mg $CaCO_3$/L. Average lead release according to water condition and stagnation time is shown in Figure 4.3. As mentioned in Section 4.6, lead release significantly increased after 4-day stagnation for some water types, therefore factorial analysis was conducted for each stagnation time independently, though results were similar between 1- and 2-day stagnation times. Average lead and copper release data can be found in Table A-2 of Appendix A.
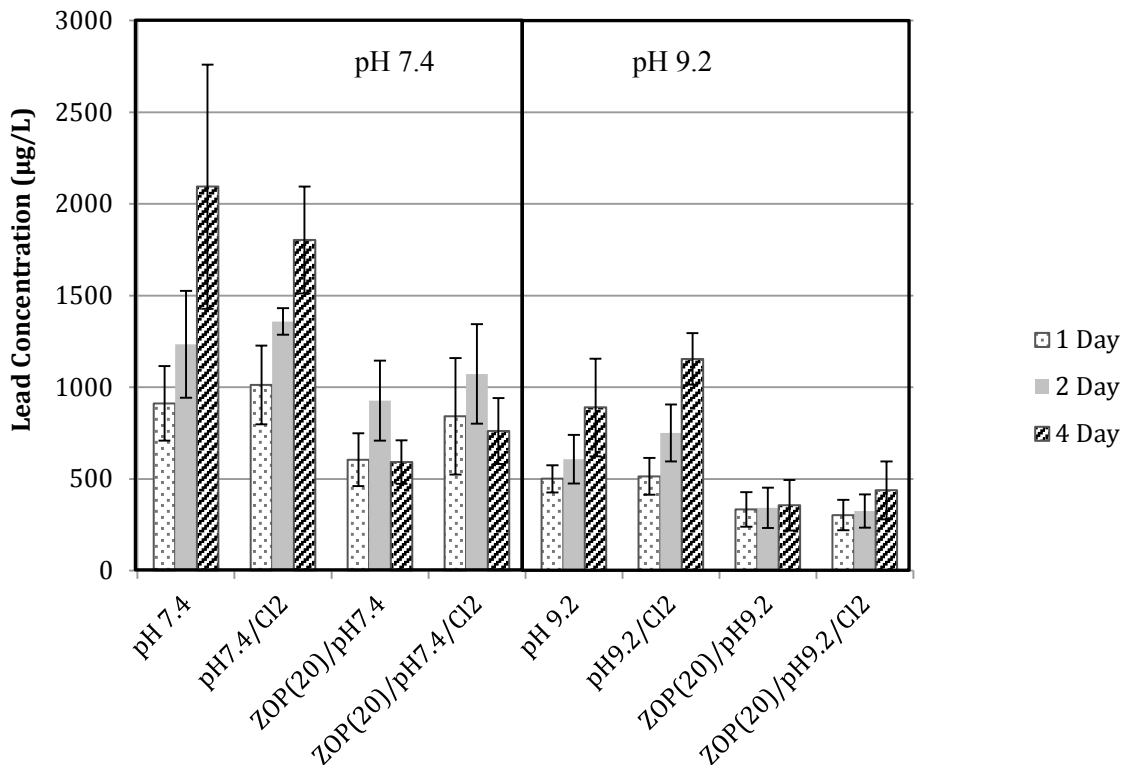
Figure 4.3 – Steady state average lead release in bulk water by stagnation time for all water conditions in with DIC(3). Average lead release decreases when pH is increased from 7.4 to 9.2 and with the addition of ZOP at both pH values. Error bars represent 95% confidence intervals.

4.7.1 Lead Release After 1- and 2-Day Stagnation

In general, low pH without corrosion inhibitor resulted in the highest average lead release. After 1- and 2-day stagnation, water condition pH7.4/DIC(3)/Cl$_2$ had the highest average lead concentration (1359 μg/L) whereas water condition ZOP(20)/pH9.2/DIC(3)/Cl$_2$ generated the lowest average lead concentration (325 μg/L) (Figure 4.3). Note that lead release was not significantly different between water conditions ZOP(20)/pH9.2/DIC(3) with and without Cl$_2$.

At both pH conditions, addition of ZOP reduced lead release. ZOP at pH 9.2 performed better than ZOP at pH 7.4: The two ZOP(20)/pH9.2/DIC(3) water conditions with and without chlorine resulted in statistically less average lead release than any of the pH 7.4 conditions (with and without ZOP). In addition, ZOP(20) at pH 7.4 performed similarly to water conditions without ZOP at pH 9.2.

Factorial analysis revealed that after 1- and 2-day stagnation times, lead release was significantly impacted by initial pH and ZOP dose but was not impacted by chlorine dose. Despite up to 5 μA increase in fill current with chlorine addition, factorial analysis showed that increases of 3 to 5 μA in current due to chlorine addition did not impact lead release in these water conditions. Increasing pH and ZOP from their low to high levels reduced lead concentration in bulk water (Figure 4.4(a)). Increasing initial pH from 7.4 to 9.2 mitigated more lead release than increasing ZOP from 0 to 20 mg PO$_4$/L. After 1-day stagnation, average lead reductions of 428.5 (p=0.001) and 211.5 μg/L (p=0) were observed when pH and ZOP dose were increased from the low to high levels, respectively. After 2-day stagnation, higher average reductions of 635 and 318 μg/L (both p=0) for pH and ZOP, respectively, were observed.
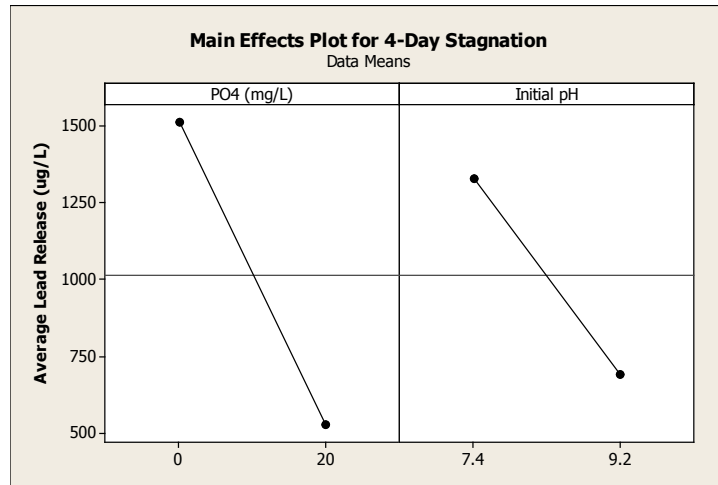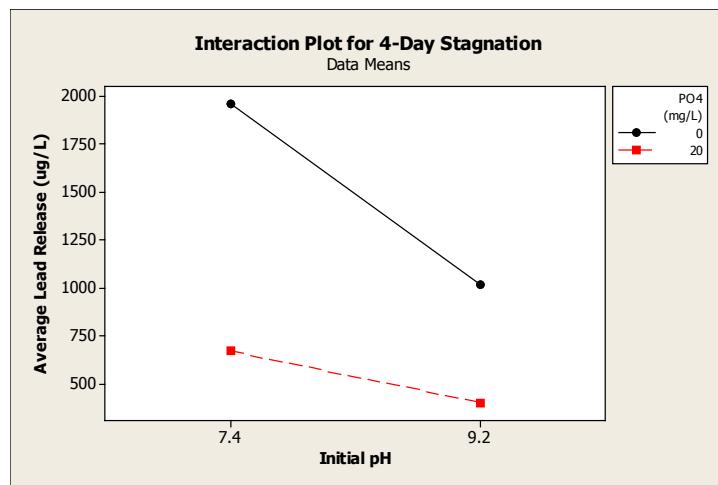
Figure 4.4 – A) ZOP and pH main effects plot for 4-Day stagnation data. Increasing PO_4 and initial pH from the low- to high-level results in less average lead release. B) Plot of interaction between ZOP and pH where effect of one variable is dependent on the level of the other variable.

4-Day Stagnation. After 4-day stagnation, ZOP dose (p=0), pH (p=0), and the interaction between ZOP dose and pH (p=0.004) significantly impacted lead release. Contrary to shorter stagnation times, ZOP had the greatest impact on lead release after 4-day stagnation, and dosing ZOP(20) resulted in an average reduction of 952 μg/L, compared to an average reduction of 605 μg/L when initial pH was increased from 7.4 to 9.2. ZOP rather than pH likely achieved better lead mitigation after 4-day stagnation beacuase of the natural decrease in pH with increased stagnation time. This will be discussed in the following section.

Increasing pH from 7.4 to 9.2 and increasing ZOP dose from 0 to 20 mg PO_4/L both reduced lead concentration, however a significant interaction between parameters means that the effect of ZOP on lead release depended on the initial pH and vice versa. This relationship is shown in Figure 4.4 (a) and (b). The addition of ZOP at pH 7.4 decreased average lead concentration from 2094 to 592 μg/L whereas the addition of ZOP at pH 9.2 only decreased average lead release from 890 to 356 μg/L. Lead concentration was reduced by 1204 and 178 μg/L at pH 7.4 and 9.2, respectively. This indicates that ZOP mitigates more lead at pH 7.4 compared to pH 9.2. This interaction between ZOP dose and initial pH also occurred after 1- and 2-day stagnation times, though the interaction was not significant. This is consistent with other studies that have found ZOP is most effective in the pH range 7.4-7.8 (Hill and Gianni, 2011). The same authors also do not suggest dosing ZOP when pH is greater than 8 because zinc can prematurely precipitate, though this was not observed in the current study. Despite ZOP being more effective at mitigating lead release at pH 7.4, overall, the water condition with ZOP at high pH, ZOP(20)/pH9.2/DIC(3), released the least amount of lead compared to the other water conditions in this factorial design.

In summary, after all stagnation times, increasing pH from 7.4 to 9.2 when ZOP was dosed reduced lead release into bulk water. Though increasing pH decreased the effectiveness of ZOP, increasing pH had a greater impact on lead mitigation and the benefits of increasing pH from 7.4 to 9.2 outweighed the decreased effectiveness of ZOP at higher pH.

4.7.2 Effect of High pH on Disinfection Potential

As stated in Section 4.7.1, raising pH improved lead mitigation compared to dosing ZOP(20) when DIC was less than 3 mg $CaCO_3$/L. However, raising pH may have other impacts on the distribution system. For example, increasing pH may result in (1) reduced disinfection potential, and (2) an increase in trihalomethane formation (THM) (Liang and Singer, 2003). At higher pH, there is a lower concentration of the strong oxidant, hypochlorous acid (HOCl), at pH 9.2 compared to 7.4. Despite the potential reduction in disinfection power at higher pH, this study did not observe significant differences between heterotrophic plate counts between water conditions at pH 7.4 and pH 9.2 (data not shown). As well, increasing pH from 6 to 8 has shown to increase THM formation but decreased other disinfection by-products, such as trihaloacetic acid formation (Liang and Singer, 2003). Though THM formation potential was not evaluated in this study, it is an important parameter to consider at the pilot- or full-scale if pH is increased for corrosion control.

4.7.3 Decrease in pH with Stagnation Time

A drawback of the current experimental set-up was that the flask-coupon systems were open to the atmosphere. Attempts were made to seal the opening, but an airtight seal was problematic and caused unnecessary coupon aggravation resulting in metals sloughing. However, in an open system, carbon dioxide can partition between the gas and aqueous phases and impact water pH (Sawyer et al., 2003).

When hydroxide is added to water, bicarbonate is converted to carbonate causing carbonic acid to convert to bicarbonate. The net effect is a rise in pH (Equations 11 and 12).

$$HCO_3^- + OH^- \rightarrow CO_3^{2-} \qquad\qquad \text{Equation 11}$$

$$H_2CO_3 + OH^- \longrightarrow HCO_3^- + H_2O \qquad\qquad \text{Equation 12}$$
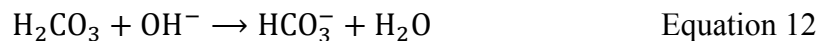
After hydroxide addition, the water becomes deficient in H_2CO_3 and CO_2 is absorbed to reestablish equilibrium with air, and an overall decrease in pH occurs (Equation 13).

$$CO_2 + H_2O \rightarrow H_2CO_3 \rightarrow HCO_3^- + H^+ \qquad \text{Equation 13}$$
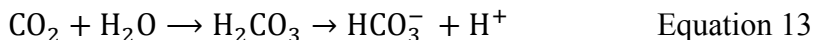
NaOH was added to increase pH to 7.4 and 9.2 (raw water pH < 6), however, pH decreased with stagnation due to the mechanism described in Equations 11-13. A decrease in pH at the anode is expected when lead is released due to galvanic corrosion (Dudi, 2004; Edwards and Triantafyllidou, 2007), however it was confirmed that even without coupons in the water and therefore no lead release, a decrease in pH was still observed in all water conditions. Average bulk water pH and lead concentrations are plotted for each water condition after 1, 2, and 4 day stagnation in Figure 4.5. Despite the largest decreases in pH when initial pH was 9.2, lead release was less than all water conditions with initial pH 7.4 indicating that lead release is not driving pH drop in bulk water.

The largest pH decreases occurred within the first 24 hours. The smallest pH decreases occurred in water types with ZOP; this is likely because phosphate in sufficient concentrations can act as a buffer against pH change (Droste, 1997). Average bulk water alkalinity and DIC is shown for the eight water conditions in Figure 4.6. As expected, alkalinity increased when ZOP(20) was dosed. NaOH addition for pH adjustment also increased alkalinity such that alkalinity between ZOP(20) at pH 7.4 and no corrosion inhibitor at pH 9.2 was not different (average 13.5 mg CaCO3/L). When ZOP(20) was dosed and pH was adjusted to 9.2, the highest alkalinity (21 mg $CaCO_3$/L) was observed.

As shown in Table 4.2, after 1-day stagnation, pH decreased by as much as 0.4 in water conditions with initial pH 7.4 and by as much as 1.8 in initial pH 9.2 water conditions. Despite pH drop, pH of water conditions with initial pH 9.2 remained significantly higher than initial pH 7.4 water conditions after 1- and 2-day stagnation, however final pH is very similar between low- and high-pH conditions after 4-day stagnation, particularly between ZOP(20)/pH7.4 and pH 9.2 conditions. This could explain why ZOP rather than
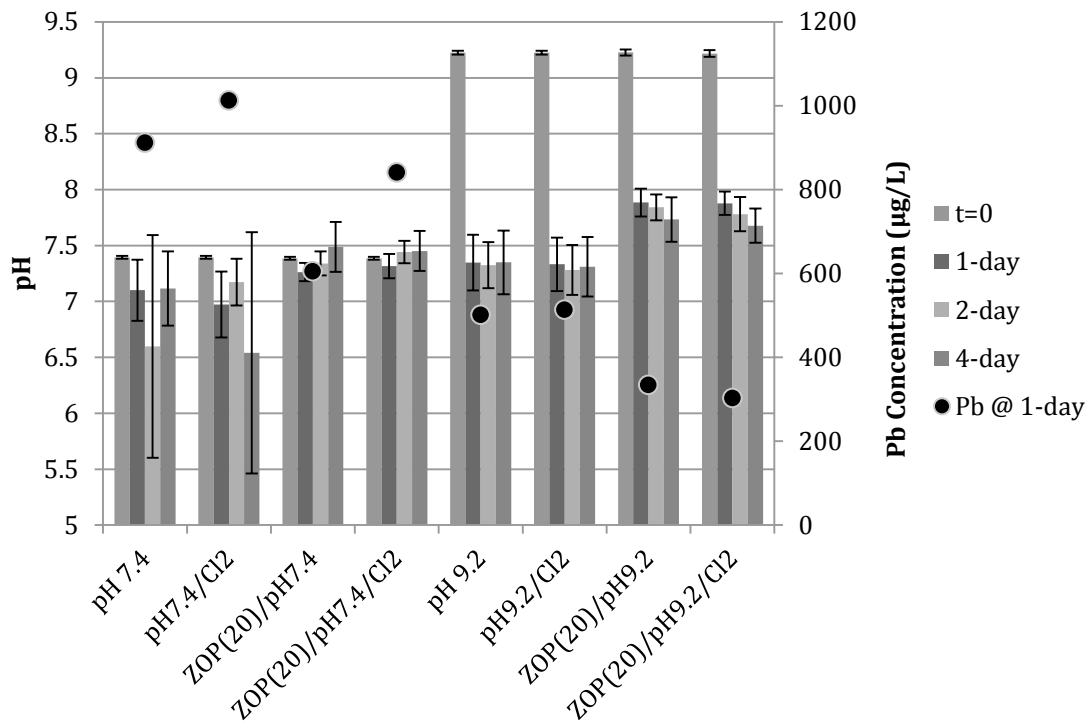
Figure 4.5 – Actual pH decrease after 1, 2, and 4 day stagnation and lead release after 1-day in DIC(3) water conditions. Greater pH decrease occurred in water conditions with low lead release indicating that atmospheric CO_2 rather than lead release is driving pH drop.
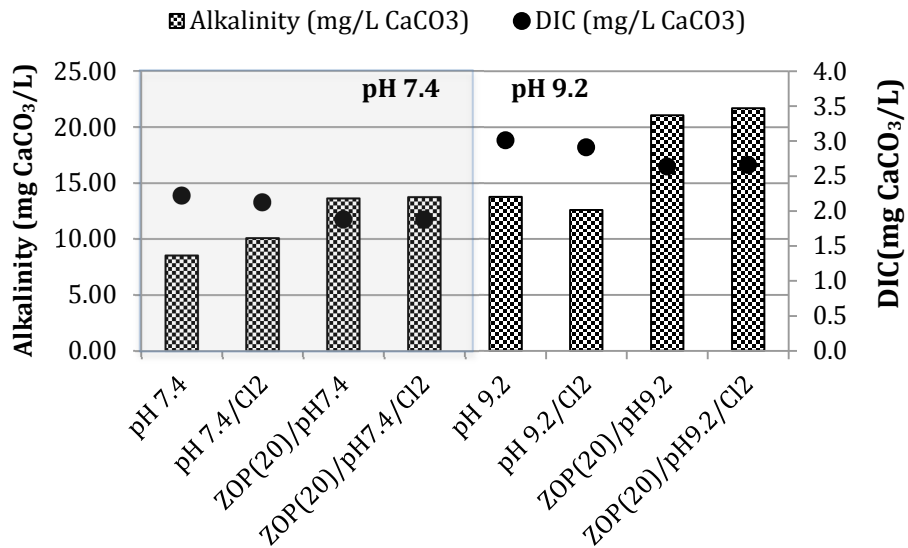
Figure 4.6 – Average alkalinity and DIC of the 8 water conditions. Data based on duplicate samples.

pH had the largest impact on mitigating lead release after 4-day stagnation. Both ZOP(20) and all pH 9.2 conditions had the least amount of pH drop. The consistently higher pH in water conditions with ZOP addition and therefore higher buffering capacity could explain why the water condition $ZOP(20)/pH9.2/\pm Cl_2$ achieved the least amount of lead release after all stagnation times.

Table 4.2 – Decrease in bulk water pH due to atmospheric CO_2 after 1, 2, and 4-day stagnation times. Value after ± represents the range of duplicate data.

		Bulk water pH		
Initial pH	Treatment	1 Day	2 Day	4 Day
7.4	pH 7.4	7.03±0.01	6.98±0	6.78±0
	pH 7.4/Cl_2	7.0±0.02	6.96±0.05	6.9±0.08
	ZOP(20)/pH 7.4	7.15±0.04	7.15±0	7.07±0
	ZOP(20)/pH 7.4/Cl_2	7.07±0	7.15±0	7.05±0.02
9.2	pH 9.2	7.59±0.15	7.38±0.05	7.03±0.01
	pH 9.2/Cl_2	7.37±0.10	7.2±0.04	6.95±0.01
	ZOP(20)/pH 9.2	7.82±0.05	7.81±0.11	7.5±0.01
	ZOP(20)/pH 9.2/Cl_2	7.77±0.05	7.75±0.07	7.41±0.07

4.7.4 Effect of Cl_2 on Lead Release

Chlorine residual was measured in bulk water and was non-detectable after 1-day stagnation. This is typical to what is observed in premise plumbing where long stagnations, higher temperatures, and reactive materials typically result in no chlorine residual in premise plumbing. As previously mentioned, Cl_2 dose did not have a significant effect on lead release and average lead release was either equivalent or greater in water conditions with chlorine compared to the same condition but without chlorine, though this was not significant in any water condition. Though chlorine has been shown to decease corrosion by oxidizing Pb(II) to the less soluble scale Pb(IV) (Switzer et al., 2006), the combination of low dose of 1.0 mg/L Cl_2 with prolonged stagnation time

removing the chlorine residual resulted in insufficient chlorine to oxidize Pb(II) scales and therefore had little impact on lead corrosion in this study. There was insufficient lead scale remaining on the lead electrodes post-experiment to analyze for Pb(II) and Pb(IV) compounds by XRD analysis.

4.8   Effect of pH, Orthophosphate, and DIC on Lead Release During Steady State

The following sections present the results from the factorial design presented in Table 3.3 where pH and OP dose were tested at 3 levels, and DIC concentration was increased from 3 mg $CaCO_3$/L to either 7 or 17 mg $CaCO_3$/L. ANOVA analysis with Tukey's method identified that mean lead concentration was not significantly different after 1-, 2-, and 4-day stagnation times for any water condition (α=0.05). As such, data and factorial analysis was conducted for all stagnation times combined.

4.8.1 Average Lead Release

A graph of average lead release for all 18 water conditions is shown in Figure 4.7. As well, average lead and copper release data can be found in Table A-2 of Appendix A. Average lead release ranged from 24 to 613 μg/L during steady-state. Lowest average lead release was in water conditions OP(20)/pH9.2/DIC(17) and highest was in OP(20)/pH7.4/DIC(7).

Overall, the highest lead concentration events occurred in water conditions dosing 20 mg/L OP as PO_4 apart from water condition OP(20)/pH9.2/DIC(17), whereas the lowest average lead concentrations were observed in water conditions dosing 10 mg/L OP as PO_4 (average lead release less than 87 μg/L). In some cases, average lead release was higher in water conditions with OP(20) addition compared to without corrosion inhibitor, and OP(20) water types exhibited the highest variation in lead concentration compared to other OP doses.
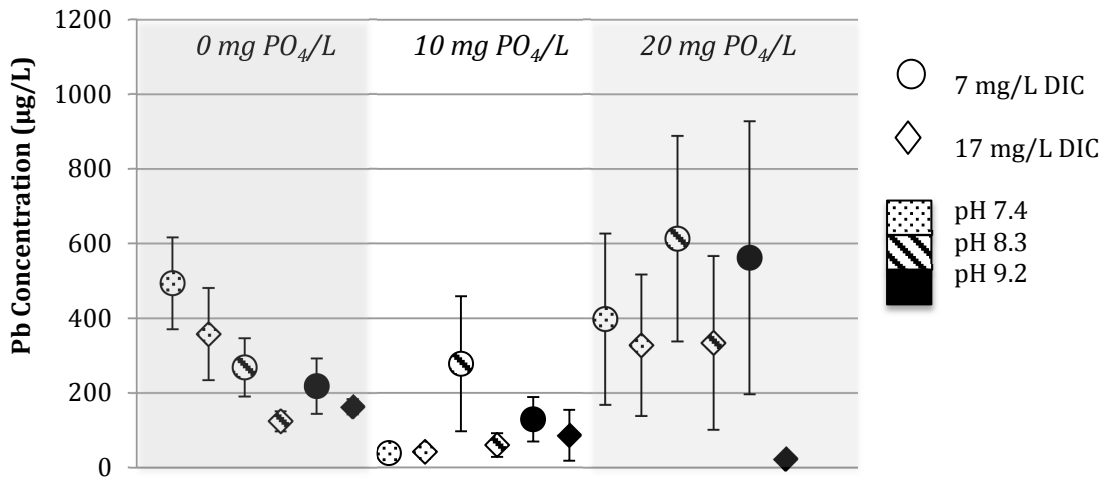
Figure 4.7 – Average lead concentration of 18 water conditions dosing OP at 0, 10, or 20 mg PO$_4$/L. Error bars represent the 95% confidence interval of the mean.
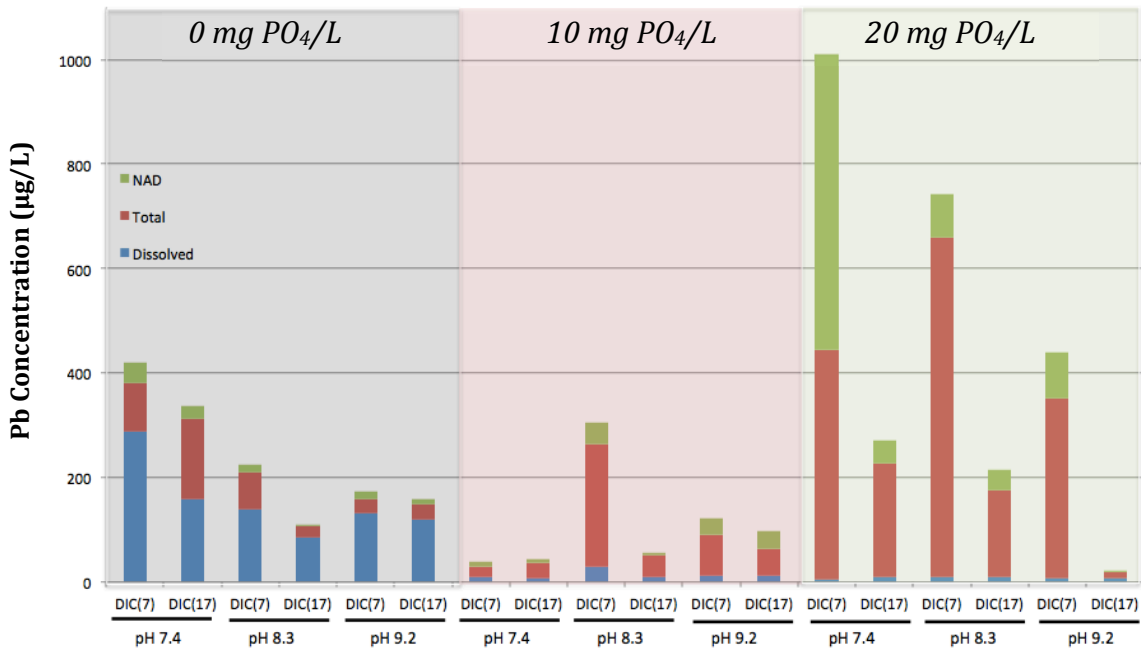
Figure 4.8 – Average dissolved, total, and NAD lead release of the 18 water conditions with OP dose of 0, 10, or 20 mg PO$_4$/L and DIC either 7 or 17 mg CaCO$_3$/L. The concentration of dissolved lead decreases when OP is dosed at either 10 or 20 mg PO$_4$/L.

62

Despite higher lead release in other OP(20) water conditions, lead release after 1, 2, or 4-day stagnation in water condition OP(20)/pH9.2/DIC(17) never exceeded 49 μg/L during steady state and average lead release was the lowest of any water condition (24 μg/L). Also, during the acclimation stage, this water condition OP(20)/pH9.2/DIC(17) never exceeded 530 μg/L. The next lowest average lead concentrations were in the two water conditions OP(10)/pH7.4 at both 7 and 17 mg/L DIC and average lead release was as low as 39 and 43 μg/L. The lowest lead release event occurred in water condition OP(10)/pH7.4/DIC(7) and released 8.8 μg/L lead whereas the highest lead release event occurred in water condition OP(20)/pH7.4/DIC(7) and was 7332 μg/L. Lead release events releasing greater than 1000 μg/L lead occurred in a number of water conditions, though the majority were when OP was dosed at 20 mg PO_4/L: five of the six water conditions dosing 20 mg PO_4/L observed the highest lead concentration events. The effect of high-dose OP will be discussed further in Section 4.13.

4.8.2 Factorial Analysis

Factorial analysis determined that DIC concentration (p=0), OP dose (p=0), and the interaction between these two parameters (p=0.049) had a significant effect on lead release whereas pH did not have a significant effect. In general, increasing DIC from 7 mg/L to 17 mg/L decreased lead concentration in bulk water. Increasing OP concentration from 0 to 10 mg PO_4/L decreased lead concentration, whereas increasing OP from 10 to 20 mg PO_4/L caused average lead concentration to increase. These relationships are shown in Figure 4.9. As well, the magnitude by which lead concentration increases when OP dose is increased to 20 mg/L depends on DIC concentration (as shown in Figure 4.10).

Increasing DIC from 7 to 17 mg $CaCO_3$/L achieved similar lead reductions when OP dose was either 0 or 10 mg PO_4/L: lead concentration was reduced by an average of 120 μg/L when DIC was increased from 7 to 17 mg $CaCO_3$/L. Whereas when OP dose was 20 mg PO_4/L, increasing DIC from 7 to 17 mg $CaCO_3$/L decreased average lead
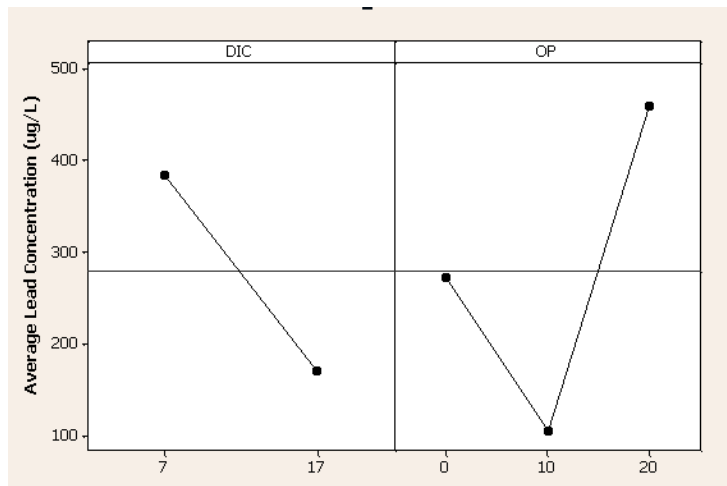
Figure 4.9 – Main effects plot displaying the effect of DIC concentration and OP dose on average lead concentration. As DIC is increased from 7 to 17 mg CaCO$_3$/L, lead release decreases, whereas lead concentration either decreases or increases depending on the OP dose.
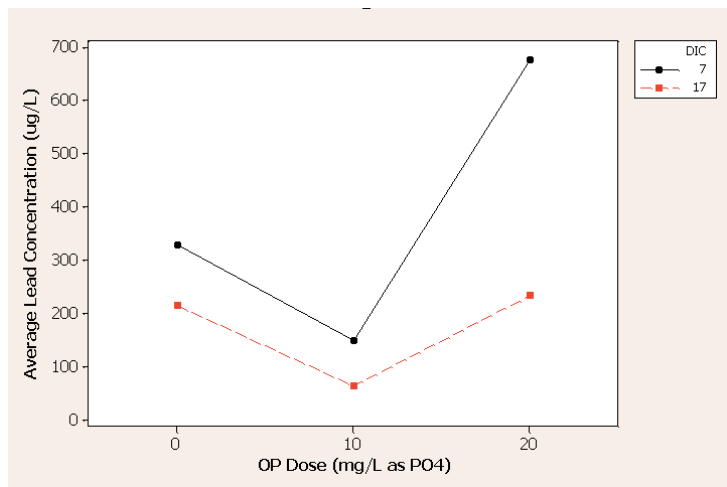
Figure 4.10 – Interaction plot displaying the effects of OP dose on lead concentration at either DIC(7) or DIC(17). Increasing DIC from 7 to 17 mg CaCO$_3$/L mitigated a higher concentration of lead when OP dose was 20 mg/L compared to 0 or 10 mg/L.

concentration by 400 μg/L, indicating that DIC(17) mitigates more lead when OP dose is 20 mg/L compared to 0 or 10 mg/L. For example, only the water condition with OP(20) but high by pH and DIC(17), OP(20)/pH9.2/DIC(17), did not exacerbate lead release compared to no corrosion inhibitor, and achieved the lowest overall average lead concentration. Even during acclimation, lead release never exceeded 530 μg/L suggesting that high DIC and pH is an effective strategy for forming a protective passivation film that protected the lead coupon against exacerbated lead release when OP dose was 20 mg PO_4/L. Though five of the six OP(20) water conditions observed increased lead release compared to OP(10) and most OP(0) conditions, increasing DIC to 17 mg $CaCO_3$/L and increasing pH to 9.2 was the most effective corrosion control strategy to reduce lead release.

4.8.2.1 Effect of OP on Dissolved and Particulate Lead

The dissolved lead, total lead, and NAD lead fractions were measured in bulk water samples. As shown in Figure 4.8, OP dosing had the largest impact on the dissolved lead fraction: the concentration of dissolved lead significantly decreases when OP is dosed at either 10 or 20 mg PO_4/L. When OP was dosed, average dissolved lead was always less than 28 μg/L whereas dissolved lead ranged from 86-287 μg/L when OP was not dosed. Other authors have found that increasing phosphate concentration decreased dissolved lead concentration (Xie and Giammar, 2011). In the current study, average dissolved lead concentration was not different between water conditions with an OP dose of 10 or 20 mg PO_4/L (α=0.05). This suggests that 10 mg PO_4/L is a sufficient OP dose to control dissolved lead in the tested water types.

Doubling OP concentration from 10 to 20 mg PO_4/L maintained equivalent dissolved lead concentrations compared to 10 mg PO_4/L, however, caused particulate lead concentration to significantly increase in 5 of the 6 water conditions. Dosing OP increased particulate lead by 60 to 800 % compared to no corrosion inhibitor. Other studies have also found that dosing OP can increase particulate lead concentration from 10 to 49% of total lead in water (Xie and Giammar, 2011). Significant increases in

65

particulate lead with increased OP dosage can be a significant public health threat: Triantafyllidou et al. (2007) simulated the dissolution of lead particles in the stomach as if they were ingested and found that Pb(IV) particulates dissolved in the simulated stomach dissolution scenario after 3 hours, suggesting a large fraction of particulate lead in drinking water could be bioavailable. The exacerbating effects of high dose OP on particulate lead stresses the importance of accurately measuring the dissolved and particulate portion of lead in drinking water samples.

4.8.3 Effect of pH

In all cases, increasing pH when no corrosion inhibitor was dosed resulted in lead mitigation. When corrosion inhibitors were dosed, however, the effect of pH on lead release depended on the corrosion inhibitor that was dosed. When ZOP(20) was dosed, increasing pH from 7.4 to 9.2 achieved overall the lowest lead concentration, whereas increasing pH with OP addition had a tendency to increase lead release. As shown in Figure 4.7, increasing initial pH from 7.4, to 8.3, and to 9.2 without OP reduces lead release, though lead had a tendency to increase with increasing pH when OP was dosed at 10 and 20 mg PO_4/L. This is consistent with other authors that found that OP film formation on lead is optimized at a pH between 7 and 8 (Schock, 1989).

Similar to the previous factorial design testing ZOP, pH did not remain constant with stagnation time due to the open-air nature of the experimental set-up. Actual average pH in bulk water of six water conditions without corrosion inhibitor after 1, 2, and 4 day stagnation times is shown in Figure 4.11. pH trends in Figure 4.11 are representative of water conditions with OP dosing as well. A combination of sodium bicarbonate, phosphate, and NaOH addition to reach DIC, phosphate, and pH targets resulted in either an overall increase or an overall decrease in pH. pH increased by as much as 0.9 is some cases.

When a water system open to the atmosphere becomes overloaded with bicarbonate with respect to a normal bicarbonate concentration in equilibrium with air, bicarbonate converts to carbonic acid by binding with a proton, and pH will rise as CO_2 is released to

66

the atmosphere. This reaction is shown in Equation 14. The overall effect of bicarbonate addition is a rise in alkalinity and a rise in pH.

$$HCO_3^- + H^+ \rightleftharpoons H_2CO_3 \rightleftharpoons CO_2 + H_2O \qquad \text{Equation 14}$$
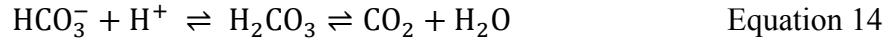
In general, bicarbonate addition initially decreased pH after 1 day stagnation but then increased pH with longer stagnation times. As the system strived to achieve a new equilibrium post bicarbonate addition, pH as well as DIC concentration was slightly changed. However, the low- and high-DIC levels remained significantly different despite DIC changes with stagnation: DIC(7) water conditions never exceeded 8.4 mg CaCO$_3$L and DIC was never below 13.9 mg CaCO$_3$/L in DIC(17) water conditions. It is theorized that the addition of bicarbonate and its effect on increasing pH with exposure to the atmosphere is likely why pH was not found to be significant in these experiments.
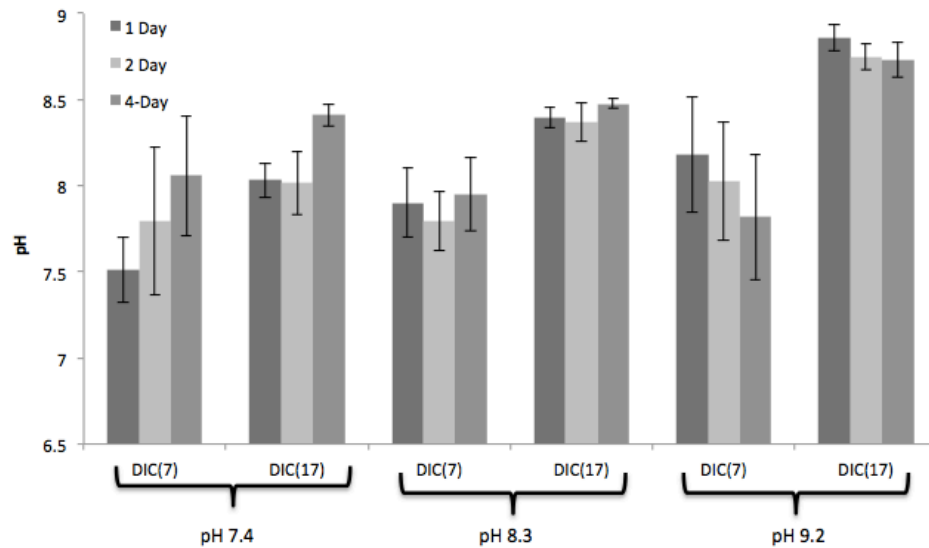
Figure 4.11 – pH after 1-, 2-, and 4-day stagnation times in water conditions without OP dosing, and representative of pH changes in water conditions at both OP doses. pH either increased or decreased with stagnation time depending on bicarbonate addition.

4.9   Effect of DIC on Lead Release Without Corrosion Inhibitor

Average DIC ranged from 2.2 to 20.1 in water conditions without corrosion inhibitor. A graph of average lead release and corresponding influent DIC concentration for the 8 water conditions tested without corrosion inhibitor is shown in Figure 4.12. Average lead release was greatest in pH 7.4 and DIC of 2.1 mg $CaCO_3$/L and was significantly higher than all other water conditions without corrosion inhibitor ($\alpha=0.05$). However, when water DIC remained low (2.7 mg/L) but initial pH was increased to 9.2, lead release was significantly higher than the three water conditions at DIC above 17 mg/L but was not different than water conditions with DIC ranging between 6.8-7.2 mg/L. The highest lead concentration events occurred in low DIC (<3 mg $CaCO_3$/L) water conditions whereas maximum lead release events were much smaller when DIC was high (>17 mg/L). Overall, a significant difference in lead release was observed between water conditions with DIC(3) compared to DIC(7) or DIC(17), whereas lead release was not significantly different between water conditions with DIC 7 and 17 mg/L. When no corrosion inhibitor is dosed, calcium carbonate precipitation on metals governs corrosion control. Increasing pH from 7.2 to pH 9.2 at DIC(3) also had a significant impact on decreasing lead release but at higher DIC concentrations, increasing pH did not have as large an effect on mitigating lead release. Therefore, increasing pH when alkalinity is below 3 mg/L has a greater impact on lead reduction than increasing pH when alkalinity is higher.

The results of this study demonstrate the potential for pH-alkalinity adjustment as a method of corrosion control, though no pH-alkalinity treatment achieved lower lead release in bulk water than water conditions with corrosion inhibitor. The lowest average lead release obtained with pH-alkalinity adjustment was 75 µg/L in water conditions pH8.3/DIC(17) (Table A.2). In contrast, recent studies have found that increasing alkalinity without corrosion inhibitor can exacerbate lead release. Tam and Elefsiniotis (2009) measured lead release from brass fittings and found that at pH 7 or 7.5, increasing alkalinity from 20 to greater than 100 mg $CaCO_3$/L resulted in a substantial increase in lead release. Detrimental impacts on lead release were also observed at much lower alkalinity: Nguyen et al. (2011a) found that increasing alkalinity from 8 to 20 mg $CaCO_3$/L increased lead release from galvanic solder by six times in low conductivity

water (CSMR=4) without corrosion inhibitor. It is suggested that the addition of bicarbonate alkalinity increased water conductivity that overpowered the benefits of carbonate alkalinity in passivation film formation. In this study, dosing bicarbonate to increase alkalinity from less than 3 to either 7 or 17 mg $CaCO_3$/L did not exacerbate lead release. This discussion highlights the importance of utility-specific studies, as corrosion control techniques can have different outcomes on lead release depending on source water.

4.10   Comparing High-Dose Corrosion Inhibitors ZOP and OP

Average lead release and the corresponding influent DIC concentration for all water types with corrosion inhibitor is shown in Figure 4.13. ZOP was tested at a dose of 20 mg PO_4/L whereas OP was dosed at either 10 or 20 mg PO_4/L. Lead release in water conditions dosing ZOP with and without chlorine were not significantly different, therefore only the two water conditions without chlorine addition were included in this analysis. As well, data from all stagnation times is averaged since it was previously shown that lead release was not different with longer stagnation time when ZOP and OP were dosed.

The highest average lead concentration was observed in the two water conditions dosing ZOP(20) and low DIC(3). ZOP(20)/pH7.4/DIC(3) released significantly higher lead than any water condition dosing corrosion inhibitor (α=0.05) whereas in the same water condition but initial water pH 9.2, average lead release was not different than two water conditions dosing OP at 20 mg PO_4/L. ZOP(20) and OP(20) water conditions had wider confidence intervals for the mean than OP(10) conditions. Overall, OP dose of 10 mg PO_4/L and DIC of 17 mg $CaCO_3$/L at all initial pH conditions performed better than all other corrosion inhibitor conditions other than OP(20)/pH9.2/DIC(17).
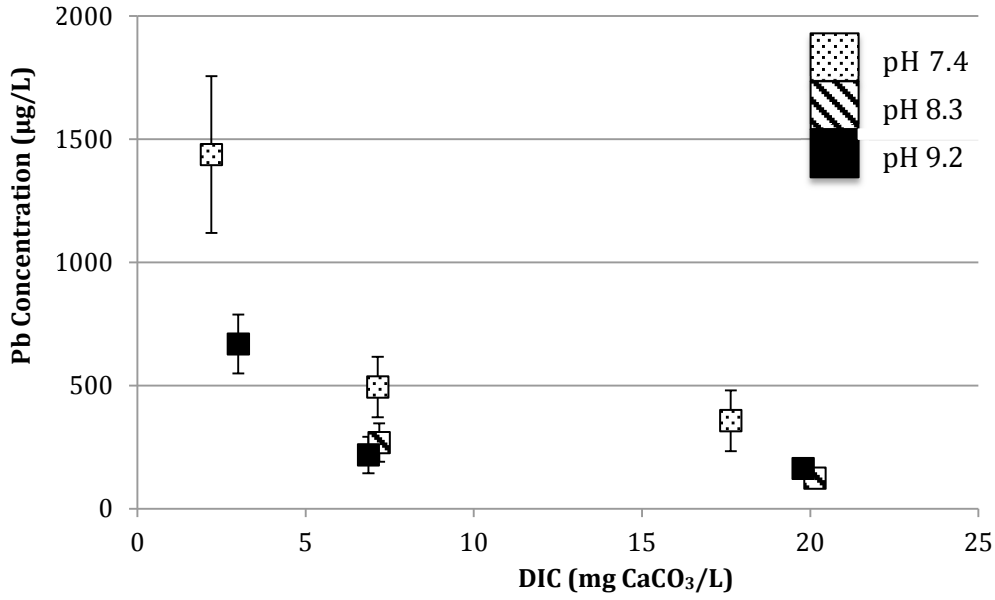
Figure 4.12 – Average steady state lead release versus influent DIC concentration of the eight water conditions without corrosion inhibitor. Lead concentration decreases as DIC and pH increase. Error bars represent the 95% confidence interval of the mean.
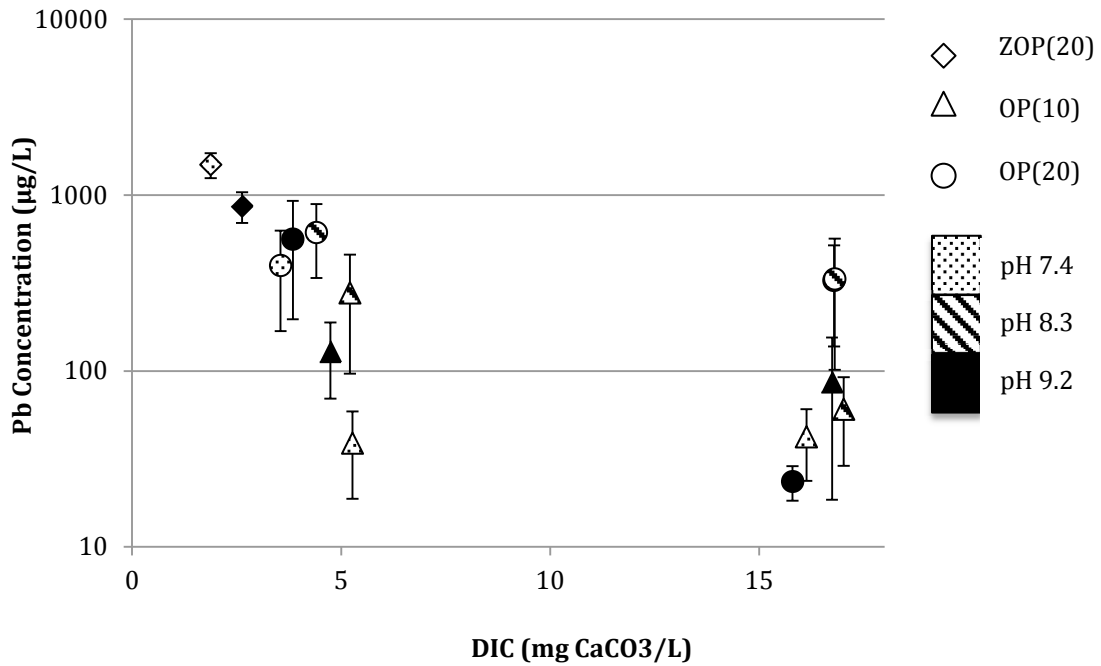
Figure 4.13 – Average steady state lead release in the 14 water conditions dosing corrosion inhibitor, either ZOP dose of 20 mg PO_4/L or OP dose of 10 or 20 mg PO_4/L. Error bars represent the 95% confidence interval of the mean.

Though ZOP corrosion inhibitor resulted in the highest lead concentrations compared to both OP doses, DIC was not consistent between corrosion inhibitor trials. Therefore, a lead concentration factor (CF_{Pb}) was calculated to compare lead mitigation with corrosion inhibitor compared to its corresponding water condition without corrosion inhibitor (CF_{Pb}=Pb concentration with corrosion inhibitor divided by Pb concentration without corrosion inhibitor). A CF_{Pb} less than 1 indicates lead was mitigated compared to no corrosion inhibitor at the same pH and DIC.

Table 4.3 – Concentration factors of all water conditions dosing corrosion inhibitors

Water Condition	CF_{Pb}
ZOP(20)/pH7.4	1.1±0.15
ZOP(20)/pH9.2	1.3±0.2
OP(10)/pH7.4/DIC(7)	0.1±0.05
OP(10)/pH8.3/DIC(7)	1.2±0.6
OP(10)/pH9.2/DIC(7)	0.7±0.4
OP(10)/pH7.4/DIC(17)	0.2±0.1
OP(10)/pH8.3/DIC(17)	0.7±0.6
OP(10)/pH9.2/DIC(17)	0.5±0.4
OP(20)/pH7.4/DIC(7)	1.0±0.6
OP(20)/pH8.3/DIC(7)	2.8±1
OP(20)/pH9.2/DIC(7)	2.7±1.6
OP(20)/pH7.4/DIC(17)	0.9±0.5
OP(20)/pH8.3/DIC(17)	3.2±2.0
OP(20)/pH9.2/DIC(17)	0.15±0.05

Average CF_{Pb} are shown in Table 4.3. Average CF_{Pb} were all below 1 when OP was dosed at 10 mg PO_4/L except for 1 water condition when pH was 7.4: OP(10)/pH7.4/DIC(17). In comparison, average CF_{Pb} when ZOP was dosed was 1.1 and 1.3 for pH 7.4 and 9.2, respectively. Three of the six water conditions with OP dosed at 20 mg PO_4/L increased lead release by a factor of 2.8 to 3.2 compared to the comparable

water type without OP. Therefore, despite overall less lead release by OP(20) compared to ZOP(20), compared to their respective water condition without corrosion inhibitor, the consequences of high dose OP on lead release is greater than for ZOP.

4.10.1 Relationship Between Current and Lead Concentration

For every pair of electrons removed from lead by galvanic current, one lead molecule can be corroded and potentially released to water. Other authors have predicted lead released by galvanic action using Equation 15 below (Dudi, 2004):

$$Maximum\ Lead\ Leaching\ (g) = \frac{I\left(\frac{Coulomb}{sec}\right) \times T(sec) \times 207.2\left(\frac{g\ of\ Pb}{mole\ of\ Pb}\right)}{1.6\times10^{-19}\left(\frac{Coulomb}{e}\right) \times 6.023\times10^{23}\times\left(\frac{Pb}{mole\ of\ Pb}\right) \times 2\left(\frac{e}{Pb}\right)} \quad \text{Equation 15}$$

Actual lead leached was calculated as a concentration, in µg/L. To calculate mass of lead leached, the lead concentration in bulk water was multiplied by 190 mL, the volume of water in each flask.

Maximum predicted lead leaching (based on measured current) versus actual lead concentrations in bulk water were plotted and two plots from representative water conditions are shown in Figure 4.14. All water conditions had significantly higher predicted lead than actual lead release (p<0.008). Maximum predicted lead overestimated actual lead release by as little as 578 µg and as much as 2129 µg (α=0.05). Other researchers have found similar trends: Dudi (2004) found that lead leaching was equal to or less than predicted lead when brass devices were connected to copper piping.

The presence of passivation scales could be responsible for the discrepancy between predicted and observed lead release. The galvanic current measurement is indicative of electrons flowing from the lead to the copper coupon, but since lead concentration in water is less than expected, lead molecules that are corroded must be retained on the surface of the electrode and not released to the bulk water. Nguyen et al. (2010) found lead release to water was four times less than the predicted value, and the majority of

'missing' lead was contained in the anodic scale or elsewhere in the apparatus (determined by mass balance). As well, galvanic current is used to measure corrosion from a galvanic connection only, whereas normal lead dissolution and deposition corrosion are not accounted for. As such, galvanic current is a direct measure of lead oxidation but not necessarily of lead release. Oxidized lead can remain on the lead coupon as a deposit or part of a corrosion film and does not necessarily release into bulk water. This study along with others, demonstrates that galvanic current measurements do not act as an accurate predictor of lead concentration in water. From a practical standpoint, relying on galvanic current between lead and copper materials may grossly overestimate the lead released to water.
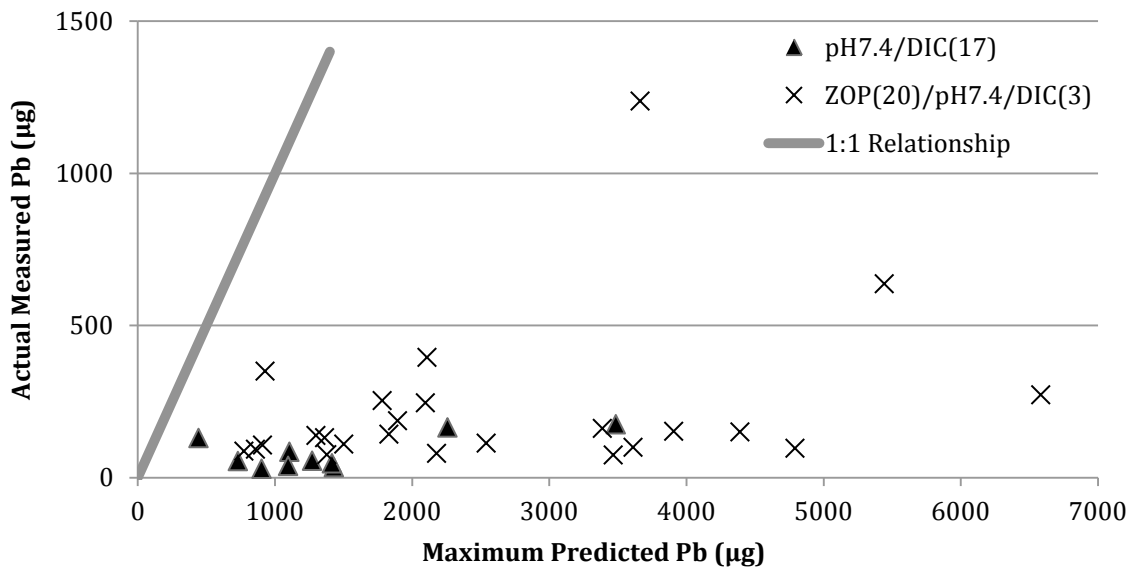
Figure 4.14 – Relationship between predicted lead release (calculated using initial current) versus actual lead release for two water conditions. Predicted lead was always higher than measured lead in bulk water.

73

4.11   Copper Release

4.11.1 Copper Release during Acclimation

Unlike lead release, there were no spikes in copper release during the acclimation phase. In fact, average copper concentration was often higher during steady state than during the acclimation phase. When DIC was 3 mg $CaCO_3$/L, either without corrosion inhibitor or with addition of ZOP(20), average copper release was less during the steady state phase than during acclimation phase in all cases. When DIC was 7 or 17 mg/L (either without corrosion inhibitor or OP), all but 3 water conditions exhibited higher copper release during steady state than during acclimation. Copper concentration was between 1.1 and 3.1 times greater during steady state than acclimation in these water types.

The highest concentration of copper in bulk water during acclimation was 316 μg/L in water condition OP(10)/pH7.4/DIC(7) and the lowest was 2 μg/L in water condition ZOP(20)/pH9.2/DIC(3). Average copper concentration during acclimation was typically within the range of 11-45 μg/L, but average concentration in water condition OP(10)/pH7.4/DIC(17) was 73 μg/L and was significantly higher than all other water conditions during acclimation except for pH7.4/DIC(3)/Cl_2.

4.11.2 Effect of pH, ZOP, and Cl_2 on Copper Release

A graph of copper concentration in bulk water as a function of stagnation time and the 8 water conditions during steady state is shown in Figure 4.15 and average copper release after 1, 2, and 4 day stagnation is shown in Table A.2 of Appendix A. No copper release event exceeded the copper aesthetic objective of 1 mg/L (Health Canada, 2012). Average copper concentrations without corrosion inhibitor were in the range of 11-19 μg/L whereas average copper concentrations in water conditions with ZOP(20) were in the range of 2.8 to 4.8 μg/L. The maximum observed copper concentration was 30 μg/L and occurred after 2-day stagnation in a water condition without ZOP. When ZOP was dosed, no bulk water concentration exceeded 9 μg/L at any stagnation time. Water condition ZOP(20)/pH9.2/Cl_2 released the least amount of copper and released less than 3 μg/L

after all three stagnation times. This was also the water condition that released the lowest average lead release.

In 6 of the 8 water types, average copper concentration was not different as stagnation time increased ($\alpha=0.05$). In water type pH9.2/DIC(3), mean concentration after 1-day stagnation was significantly less than after 2- and 4-days, and in water type pH9.2/DIC(3)/Cl$_2$, mean copper concentration after 2-days was significantly higher than after 1- and 4-days, though 1- and 4-day were not different from one another. Since only 1 stagnation time was different than the other 2 stagnation times in both of these water types, factorial analysis was conducted with all three stagnation times combined.
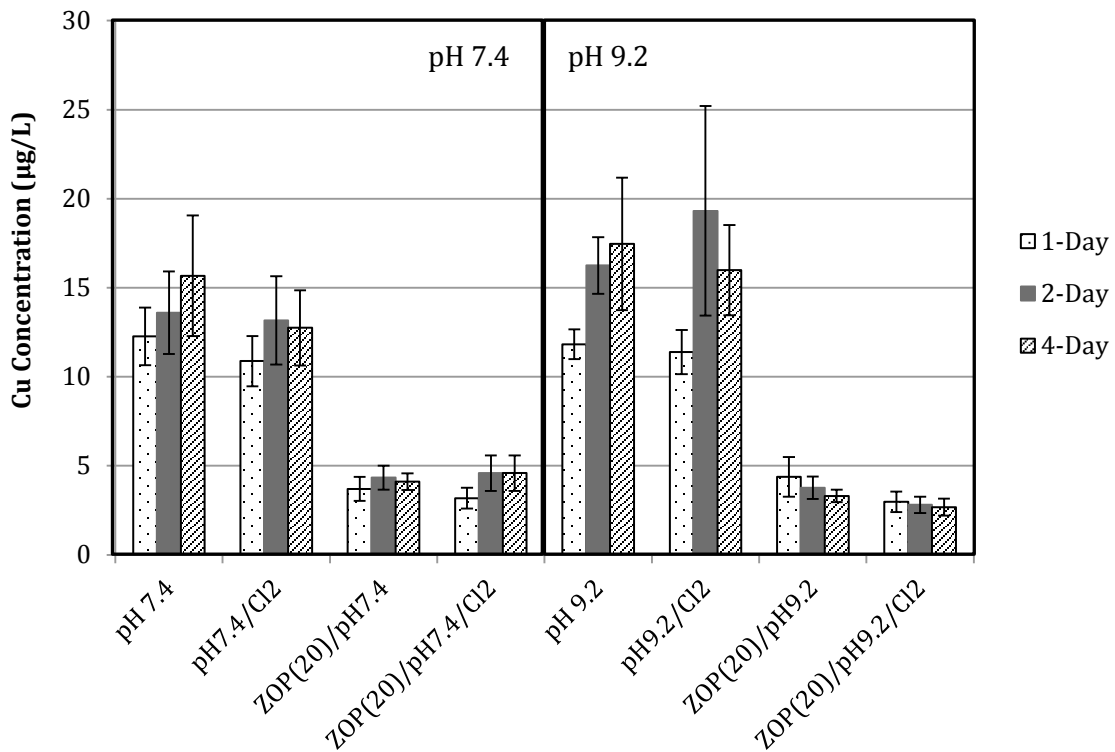
Figure 4.15 – Average copper in bulk water after 1-, 2-, and 4-day stagnation times in low alkalinity water with or without ZOP addition. Error bars represent the 95% confidence interval of the mean. ZOP addition reduced copper concentration in bulk water to below 5 μg/L at both pH conditions.

Factorial analysis identified that only ZOP dose had a significant impact on copper concentration in bulk water and pH and chlorine did not significantly impact copper concentration. Increasing ZOP from 0 to 20 mg PO_4/L decreased average copper concentration by 10.6 µg/L (p=0). Mean copper concentration was not different between all conditions dosing ZOP, and similarly, copper concentration was not different between all conditions not dosing ZOP after 1- and 4-day stagnation times. As well, ZOP was equally as effective at reducing copper release at pH 7.4 and 9.2, unlike the significant interaction effect between ZOP and pH whereby ZOP was more effective at mitigating lead release when pH was 7.4 compared to 9.2

4.11.3 Effect of pH, OP, and DIC on Copper Release

4.11.3.1 Average Copper Release

Average copper concentration for all water conditions is shown in Figure 4.16 and average copper release after 1, 2, and 4 day stagnation is shown in Table A.2 of Appendix A. Average copper concentration ranged from 22 to 56 µg/L during steady state and was well below the aesthetic objective of 1 mg/L (Health Canada, 2012) in all water conditions. Average copper release in water conditions with or without OP at DIC(7) or DIC(17) was always above 20 µg/L. In comparison, in water conditions with DIC(3) with or without ZOP, average copper release never exceeded 20 µg/L.

The majority of copper release was in the dissolved form: dissolved copper comprised 58 to 87% of copper in bulk water. The lowest copper release event during steady state was 11.3 µg/L, in a water condition dosing OP(20). The maximum copper concentration event was 202.3 µg/L in water condition pH7.4/DIC(7) and three other water conditions, either with or without OP(20), had copper concentration events in the range of 100-200 µg/L. The three lowest average copper concentration was in water conditions pH8.3/DIC(7), OP(20)/pH8.3/DIC(7), and OP(20)/pH9.2/DIC(17) (averages between 22 and 27 µg/L) and were the only three water conditions with average copper release significantly lower

than the two water conditions that released the highest copper concentrations, OP(10)/pH8.3/DIC(17) and pH9.2/DIC(17) with average copper between 53 and 56 µg/L.
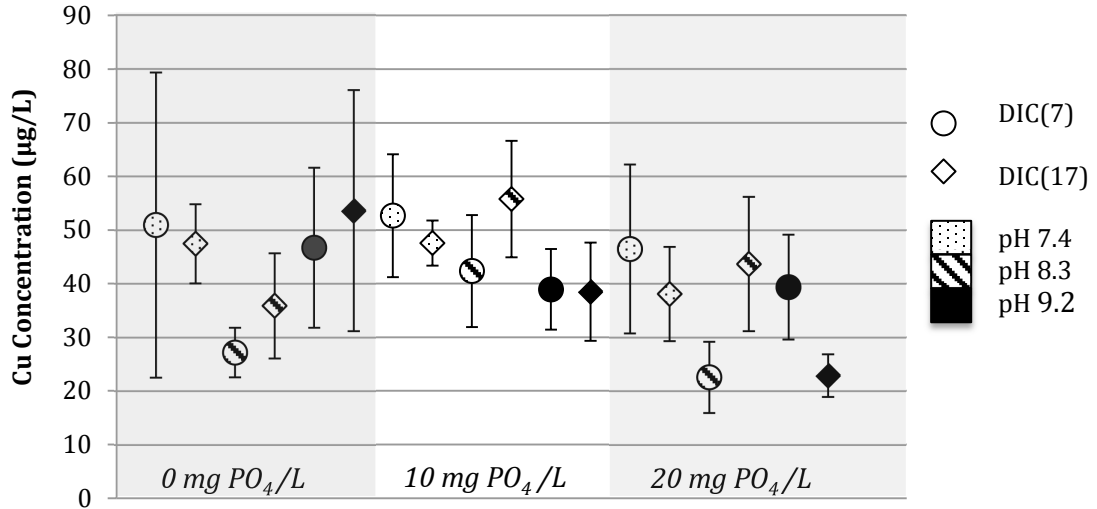
Figure 4.16 – Average copper concentration in 18 water conditions with OP dose of 0, 10 or 20 mg PO₄/L. Error bars represent the 95% confidence interval of the mean.

4.11.3.2 Factorial Analysis

Copper concentration in bulk water was not statistically different after 1, 2, or 4 day stagnation in all water conditions except for one water condition: In water condition OP(10)/pH9.2/DIC(7), mean copper concentration after 4-day stagnation was greater than mean copper concentration after 1-day stagnation ($\alpha=0.05$). Therefore, factorial analysis was conducted by combining all data from the three stagnation times. Initial pH (p=0.009), orthophosphate dose (p=0.003), and the interaction between pH and orthophosphate dose (p=0.004) had a significant effect on copper concentration.

The effect of increasing pH and OP dose on copper concentration was dependent on the level of the alternate parameter. As shown in Figure 4.17, at both initial pH 7.4 and 8.3, increasing OP dose from 0 to 10 mg PO₄/L resulted in an increase in average copper

concentration, but increasing OP dose to 20 mg PO_4/L decreased average copper concentration. When initial pH was 9.2, however, increasing OP dose always decreased average copper concentration.
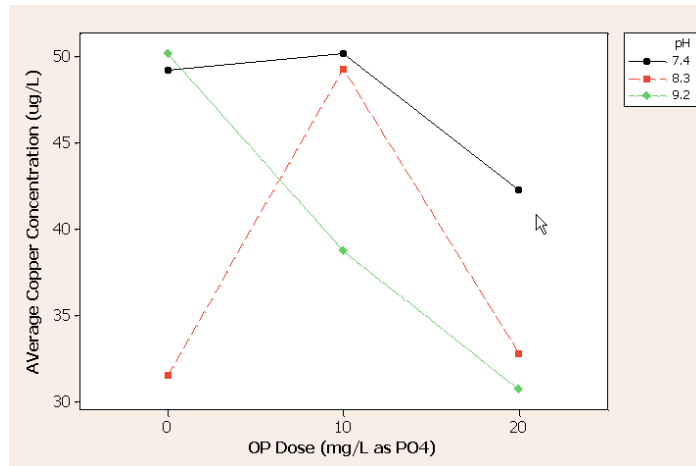
Figure 4.17 – Interaction plot demonstrating the effects of pH and OP dose on copper concentration. At pH 7.4 and 8.3, increasing OP dose from 0 to 10 to 20 mg PO_4/L increases and then decreases copper concentration, respectively. When pH is 9.2, increasing OP dose always decreases copper concentration.

4.11.4 Relationship Between Lead and Copper Release

The impacts of corrosion inhibitor dose on lead and copper release was different between OP and ZOP.

Figure 4.18 shows the effect of ZOP dose on lead and copper release. When ZOP dose was increased from 0 to 20 mg PO_4/L, both lead and copper concentrations decreased. The relationship between lead and copper and OP dose is shown in Figure 4.19. Figure 4.19 shows that when OP dose was increased from 0 to 10 mg PO_4/L lead release decreased, whereas increasing the dose from 10 to 20 mg PO_4/L increased lead release. The opposite relationship existed for copper release: increasing OP dose from 0 to 10 mg PO_4/L increased copper release whereas increasing the dose from 10 to 20 mg PO_4/L.
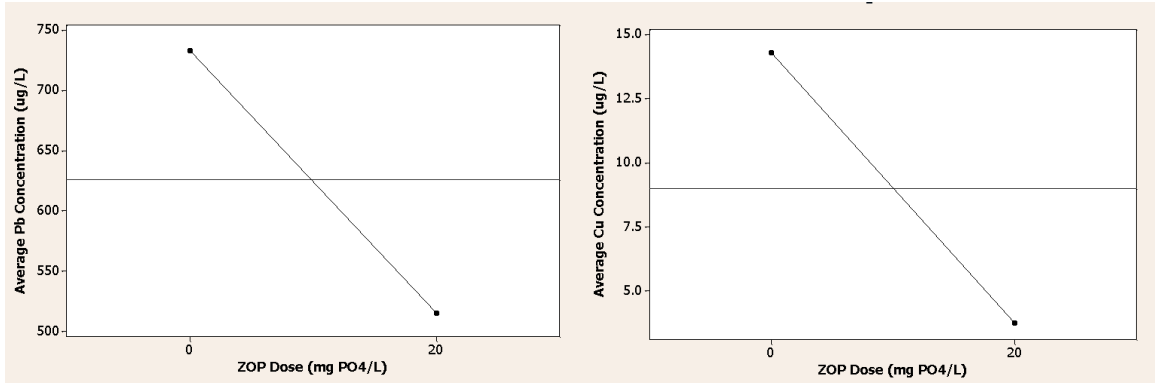
Figure 4.18 – Main effects plots of lead and copper versus ZOP dose (after 1-day stagnation). When ZOP dose was increased from 0 to 20 mg PO_4/L, both lead and copper concentration in bulk water decreased.
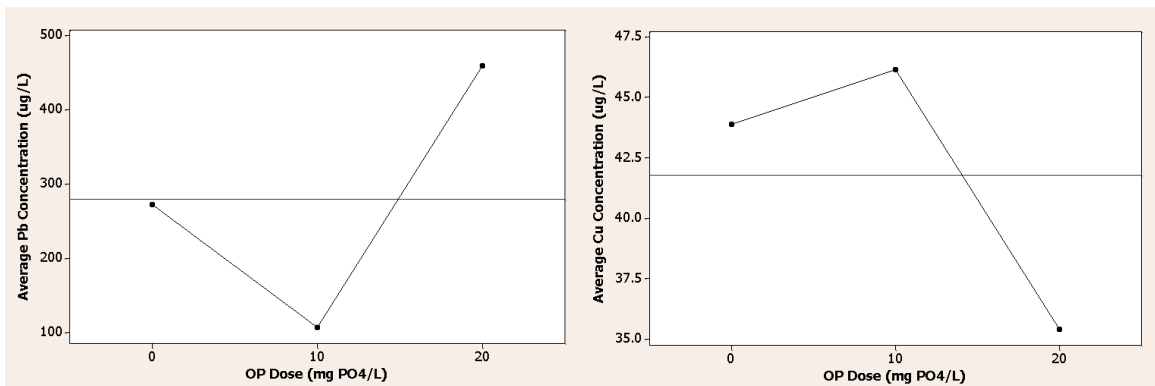
Figure 4.19 – Main effects plots of lead and copper versus OP dose (all stagnation times combined). When OP dose increases from 0 to 10 mg PO_4/L, lead release decreases and copper release increases, but when OP dose was increased from 10 to 20 mg PO_4/L, lead release increases and copper release decreases.

4.12   Elemental Analysis of Lead Coupons

Pipe scales were scraped from lead coupons and analyzed by EDS and XRD. Only the 18 lead coupons from the factorial design analyzing OP doses of 0, 10 or 20 mg PO_4/L were analyzed by XRD. Insufficient scale existed on lead coupons from water conditions testing ZOP and therefore XRD analysis was not possible. As well, XRD analysis was unable to measure the relative proportions of compounds due to the small sample size.

4.12.1 Without Corrosion Inhibitor

Coupons submerged in water conditions without corrosion inhibitor had dark films covering the portion of the coupon that was submerged in water. Many had white films at the water line, and three coupons with pH 8.3 and 9.2 had orange islands close to the bottom of the coupon. An image of the lead and copper coupon from water condition pH9.2/DIC(7) is shown in Figure 4.21 and can be compared to coupons prior to exposure to water in Figure 4.20. All water conditions identified the presence of $PbCO_3$ (Table 4.4). When corrosion inhibitor was not dosed, only two other compounds were identified in corrosion scales: Two Pb(II) oxides, PbO and Pb_5O_8. Only pH7.4/DIC(7) and pH7.4/DIC(17) did not contain PbO or Pb_5O_8 in pipe scales, respectively. In descending weight percent (wt%), EDS analysis identified lead, oxygen, carbon, and aluminum as present on lead coupons without corrosion inhibitor. Calcium was occasionally present but weight percent never exceeded 4.7 wt% (only DIC<3.5 mg/L water conditions). In general, EDS analysis confirmed that a lead carbonate scale dominated corrosion control when no corrosion inhibitor was dosed as the carbon wt% on lead coupons decreased when corrosion inhibitor was dosed.

SEM imaging identified a similar corrosion film on the surface of all lead plates without corrosion inhibitor (Figure 4.22). As DIC increased from 3 to 7 or 17 mg $CaCO_3$/L, dendritic corrosion products about 1 nm wide were present, particularly at pH 8.3 and 9.2 (Figure 4.23). A closer image of the dendritic structure shows geometrical shapes, rather than rod-like species (Figure 4.24).
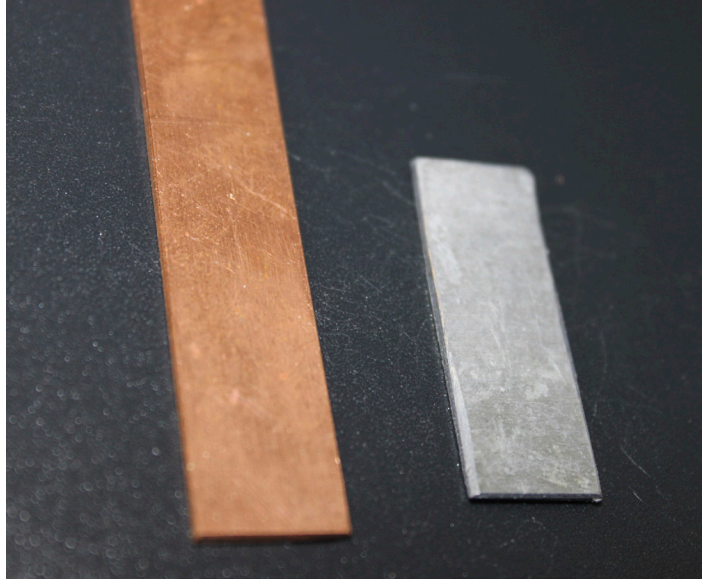
Figure 4.20 – Typical copper (left) and lead (right) coupons prior to exposure to water conditions.
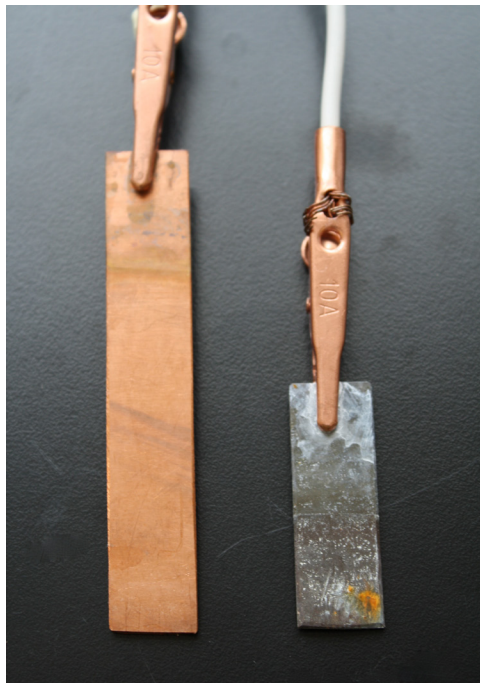
Figure 4.21 – Post-experiment copper (left) and lead (right) coupons from water condition pH9.2/DIC(3). Without corrosion inhibitor, portion of Pb coupon submerged in water was covered with a dark film that is likely lead carbonate scale.
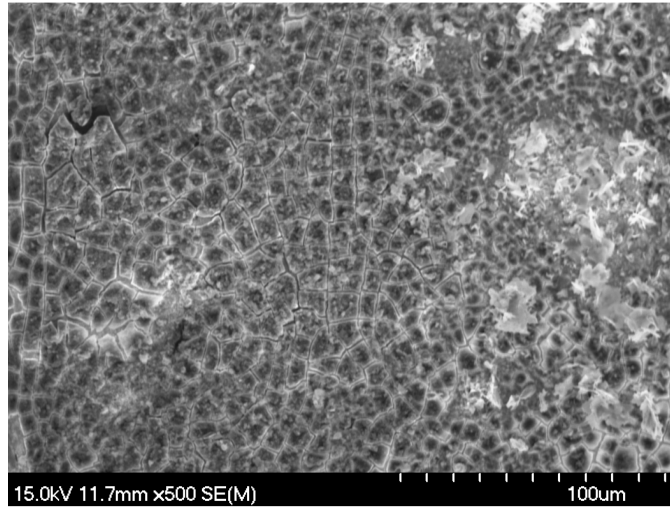
Figure 4.22 – Corrosion film on lead coupon without corrosion inhibitor in water condition pH8.3/DIC(7).
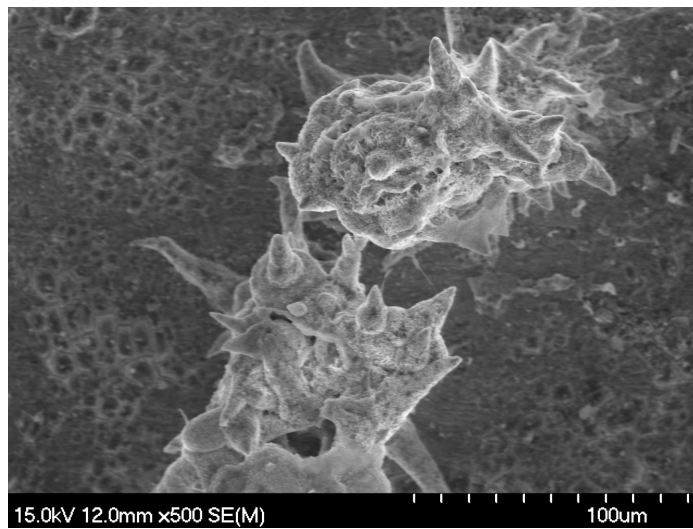
Figure 4.23 – Dendritic structure on lead coupon from water condition pH8.3/DIC(17).
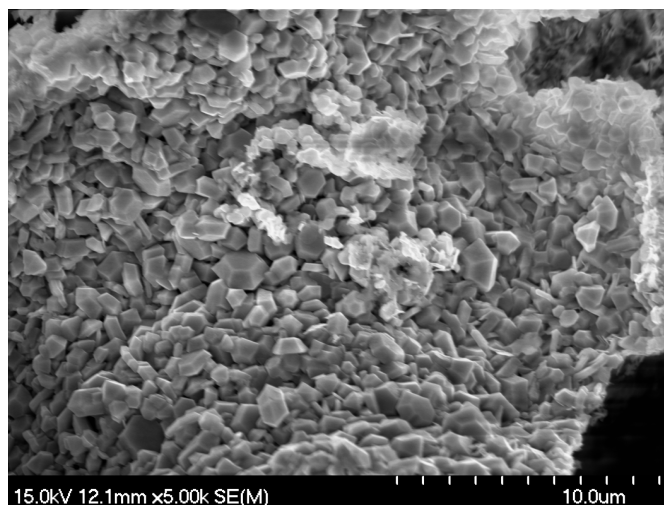
Figure 4.24 – Higher magnification of the dendritic structure on lead coupon from water condition pH8.3/DIC(17). Geometrical shapes, rather than rod-like structures were present.

4.12.2 Orthophosphate Corrosion Inhibitor

When OP was dosed at either 10 of 20 mg PO_4/L, lead coupons in water conditions typically had dark films similar to films observed when no corrosion inhibitor was dosed, however, white corrosion products overlaid the dark film and covered a portion or the entire area submerged in water. Some coupons had localized white and orange speckles. An example of a typical lead and copper plate in a water condition dosing OP(10) is shown in Figure 4.25. Lead coupons in water conditions with OP dosed at 20 mg PO_4/L looked similar to coupons exposed to OP doses of 10 mg PO_4/L, however the white film typically covered the entire submerged area, and larger white corrosion products, or tubercles, extended typically from the bottom of the coupon. These large white tubercles were not securely attached and likely contributed to the outlier lead concentration events observed in water conditions with OP at 20 mg PO_4/L. Figure 4.26 shows a lead and copper coupon from a DIC(7) and initial pH 7.4 water condition with OP dose of 20 mg PO_4/L.

Surface scales when dosing OP consisted of lead carbonates, lead oxides, and lead phosphates (shown in Table 4.4). All 12 water conditions with OP addition produced a

lead carbonate film on the lead surface whereas all but three water conditions contained the Pb(II) oxide, PbO, and half of the water conditions produced a Pb_5O_8 scale (also a Pb(II) species) on the lead coupon. The presence of PbO_2, a Pb(IV) compound, was detected on 3 of the 12 coupons that dosed OP at either 10 or 20 mg PO_4/L. According to the Pourbaix diagram for the $Pb-H_2O-CO_3$ system (shown in Figure 2.3), when pH is between 7.4 and 9.2, lead(II) carbonates form readily between -0.5 and 1 V. When potential is increased to above 1 within the pH range of natural waters, the Pb(IV) compound PbO_2 is preferentially formed. The production of Pb(IV) compounds can occur when Pb(II) compounds are oxidized, and a strong oxidant, such as oxygen or chlorine, is often necessary for oxidation of Pb(II) to occur. Though the chlorine concentration was below detection in these water types and it has also been found that the presence of orthophosphate can inhibit the formation of Pb(IV) oxides (Lytle et al., 2009), the open-air experimental set-up may have created a sufficiently oxidizing system within these water conditions to promote the oxidation of Pb(II) to Pb(IV) scales.

Lead phosphates played a role in film passivation when OP was dosed. Two lead phosphates, either $Pb_5(PO_4)_3Cl$ (chloropyromorphite), or $Pb_3(PO_4)_2$, or both species, were present on all lead coupons when OP was dosed. EDS analysis identified that the main elements on lead surfaces with OP addition were lead, oxygen (O), carbon (C), aluminum (Al), phosphorus (P), and calcium (Ca). In general, carbon wt% decreased when OP was dosed compared to no inhibitor; the same trend occurred with the addition of ZOP. A decrease in carbon wt% and an increase in phosphorus wt% suggests that lead phosphates are present and contribute towards passivation on lead coupons. Phosphorus wt% ranged from 2.9 to 9.1 % on coupons that dosed ZOP and ranged from 5.6 to 8.1 % on coupons that dosed OP at either 10 or 20 mg PO_4/L.

As shown in Table 4.4, lead scales of all six coupons in water conditions that dosed OP(20) contained the mineral chloropyromorphite whereas only 3 of the 6 lead coupons in water conditions that dosed OP(10) contained scales with the mineral chloropyromorphite. Coupons in water conditions with OP(10) all either contained chloropyromorphite or $Pb_3(PO_4)_2$, and both were present in water condition OP(10)/pH7.4/DIC(17). An interesting finding was that $Pb_3(PO_4)_2$ was only present on

Figure 4.25 – Post-experiment lead and copper coupons from water condition OP(10)/pH7.4/DIC(7). Dark lead carbonate scale is present beneath a white lead oxide layer and lead phosphate layer.

Figure 4.26 – Post-experiment copper and lead coupons from water condition OP(20)/pH7.3/DIC(7). White corrosion tubercles are extending from the lead surface.

Table 4.4 – Crystalline phases identified on lead coupons exposed to OP, pH adjustment, and DIC adjustment

	Crystalline Phase					
	$PbCO_3{}^{\phi}$	PbO	PbO_2	Pb_5O_8	$Pb_5(PO_4)_3Cl^{\S}$	$Pb_3(PO_4)_2$
Water Condition	Pb(II)	Pb(II)	Pb(IV)	Pb(II)	Pb(II)	Pb(II)
pH7.4/DIC(7)	X	X				
pH7.4/DIC(17)	X			X		
pH8.3/DIC(7)	X	X		X		
pH8.3/DIC(17)	X	X		X		
pH9.2/DIC(7)	X	X		X		
pH9.2/DIC(17)	X	X		X		
OP(10)/pH7.4/DIC(7)	X	X				X
OP(10)/pH7.4/DIC(17)	X	X		X	X	X
OP(10)/pH8.3/DIC(7)	X	X		X	X	
OP(10)/pH8.3/DIC(17)	X	X				X
OP(10)/pH9.2/DIC(7)	X		X		X	
OP(10)/pH9.2/DIC(17)	X					X
OP(20)/pH7.4/DIC(7)	X		X		X	
OP(20)/pH7.4/DIC(17)	X	X			X	
OP(20)/pH8.3/DIC(7)	X	X		X	X	
OP(20)/pH8.3/DIC(17)	X	X	X	X	X	
OP(20)/pH9.2/DIC(7)	X	X		X	X	
OP(20)/pH9.2/DIC(17)	X	X		X	X	

$^{\phi}$Cerrusite
§chloropyromorphite

coupons with OP(10) and was identified on four of the six coupons, whereas $Pb_3(PO_4)_2$ was not identified on any coupon dosing OP(20). Increases in lead release were observed when OP dosed was increased from 10 to 20 mg/L, and the physical and crystalline differences in lead scale may allude to why lead release was different between these water conditions.

Other studies have shown the formation of $Pb_3(PO_4)_2$ on lead pipe (Lytle et al., 2009) however it is less thermodynamically stable than other lead minerals. Chloropyromorphite is the most stable lead mineral under normal environmental conditions and other lead solids tend to transform to chloropyromorphite via a dissolution-re-precipitation mechanism with sufficient OP and chloride concentration (Nriuagu, 1974). Therefore, the presence of $Pb_3(PO_4)_2$ on coupons that dosed OP(10) could suggest that chloride concentration was limiting, and the formation of $Pb_5(PO_4)_3Cl$ could not occur. However, influent chloride concentration (mg/L) was not significantly different between any of the water conditions (with or without OP) ($\alpha=0.05$). It is not well understood why chloropyromorphite formation was preferred over $Pb_3(PO_4)_2$ when OP dose was 20 mg PO_4/L. This will be discussed further in section 4.13.

4.13   The Impact of High-Dose Corrosion Inhibitor on Lead Release

The effect of high-dose corrosion inhibitor was dependent on corrosion inhibitor type and dose. When ZOP was dosed in water with low DIC (<3 mg/L), 20 mg PO_4/L reduced lead concentration in bulk water in all cases, and copper release significantly decreased as well. In comparison, OP dosed at 10 mg/L significantly decreased lead release whereas OP dose of 20 mg/L significantly increased lead release compared to no corrosion inhibitor in some water conditions. Previous research has suggested that high doses of OP corrosion inhibitor (9.3 mg PO_4/L) can increase water conductivity to such an extent that lead release is increased (Nguyen et al., 2011a). As mentioned in Section 4.4.3, increasing DIC from 7 to 17 mg/L significantly increased conductivity, but increasing PO_4 concentration from 10 to 20 mg/L did not significantly increase conductivity. As

shown in Figure 4.27, conductivity of water conditions with similar DIC levels at either 10 or 20 mg PO_4/L are not significantly different. Therefore, conductivity was not higher in all OP(20) compared to OP(10) water conditions and can not be attributed to the exacerbated lead release compared to no corrosion inhibitor observed in five of the six OP(20) water conditions.

Physical observations of the lead plates and XRD analysis suggest that differences in lead passivation exist between the two OP doses. For example, higher variation in lead release resulting from sloughing events over the experimental duration support the theory that tubercles were more readily formed when OP was dosed at 20 mg PO_4/L. As well, increasing OP dose from 10 to 20 mg PO_4/L increased particulate lead but not dissolved lead, which is characteristic of tubercle sloughing.

The reason for increased tubercle formation could be related to microbial growth. As mentioned in section 3.1, water used for experimentation was filtered water from JDKWSP. Since no chlorine was dosed in this experimental design, influent water may have contained native bacteria. The relationship between tubercles and bacteria has been reported in the literature: Chen et al. (2013) identified bacterial communities within cast
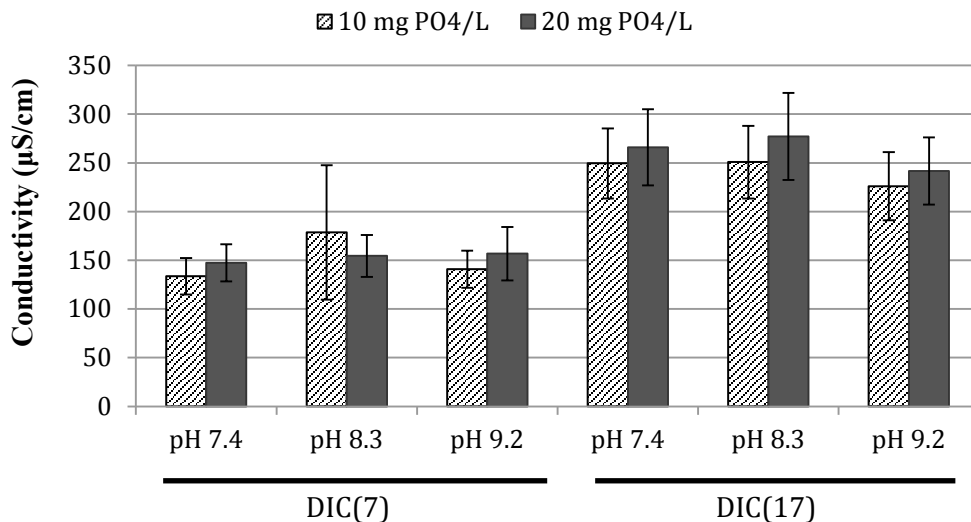
Figure 4.27 – Conductivity in water conditions with either 10 or 20 mg PO_4/L. Conductivity of bulk water with DIC(7) were always lower than conductivity in bulk water with DIC(17).

iron pipe tubercles and these communities were the same as bacterial members in the bulk water. Anaerobic, sulfate-reducing bacteria have been identified within acidic tubercle interiors and were easily removed from the pipe wall when water velocity was high (Tuovinen et al., 1980).

Differences in microbial concentrations could be related to the concentration of phosphorus in the bulk water. Research has shown that phosphorus can contribute to bacterial regrowth in the distribution system (Chen et al., 2013; Lehtola et al., 2002) and that microbial growth in drinking water can be limited by phosphorus concentration (Fang et al., 2009; Lehtola et al., 2001). It is theorized that increasing OP concentration from 10 to 20 mg PO_4/L increased the microbial population in the bulk water and increased tuberculation and therefore sloughing of metals into the bulk water.

Though biological activity was not monitored during the study with OP addition, a potential indication of increased biological activity in OP(20) water conditions is the presence of chloropyromorphite scale on OP(20) lead coupons. Phosphate has been used to immobilize lead in soil for soil remediation by forming insoluble lead phosphate complexes such as pyromorphite, and while this reaction was believed to consist of purely chemical reactions, Rhee et al. (2012) recently found that microbial activities may also contribute to pyromorphite formation in soils. Therefore, the presence of chloropyromorphite on all lead plates from OP(20) water conditions may be indicative of increased microbial activity in these water types.

Despite higher lead release in most OP(20) water conditions, the water condition OP(20)/pH9.2/DIC(17) had the lowest average lead release of any water condition (with or without corrosion inhibitor). Tuberculation was visibly less on the lead coupon compared to other OP(20) water conditions. Factorial analysis indicated that increasing DIC had a significant impact on reducing lead release, and increasing DIC from 7 to 17 mg $CaCO_3$/L had the largest impact on reducing lead release when OP was 20 mg/L (Figure 4.10). Therefore, it is suspected that high DIC of 17 mg $CaCO_3$/L and high pH 9.2 were sufficient in preventing tuberculation and decreasing the potential for microbial

habitat and therefore microbial corrosion.

4.14   Copper Coupons Scale Analysis

When no corrosion inhibitor was dosed, C, O, Cu, and Pb were the dominant elements identified on copper coupons. Trace amounts of Al were also identified on some plates. Pb wt% on copper coupons decreased as DIC increased: Pb wt% was between 16 and 59 when DIC was less than 3 mg/L whereas it did not exceed 4 wt% when DIC was either 7 or 17 mg/L. This data suggests that increasing DIC as well as dosing OP may control deposition corrosion better than low DIC water and ZOP corrosion inhibitor.

EDS analysis did not identify any compositional differences in copper coupons between conditions with and without OP. Similar to when no corrosion inhibitor was dosed, C, O, Cu and occasionally Pb were the only elements identified on copper coupons with OP addition. In contrast, there were distinct differences between elemental analysis of copper coupons with and without ZOP addition in DIC(3) water conditions. In general, C, O, Cu, Pb, Zn, and P were identified on copper coupons with ZOP addition. Ca and Al were also present on most coupons in trace amounts. A decrease in C wt% and an increase in O wt% occurred when ZOP was dosed compared to no ZOP suggesting that oxide scales played a role in copper coupon passivation when ZOP was dosed. As well, P wt% was between 7.9 and 13.6 on copper coupons with ZOP addition. In comparison, P was not detected on copper coupons without corrosion inhibitor or with OP addition.

4.14.1 The Role of Zinc in Copper Corrosion Mitigation

As was previously mentioned, ZOP addition was the only corrosion control strategy that significantly reduced copper concentration, whereas OP was found to significantly increase copper concentration in some cases. Phosphorus deposition onto copper coupons only in the presence of zinc suggests that zinc promoted P deposition onto copper coupons and protected the copper cathode from corrosion. Other authors have also found

that more phosphate deposited on the pipe when zinc was present that potentially inhibited nonuniform copper corrosion (Lattyak, 2007; Scheffer, 2006).

Zn wt% ranged from 13 to 30 % on copper electrodes. EDS analysis identified higher Zn wt% than P wt% on copper coupons. A higher Zn:P wt% ratio could indicate higher zinc concentration on the surface that protects the cathode copper. Elemental coloured maps were created with EDS data to show the deposition of elements on copper and lead coupons. Elemental maps for copper and lead coupons of the water condition ZOP(20)/pH7.4/DIC(3) are shown in Figure 4.28 and Figure 4.29, respectively. On the copper coupon, zinc and phosphorus are evenly distributed over the entire plate. On the lead coupon, however, phosphorus and lead deposition cover the plate, suggesting even lead-phosphate passivation, whereas zinc deposition is localized (green in Figure 4.29). The presence of zinc and phosphate on the copper surface is breaking the connection between the copper coupon and the electrolyte and potentially reducing copper release in water conditions with ZOP addition. The localized deposition of zinc on the lead anode suggests that zinc plays a minimal role in lead corrosion control at the anode.

4.14.1 Downstream Impacts of High-Dose Corrosion Inhibitor

Within the Health Canada Guidelines for Drinking Water Quality (Health Canada, 2012) zinc is regulated as an aesthetic objective (5 mg/L) and no objective has been identified for phosphate in drinking water. In spite of the benefits of high-dose ZOP for control of copper corrosion, and the demonstrated benefits of a ZOP dose of 10 mg PO_4/L on reducing lead release, the downstream impacts of high zinc and/or phosphate doses must be considered. Research has shown that phosphorus loads may exacerbate bacterial growth in the distribution system (Lehtola et al., 2001; Miettinen et al., 1997) and the impacts of microbially induced corrosion should be considered. High zinc and phosphorus concentrations could also have implications on the water quality of receiving water bodies if wastewater is discharged without treatment. Studies have shown that zinc is toxic to fish (Burton et al., 1972; Skidmore, 1964) and zinc can reduce reproduction in
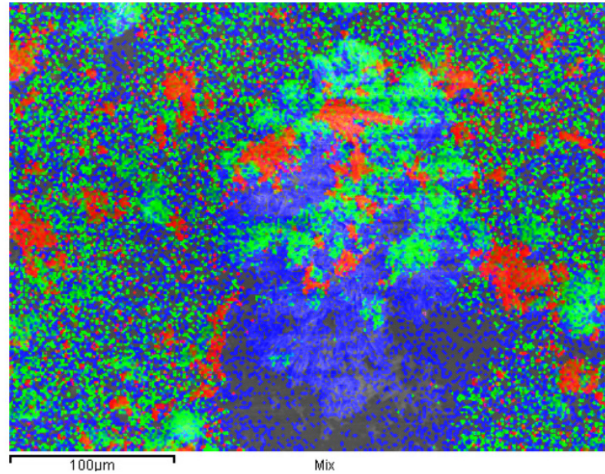
Figure 4.28 – EDS elemental map of copper coupon from ZOP(20)/pH7.4/DIC(3) water condition. Green represents phosphorus, blue is zinc, and red is lead. Zinc and phosphorus are distributed evenly over the copper surface.
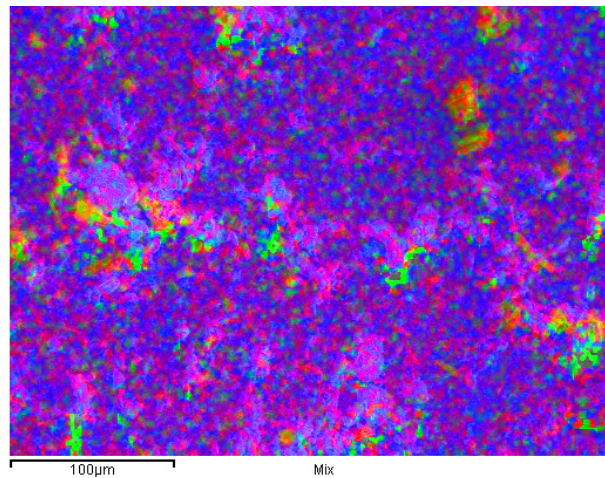
Figure 4.29 – Image of lead coupon from ZOP(20)/pH7.4/DIC(3) water condition. Blue represents lead, red is phosphorus, and green is zinc deposition. Phosphorus (in red) covers the lead plate evenly, whereas zinc deposition is more localized.

certain fish species (De Schamphelaere et al., 2004). As well, though phosphorus is non-toxic to aquatic organisms, phosphorus inputs increase the risk of eutrophication and oxygen depletion of receiving waters (Schindler et al., 2008). Therefore, to prevent the downstream effects of zinc and phosphorus loads, wastewater treatment will be impacted.

4.15   Ellipsometry: An Optical Tool for Analysis of Drinking Water Films

4.15.1 Ex-situ Ellipsometric Measurements on Lead Sputtered Plates

The potential for measuring corrosion film thickness using ex-situ ellipsometry was attempted using lead sputtered plates. The optical constants of a dry lead sputtered plate in air were measured, and then the lead sputtered plate was soaked in JDKWSP tap water overnight, allowed to air dry, and the optical constants were re-measured 24 hours later to determine a change in lead film properties and thickness.

It was assumed that the lead sputtered plate was opaque, and a B-spline model was used to determine the optical properties of the film based. However, an analysis of the *pseudo n* parameters identified that the film was not opaque and it is speculated that the light beam penetrated through the sputtered lead film and was "seeing" the glass underneath the sputtered lead.

The benefit of an opaque film is that all light is reflected off the film, and therefore the thickness of the opaque film does not need to be considered; this reduces the number of unknown sample properties (Hilfiker et al., 2008). A potential solution was to sputter a thicker lead film to create an opaque substrate, however, a lead sputtered film between 20 and 50 nm was not reflective enough and there was insufficient reflected light off the surface to perform ellipsometric measurements.

Another issue with the lead sputtered plate was that the lead film was partially absorbing

at the surface. As such, depositing a thicker opaque lead sputtered film would not entirely resolve the issue as the film was also partially absorbing at the surface. In a transparent substrate, the extinction coefficient, k, is equal to zero and does not need to be determined by the model. However, with absorbing films, there are more unknown sample properties than measured values. The B-Spline model cannot simultaneously fit for n, k, and film thickness of a partially absorbing film. As such, the lead films cannot be adequately modeled with the B-Spline model, and other models were considered to determine the optical constants and therefore thickness of the passivation film on lead.

An effective medium approximation (EMA) could potentially work for this system as EMA model determines thickness of a film but not independently of n and k. Since metal films typical have a large amount of variation across the surface, determining n and k at each sample point may be the most effective method for film thickness determination. This analysis was not conducted on the sample, however. This study demonstrated the complexity that exists in measuring film thickness of thin absorbing metallic films and that the EMA model should be considered in future ellipsometric metal oxide film analysis.

4.15.2 Protein Adsorption on Copper Coupon

The role of bacteria in lead and copper corrosion is not well understood in the literature and the current study suggests that bacterial corrosion may have exacerbated lead release in water conditions with OP(20). A methodology for quantifying bacteria at the metal-water interface would provide insight of the role of bacteria on lead and copper corrosion.

In literature, a method for quantifying adsorbed protein layers at the protein/metal interface using an in-situ spectroscopic ellipsometry technique has been described by other authors (Byrne et al., 2009; McArthur et al., 2010). These studies are relevant to drinking water as the attachment of biofilm onto metallic surfaces is similar to the concept of adsorbed protein onto metal surfaces; biofilm initially attach to surfaces, including metallic distribution system piping, using exopolysaccharides and proteins (Gu,

2009). A nanoscale evaluation of protein attachment onto metallic surfaces in chlorinated drinking water could provide insight into the effect of chlorine on biofilm attachment. Therefore, in-situ ellipsometry was applied to assess the effect of chlorine concentration on protein (simulating biofilm) attachment to copper surfaces.

Copper sputtered plates were used in place of lead, and fibrinogen protein was used to simulate the proteins involved with biofilm attachment as this protein has been used in previous studies with success (McArthur et al., 2010). Fibrinogen protein is transparent, and can be modeled by the Cauchy model, as shown in Figure 4.30(b).

4.15.3 In-situ Ellipsometry Methodology

Firstly, a copper sputtered plate was loaded into the flow cell and the cell was filled with PBS. The plate was allowed to sit for 2 hours prior to ellipsometric measurements to stabilize the metal surface in PBS as PBS solution was found to modify the metallic film's surface properties (data not shown). Next, the parameters Ψ and Δ were measured in duplicate at 39 pts along the centerline of the copper plate. This data was used to determine the n and k values of copper in PBS solution prior to the addition of protein or chlorine (optical model shown in Figure 4.30(a)). The n and k values of PBS and fibrinogen are consistent with values used by other researchers (McArthur et al., 2010). A 1 mg/mL fibrinogen in PBS solution was pumped through the cell (2.5 mL/min, laminar) for 10 minutes. Flow was stopped and Ψ and Δ were measured at the 39 points along the plate in duplicate. The optical model used for generating protein thickness is shown in Figure 4.30(b). This stage represents the determination of the initial protein film thickness. Next, PBS with either 0, 0.2 or 1 mg Cl_2/L was pumped for 10 mins, and ellipsometric measurements were once again measured and fit for film thickness followed by a second identical rinse and measurement cycle. A summary of the in-situ procedure is shown in Figure 4.31.

Protein thickness ranged from 1.5 to 2.3 nm between the three runs. As can be seen in Figure 4.32, protein film thickness decreases along the entire length of the plate after

rinsing with 0.2 mg Cl$_2$/L except for an increase in film thickness after the rinsing stage at the 27th position from the leading edge. Increases in protein thickness may have occurred as protein were dislodged from the plate surface and then reattached downstream. A similar trend of decreasing protein thickness after rinsing was observed after every rinse type; protein thickness always decreased after rinsing and was independent of chlorine dose.

a)   b)

| PBS [n=1.335; k=0] | Cauchy |
| Protein [n=1.57; k=0] | Cauchy |

| PBS [n=1.335; k=0] | Cauchy |
| Copper [n(x), k(x)] | |

| Copper [n(x), k(x)] | |
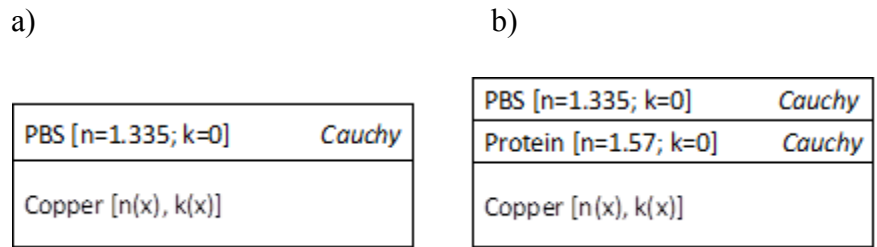
Figure 4.30 – Optical models used for (a) fitting refractive indices for the metallic Cu film in PBS, and (b) determining the thickness of adsorbed protein layer before and after rinse cycles.
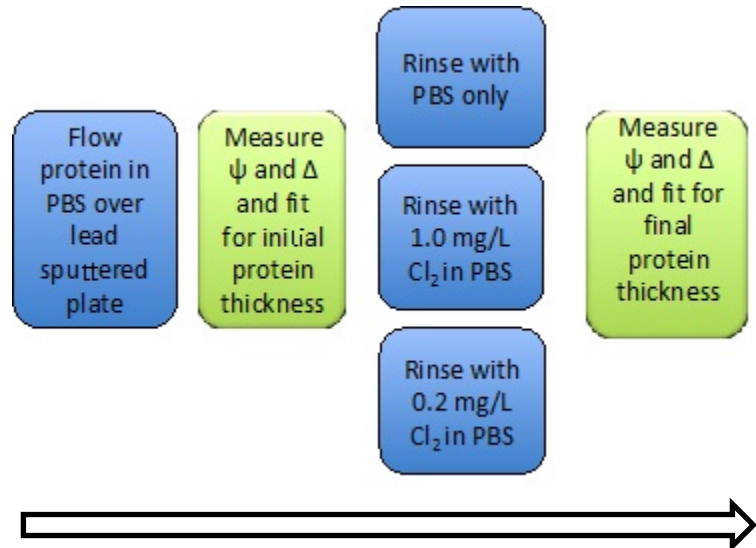
Figure 4.31 – In-situ ellipsometry procedure for determining the effect of chlorine dose on protein film thickness.

In Figure 4.33, the ratio of protein thickness after the 2nd rinse ($L_{f,f}$) divided by the initial protein thickness ($L_{f,f}/L_{f,0}$) is plotted. An $L_{f,f}/L_{f,0}$ ratio smaller than 1 indicates final film thickness is less than initial film thickness. The $L_{f,f}/L_{f,0}$ ratio was less than 1 for all three Cl_2 rinse conditions indicating that final protein thickness was less than initial film thickness. As well, there was no significant difference in $L_{f,f}/L_{f,0}$ between rinsing with 0, 0.2, or 1 mg Cl_2/L in PBS solution.

Overall, the data does not provide substantial insight into the effects of chlorine on protein thickness for various reasons. Firstly, limited data was generated from this set-up because the method of protein adsorption onto copper surfaces was not easily reproducible. There were consistent issues with the copper plates including discoloration when in contact with water and air (which was speculated to be copper oxide formation on the plate), and the model often returned a protein thickness of -1. The return of -1 nm thickness raised questions as to whether the protein was being completely removed from the plate. Secondly, protein thickness decreased after every wash type, including PBS without chlorine. It is unknown whether the initial protein thickness measurement represents adsorbed protein or simply protein which had settled out of solution onto the copper plate. Overall, these results cannot determine whether the effect of chlorine on protein attachment is more significant than the effect of flow (abrasion) on protein attachment.
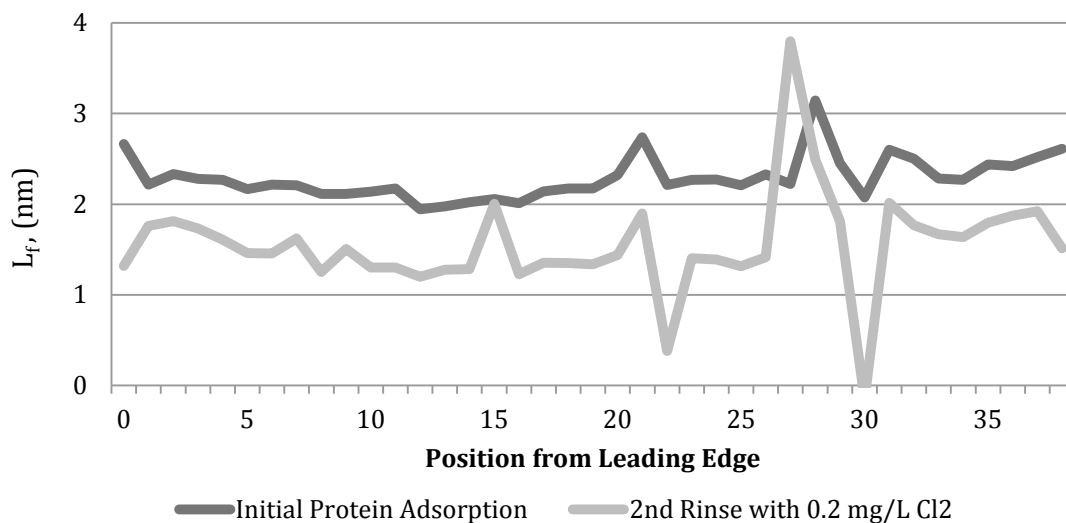
Figure 4.32 – Protein film thickness (L_f, in nm) before and after the second rinse with 0.2 mg Cl_2/L. Along the length of the plate, film thickness decreased after rinsing with 0.2 mg Cl_2/L.
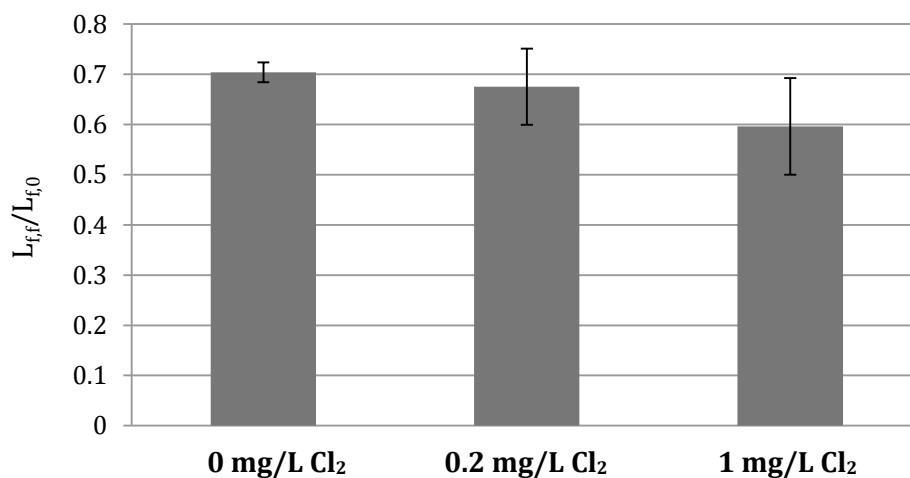
Figure 4.33 – Average film thickness after 2nd rinse divided by initial film thickness, $L_{f,f}/L_{f,0}$, over length of the copper coupon. Error bars represent the 95% confidence interval. $L_{f,f}/L_{f,0}$ was not significantly different between rinse types.

4.15.3.1 Recommendations

Recommendation for future development of this method include:

1. Allow plate to sit with protein solution for longer period
2. Conduct a trial with alternating rinse and measurement cycles and determine if at any point continual rinsing no longer decreases protein thickness.
3. Use lead sputtered plates instead of copper to avoid discolouration of plates.
4. Conduct experiment using the simpler ex-situ methodology rather than in-situ.
5. Develop a methodology to adequately model absorbing lead or copper films prior to evaluating the effects of protein and chlorine on lead and copper surfaces.

CHAPTER 5   CONCLUSION AND RECOMMENDATIONS

5.1   Summary of Objectives and Main Findings

Galvanic corrosion between lead and copper in drinking water distribution systems has shown to be a major contributor to lead and copper levels in drinking water. Galvanic corrosion can increase lead concentrations to above what would occur for lead pipe alone, and galvanic currents can be sustained for long periods of time causing a significant public health threat. Understanding the water quality parameters that encourage galvanic corrosion in low alkalinity water (DIC<20 mg $CaCO_3$/L) will be beneficial for improving corrosion control. Corrosion control has shown to be a site-specific issue and the role of high-dose corrosion inhibitors has not been studied in depth for lead corrosion in low alkalinity water. This bench-scale study examined the effects of pH conditions, high-dose ZOP and OP corrosion inhibitors, and buffering capacity through alkalinity adjustment on galvanic corrosion between lead and copper and sought to answer the following questions:

1. How does the high-dose corrosion inhibitor strategy compare to pH and/or alkalinity adjustment strategies with respect to lead and copper release?

2. What are the main corrosion products formed by each strategy?

3. Can in-situ ellipsometry be a useful tool for quantifying passivation film formation?

Table 5.1 below presents a summary of the main findings from this study.

Table 5.1 – Summary of results

Research Focus	Finding
Particulate Lead	• Samples with turbidity less than 1 NTU can also contain significant portions of particulate lead.
Acclimation Stage	• Highest copper concentrations occurred during acclimation when either no corrosion inhibitor or ZOP was dosed. When OP was dosed, however, copper concentration was 1.1 to 3.1 times greater during steady state than during acclimation. • Without corrosion inhibitor, higher DIC and higher pH reduced average lead release during the acclimation period and prevented high lead release events likely caused by sloughing. • In water conditions with corrosion inhibitor (either ZOP or OP), lead concentration in bulk water exceeded 1000 μg/L at least once, whereas lead release never exceeded 530 μg/L in water conditions with corrosion inhibitor and high DIC and initial pH 9.2.
Steady-State: ZOP addition versus pH adjustment in low DIC water	• In DIC(3) water conditions, increasing pH had the most significant impact on reducing lead release. • ZOP(20) also significantly reduced lead release, and mitigated a higher concentration of lead when pH was 7.4 compared to 9.2. • The combination of high pH and ZOP addition resulted in the lowest concentration of lead in bulk water.
Steady-state: OP addition versus pH-alkalinity adjustment	• OP addition significantly reduced dissolved lead compared to no corrosion inhibitor and dissolved lead was always less than 28 μg/L. • Increasing OP dose from 10 to 20 mg PO_4/L did not significantly reduce dissolved lead concentration but significantly increased particulate lead in 5/6 water conditions. • Lead release was best mitigated by OP(10) and DIC(17) mg $CaCO_3$/L. Most OP(20) conditions exacerbated lead release compared to no corrosion inhibitor

Steady-state: OP addition versus pH-alkalinity adjustment (cont.)	• Tubercles were observed on lead plates when OP(20) was dosed and it is theorized that a higher dose of OP increased bacterial corrosion and tuberculation and therefore lead release in OP(20) conditions.
Elemental Scale Analysis	• XRD analysis of lead coupons in DIC 7 or 17 mg $CaCO_3$/L water conditions showed that lead carbonates and lead oxides were present on all coupons with or without corrosion inhibitor. • Lead phosphates, including chloropyromorphite and $Pb_3(PO_4)_2$ were present on coupons exposed to OP. • Dominant presence of chloropyromorphite on OP(20) lead coupons may be indicative of microbial activity.
Steady State Copper release	• Copper concentration was only significantly reduced with addition of ZOP(20) at both pH conditions and decreased copper by an average of 10 μg/L. Average copper release was always below 5 μg/L when ZOP was dosed. • Zinc is believed to promote phosphate deposition on copper and mitigate copper corrosion. • Average Copper concentration was between 22 and 56 μg/L when OP was dosed • Copper increased with OP(10) and decreased with OP(20) addition, whereas the opposite effect occurred for lead release.
Ellipsometry	• Lead sputtered onto a glass plate was a partially absorbing film that may require an EMA model to determine film thickness. • Data was inconclusive as to whether chlorine concentration affects protein adsorption onto copper.

5.2 Concluding Remarks

The impact of pH, buffering capacity, and corrosion inhibitors on lead release was compared in this study. When no corrosion inhibitor was dosed, increasing DIC from 3 mg $CaCO_3$/L to 7 or 17 mg $CaCO_3$/L had the greatest impact on reducing lead release. As well, increasing pH when DIC was 3 mg $CaCO_3$/L had a greater impact on reducing lead release than when DIC was higher. Compared to ZOP, pH had the greatest impact on reducing lead release when DIC was below 3 mg $CaCO_3$/L, however the combination of increased pH and ZOP corrosion inhibitor was the best corrosion control strategy overall. When DIC was increased and OP was dosed, OP dose most significantly impacted lead release. Though 20 mg PO_4/L often had detrimental effects on lead release, a high-dose of 10 mg PO_4/L overall mitigated the most lead release. It is eluded that increasing OP dose to 20 mg PO_4/L increased microbial activity in the bulk water and exacerbated lead release.

Lead carbonates and lead oxides were present on all lead coupons, and the dominance of lead phosphates occurred when OP was dosed (no analysis conducted on ZOP lead coupons). Chloropyromorphite was on OP(20) lead coupons but not OP(10) coupons which may also elude to an increase in microbial corrosion in OP(20) water conditions. The presence of zinc improved phosphate deposition onto copper coupons and played a role in mitigating copper release whereas copper release was occasionally increased in the presence of OP without zinc.

Metal passivation and biofilm attachment mechanisms are not well understood at the nanometer-scale though they are known to play a major role in corrosion in drinking water. This study attempted to use an optical tool, ellipsometry, to measure anodic oxide films and to measure the effects of chlorine on protein attachment. Many challenges existed with the technique, including modeling the metal substrate as an absorbing film. As such, troubleshooting with respect to modeling metal absorbing films is necessary before ellipsometry can be an effective tool within the water industry.

5.3   Recommendations

5.3.1 Galvanic Studies at the Bench-Scale

When analyzing metals samples, it is recommended that a cohort of samples be analyzed with both direct and NAD methods regardless of sample turbidity to identify water conditions that exhibit significant portions of particulate lead. As well, this study identified changes in dissolved lead portions with addition of OP, and it would have been beneficial to have measured dissolved lead fractions in water conditions dosing ZOP. Therefore, due to the effects of corrosion inhibitor on lead and copper particulate and dissolved fractions, a complete analysis of metals during galvanic studies is recommended.

Dump-and-fill experiments are a common methodology used for bench-scale studies of lead and copper galvanic corrosion. This study identified the role of CO_2 on pH when the system is open to the atmosphere. It is recommended that bench-scale dump-and-fill studies be conducted in closed-systems to better mimic distribution system conditions and to reduce pH changes due to atmospheric CO_2. As well, this study found that there was no statistical difference in lead concentration between 1- and 2-day stagnation times; one short (1-day) and long (4-day) stagnation time would have been sufficient and reduced the water analysis workload on a weekly basis.

Current was measured over the course of the experiment and demonstrated that current is not directly correlated to lead release in the bulk water. Therefore, current should not be a used as a determinant of high metals concentrations in a galvanic cell. However, actual lead and copper concentrations in the bulk water compared to the measured current potential can speak to the effectiveness of passivation films on the metal surfaces.

This study eluded that microbial corrosion may have played a role in increasing corrosion in water conditions with high doses of OP (20 mg PO_4/L). The role of microbial corrosion within a copper and lead galvanic cell is difficult to determine, however monitoring additional water quality parameters would have been beneficial to help

elucidate the role of microbial corrosion. For example, dissolved oxygen, ORP, and analysis of bacterial activity (i.e. heterotrophic plate counts, adenosine triphosphate, and assimilable organic carbon) would have provided additional information with respect to oxygen concentration cells, lead passivation potential, and bacterial communities, respectively. It would also be beneficial to determine whether phosphate is the limiting factor for bacterial growth in JDKWSP filtered water. Fang et al. (2009) conducted a similar analysis using annular reactors and would be a good reference for conducting this analysis.

While this study used copper and lead sheet metal submerged in test water, the next step would be to evaluate the effects of high-dose corrosion inhibitors and pH-alkalinity adjustment with lead and copper pipe sections harvested from the distribution system. The advantage of using new sheet metal is that the metal has not been pre-exposed to one water type whereby passivation scale formation has already occurred on the metal, however distribution pipe materials and geometry are different than the current sheet metal set-up. Though premise plumbing pipe sections would require longer acclimation periods, they would represent premise plumbing materials better that the bench-scale sheet metal set-up of the current study.

5.3.2 Galvanic Corrosion Studies at the Pilot-Scale

The results found in the current bench-scale study are limited due to the controlled nature of the experimental set-up and simplification of the premise plumbing scenario. It is recommended that pilot-scale experiments, such as pipe sections or a larger pipe-loop configuration, be conducted to confirm the bench-scale findings.

This study identified that increasing alkalinity and pH can reduce lead corrosion particularly in water conditions without corrosion inhibitor, though neither an optimal alkalinity concentration nor pH was identified. This study also identified that high doses of orthophosphate corrosion inhibitor can have detrimental effects on lead release, though this only occurred with OP addition. As well, ZOP was the only parameter tested that was

effective in reducing copper release.   Therefore, the following recommendations are suggested for future pilot-scale studies:

1. Conduct trials with a range of phosphate doses (including low- and high-doses) to determine optimal dose of corrosion inhibitor.
2. Conduct high-dose corrosion inhibitor tests with ZOP and OP at constant alkalinity.
3. Consider zinc addition in systems where copper corrosion is a concern.
4. Investigate increasing pH in smaller increments to determine if slight increases in pH can be beneficial.
5. Determine if increasing pH for corrosion control has an effect on THM formation.
6. Consider cost effects of increasing pH and alkalinity versus corrosion inhibitor.

BIBLIOGRAPHY

APHA (American Public Health Association). (1995). American Water Works Association and Water Environment Federation. Standard methods for the examination of water and wastewater (19th ed.). American Public Health Association, Washington, DC.

APHA (American Public Health Association). (2012). American Water Works Association and Water Environment Federation. Standard methods for the examination of water and wastewater (22nd ed.). American Public Health Association, Washington, DC.

Arnold, R.B. Jr. and Edwards, M. (2012). Potential reversal and the effects of flow pattern on galvanic corrosion of lead. *Environmental Science and Technology,* **46(20)**: 10941-10947.

Berthouex, P.M. and Brown, L.C. (2002). Statistics for environmental engineers (2nd ed.). Lewis Publishers, Boca Raton, FL, USA.

Burton, D. T., Jones, A. H., and J. Cairns. (1972a). Acute zinc toxicity to rainbow trout (Salmo gairdneri): Confirmation of the hypothesis that death is related to tissue hypoxia. *Journal of the Fisheries Research Board of Canada*, **29**:1463-1466.

Byrne, T.M., Lohstreter, L., Filiaggi, M.J., Bai, Z., and Dahn, J.R. (2009). Quantifying protein adsorption on combinatorially sputtered Al-, Nb-, Ta- and Ti-containing film with electron microprobe and spectroscopic ellipsometry. *Surface Science,* **603**: 992-1001.

Cantor, A.F., Park, J.K., and Vaiyavatjamai, P. (2003). Effect of chlorine on corrosion in drinking water systems. *Journal of the American Water Works Association***, 95(5)**: 112-123.

Cartier, C., Arnold Jr., R. B., Triantafyllidou, S., Prévost, M., and Edwards, M. (2012a). Effect of flow rate and lead/copper pipe sequence on lead release from service lines. *Water Research*, **46**: 4142-4152.

Cartier, C., Doré, E., Laroche, L., Nour, S., Edwards, M., and Prévost, M. (2013). Impact of treatment on Pb release from full and partially replaced harvested lead service lines (LSLs). *Water Research,* **47(2)**: 661-671.

Cartier, C., Nour, S., Richer, B., Deshommes, E., and Prévost, M. (2012b). Impact of water treatment on the contribution of faucets to dissolved and particulate lead release at the tap. *Water Research*, **46**: 5205-5216.

Chen, L., Jia, R.-B., and Li, L. (2013). Bacterial community of iron tubercles from a drinking water distribution system and its occurrence in stagnant tap water. *Environmental Science Processes & Impacts,* **15(7):** 1332-1340.

Churchill, D.M., Mavinic, D.S., Neden, D. G., and MacQuarrie, D.M. (2000). The effect

of zinc orthophosphate and pH – alkalinity adjustment on metal levels leached into drinking water. *Canadian Journal of Civil Engineering*, **27(6)**: 33-43.

Craig, B., and Anderson, D. (Eds.). (1995). Handbook of corrosion data (2nd Ed.). ASM International, OH, USA.

De Laet, J., Vanhellemon, J., Terryn, H., and Vereecken, J. (1992). Characterization of various aluminum oxide layers by means of spectroscopic ellipsometry, **A 54**: 72-78.

De Schamphelaere, K.A., Canli, M., Van Lierde, V., Forrez, I., Vanhaecke, F., and Janssen, C.R. (2004). Reproductive toxicity of dietary zinc to Daphnia magna. *Aquatic Toxicology,* **70(3**): 233-244.

Deshommes, E., Laroche, L., Nour, S., Cartier, C., and Prévost, M. (2010). Source and occurrence of particulate lead in tap water. *Water Research*, **44**: 3734-3744.

Dodrill, D.M. and Edwards, M. (1995). Corrosion control on the basis of utility experience. *Journal American Water Works Association*, **87(7)**: 74-85.

Douglas, I., Guthmann, J., Muylwyk, Q., and Snoeyink, V. (2004). Corrosion control in the City of Ottawa — Comparison of alternatives and case study for lead reduction in drinking water. In: Robertson, W. and Brooks, T. (Ed.). 11th Canadian National Drinking Water Conference and Second Policy Forum. Calgary, Alberta, Canada. April 3 - 6.

Droste, R.L. (1997). Theory and practice of water and wastewater treatment (6th ed.). John Wiley & Sons, New Jersey.

Dudi, A. (2004). Reconsidering lead corrosion in drinking water: Product testing, direct chloramine attack and galvanic corrosion. (Master of Science dissertation). Virginia Polytechnic Institute and State University, Blacksburg, VA, USA.

Edwards, M. and McNeill, L.S. (2002). Effect of phosphate inhibitors on lead release from pipes. *Journal of the American Water Works Association*, **94(1)**: 79-90.

Edwards, M. and Triantafyllidou, S. (2007). Chloride-to-sulfate mass ratio and lead leaching to water. *Journal of the American Water Works Association,* **99(7)**: 96-109.

Edwards, M., Bosch, D., Loganathan, G. V., and Dietrich, A.M. (2003). The future challenge of controlling distribution system water quality and protecting plumbing infrastructure: Focusing on Consumers. Proceedings of the IWA Leading Edge Conference in Noordwijk, Netherlands.

Edwards, M., Marshall, B., Zhang, Y., and Lee, Y. (2005). Unintended conseqences of chloramine hit home. In Proceedings of the WEF Disinfection Conference. Mesa, Arizona.

Elfland, C., Scardina, P., and Edwards, M. (2010). Lead-contaminated water from brass plumbing devices in new buildings. *Journal American Water Works Association,* **102(11)**: 66-76.

Fang, W., Hu, J.Y., and Ong, S.L. (2009). Influence of phosphorus on biofilm formation in model drinking water distribution systems. *Journal of Applied Microbiology,* **106**: 1328-1335.

Goh, K.H., Lim, T.T., and Chui, P.C. (2008). Evaluation of the effect of dosage, pH and contact time on high-dose phosphate inhibition for copper corrosion control using response surface methodology (RSM). *Corrosion Science,* **50(4)**: 918-927.

Grass, G. and Rending, C. (2001). Genes involved in copper homeostasis in *Escherichia coli*. *Journal of Bacteriology,* **183(6)**: 2145-2147.

Gu, J.-D. (2009). Corrosion, microbial. In Schaechter, M (Eds.), Encyclopedia of Microbiology (3rd ed.), Elsevier Inc., Oxford, UK.

Health Canada (2012). Guidelines for Canadian drinking water quality – summary table. Water, Air, and Climate Change Bureau. Healthy Environments and Consumer Safety Brand, Health Canada, Ottawa, Ontario.

Hilfiker, J. N., Singh, N., Tiwald, T., Convey, D., Smith, S. M., Baker, J. H., & Tompkins, H. G. (2008). Survey of methods to characterize thin absorbing films with spectroscopic ellipsometry. *Thin Solid Films*, **516(22)**: 7979-7989.

Hill, C.P. and Gianna, R. (2011). Water quality monitoring and assessment of internal corrosion and increased metals concentrations. In Internal corrosion control in water distribution systems – Manual of water supply practices, M58. AWWA, Denver, Colorado.

Johnson, B., Yorton, R., Tran, T., and Kim, J. (1993). Evaluation of corrosion control alternatives to meet the lead and copper rule for eastern Massachusetts. *Journal New England Water Works Association.* **107(1)**: 24 – 45

Karalekas, P.C., Ryan, C.R., and Taylor, F.B. (1983). Control of lead, copper, and iron pipe corrosion in Boston. *Journal of the American Water Works Association*, **75(2)**: 92-95.

Kim, E. J. and Herrera, J. E. (2010). Characteristics of lead corrosion scales formed during drinking water distribution and their potential influence on the release of lead and other contaminants. *Environmental Science and Technology,* **44**: 6054-6061.

Koch, G.H., Brongers, M.P.E., Thompson, N.G., Virmany, Y.P., and Payer, J.H. (2001). Corrosion Cost and Preventative Strategies in the United States.

Lattyak, R. (2007). Non-uniform copper corrosion in potable water: theory and practice. (Master of Science Dissertation). Virginia Polytechnic Institute and State University, Blacksburg, VA, USA.

Lehtola, M.J., Miettinen, I.T., and Martikainen, P.J. (2002). Biofilm formation in drinking water affected by low concentration of phosphorus. *Canadian Journal of Microbiology,* **48**: 494-499.

Lehtola, M. J., Miettinen, I.T., Vartiainen, T., Myllykangas, T. and Martikainen, P.J. (2001). Microbially available organic carbon, phosphorus, and microbial growth in ozonated drinking water. *Water Research,* **35(7)**: 1635-1640.

Lewandowski, B. R., Lytle, D. A., and Garno, J.C. (2010). Nanoscale investigation of the impact of pH and orthophosphate on the corrosion of copper surfaces in water. *Langmuir*, **26(18)**: 14671-14679.

Liang, L. and Singer, P.C. (2003). Factors influencing the formation and relative distribution of haloacetic acids and trihalomethances in drinking water. *Environmental Science and Technology,* **37**: 2920-2928.

Liu, H., Korshin, G. V., and Ferguson, J. F. (2008). Investigation of the kinetics and mechanisms of the oxidation of cerussite and hydrocerussite by chlorine. *Environmental Science and Technology,* **42(9)**: 3241– 324

Lytle, D.A. and Schock, M.R. (2005). Formation of Pb(IV) oxides in chlorinated water, *Journal American Water Works Association*, **97(11)**: 102-114.

Lytle, D.A. and Schock, M.R. (2008). Pitting corrosion of copper in waters with high pH and low alkalinity. *Journal of the American Water Works Association,* **100(3)**: 115-128.

Lytle, D.A., Schock, M.R., and Scheckel, K. (2009). The inhibition of Pb(IV) oxide formation in chlorinated water by orthophosphate. *Environmental Science & Technology,* **43**: 6624-6631.

McArthur, M.A., Byrne, T.M., Sanderson, R.J., Rockwell, G.P., Lohstreter, L.B., Bai, Z., Filiaggi, M.J., and Dahn, J.R. (2010). An in situ study of protein adsorption on combinatorial Cu-Al films using spectroscopic ellipsometry. *Colloids and Surfaces B:Biointerfaces*, **81(1)**: 58-66.

McNeill, L.S. and Edwards, M. (2002). Phosphate inhibitor use at US utilities. *Journal American Water Works Association,* **94(7)**: 57-63.

Miettinen, I.T., Vartiainen, T., and Martikainen, P.J. (1997). *Applied and Environmental Microbiology*, **63(8)**: 3242-3245.

Nadagouda, M.N, Schock, M., and Metz, D. (2008). Effect of phosphate inhibitors on the

formation of lead phosphate. carbonate nanorods, microrods, and dendrite structures. *Crystal Growth & Design*, **9(4)**: 1798-1805.

Nadagouda, M.N., White, C., and Lytle, D. (2011). Lead pipe scale analysis using broad-bean argon ion milling to elucidate drinking water corrosion. *Microscopy and Microanalysis*, **17**: 284-291.

Nguyen, C.K., Clark, B.N., Stone, K.R., and Edwards, M.A. (2011a) Role of chloride, sulfate, and alkalinity on galvanic lead corrosion. *Corrosion Science*, **67(66)**: 065005.

Nguyen, C., Stone, K.B., Dudi, A., and Edwards, M.A. (2010). Corrosive microenvironments at lead solder surfaces arising from galvanic corrosion with copper pipe. *Environmental Science & Technology*, **44**: 7076-7081.

Nguyen, C. K., Stone, K.B., Edwards, M. (2011b). Chloride-to-sulfate mass ratio: Practical studies in lead solder galvanic corrosion. *Journal American Water Works Association*. **103(1)**: 81-92.

NRC. (2006). Drinking water distribution systems: Assessing and reducing risks. The National Academies Press, Washington D.C.

Ohtsuka, T., Masuda, M., and Sato, N. (1985). Ellipsometric study of anodic oxide films on titanium in hydrochloric acid, sulfuric acid, and phosphate solution. *Journal of Electrochemical Science and Technology*, **132(4)**: 787-792.

Pinto, J.A., McAnally, A.S., and Flora, J.R. (1997). Evaluation of lead and copper corrosion control techniques. *Journal of Environmental Science and Health,* **A32(1)**: 31-53.

Revie, R.W. and Uhlig, H.H. (2008). Corrosion and Corrosion Control: An Introduction to Corrosion Science and Engineering, Fourth Edition. John Wiley & Sons, Inc., New Jersey.

Reyes, A., Letelier, M.V., De ka Iglesia, R., González, B. and Lagos, G. (2008). Microbiologically induced corrosion of copper pipes in low-pH water. *International Biodeterioration & Biodegradation,* **61**: 135-141.

Rhee, Y.J., Hillier, S., and Gadd, G.M. (2012). Lead transformation to pyromorphite by fungi. *Current Biology*, **22(3)**: 237-241.

Salvato, J., Nemero, N.L., and Agardy, F.J. (2003). Environmental Engineering (5th ed.). John Wiley and Sons: New Jersey.

Sato, N., Kudo, K., and Noda, T. (1971). The anodic oxide film on iron in neutral solution. *Electrochimica Acta*, *16*(11), 1909-1921.

Sawyer, C.N., McCarty, P.L., and Parkin, G.F. (2003). Chemistry for Environmental Engineering and Science. McGraw-Hill, New York.

Scheffer, G. J. A. (2006). Investigation of copper pitting propensity using bench and field scale testing. (Master's dissertation). Virginia Tech, Blacksburg.

Schindler, D.W., Hecky, R.E., Findlay, D.L., Stainton, M.P., Parker, B.R., Paterson, M.J., Beaty, K.G., Lyng, M. and Kasian, S.E.M. (2008). Eutrophication of lakes cannot be controlled by reducing nitrogen input: Results of a 37-year whole-ecosystem experiment. *PNAS,* **105(32)**: 11254-11258.

Schneider, O. D., LeChevallier, M.L., Reed, H.F., and Corson, M.J. (2007). A comparison of zinc and nonzinc orthophosphate-based corrosion control. *Journal American Water Works Association*, **99(11)**: 103–113.

Schock, M. R. (1989). Understanding Corrosion Control Strategies for Lead. *Journal American Water Works Association*, **81(7)**: 88–100.

Schock, M.R. (1990). Internal corrosion and deposition control (4th Ed). In AWWA (Eds.), Water quality and treatment (997-1111). NY, McGraw-Hill, Inc.

Schock, M.R., Lytle, D.A., and Clement, J.A. (1995). Effect of pH, DIC and orthophosphate on drinking water cuprosolvency. U. S. EPA Office of Research and Development Report, EPA/600/R-95/085.

Schock, M.R., Wagner, I., and Oliphant, R. (1996). Corrosion and solubility of lead in drinking water (2nd Ed.). In AWWARF (Eds.), Internal corrosion of water distribution systems (131-230). Denver, CO, AWWA.

SDWA (Safe Drinking Water Act). 42 USC § 300g–6 (1996).

Skidmore, J.F. (1964). Toxicity of zinc compounds to aquatic animals, with special reference to fish. *The Quarterly Review of Biology,* **39(3)**: 227-248.

Smil, V. (2000). Phosphorus in the environment: natural flows and human interferences. *Annual Review of Energy and the Environment*, **25**: 53-88.

Snoeyink, V. and Wagner, I. (1996). Principles of corrosion of water distribution systems (2nd Ed.). In AWWARF (Eds.), Internal corrosion of water distribution systems (1-27). Denver, CO: AWWA.

Switzer, J.A., Rajasekharan, V.W., Boonsalee, S., Kulp, E.A., and Bohannan, E.W. (2006). Evidence that monochloramine disinfectant could lead to elevated Pb levels in drinking water. *Environmental Science and Technology*, **40(10)**: 3384-3387.

Tam, Y.S. and Elefsiniotis, P. (2009). Corrosion control in water supply systems: Effect

of pH, alkalinity, and orthophosphate on lead and copper leaching from brass plumbing. *Journal of Environmental Science and Health Part A,* **44**: 1251-1260.

Triantafyllidou, S. and Edwards, M. (2011). Galvanic corrosion after simulated small-scale partial lead service line replacements. *Journal of the American Water Works Association,* **103(9)**: 85-99.

Triantafyllidou, S., Parks, J. and Edwards, M. (2007). Lead particles in potable water. *Journal of the American Water Works Association*, **99(6):** 107-117.

Tuovinen, O.H., Button, K.S., Vuorinen, A., Carlson, L., Mair, D.M. and Yut, L.A. (1980). Bacterial, chemical and mineralogical characteristics of tubercle in distribution pipelines. *Journal American Water Works Association,* **72(11)**: 626-635.

Vasquez, F.A., Heaviside, R., Tang, Z., and Taylor, J.S. (2006). Effect of free chlorine and chloramines on lead release in a distribution system. *Journal of the American Water Works Association,* **92(2)**: 144-154.

Wang, Y., Jing, H., Mehta, V., Welter, G.J., and Giammar, D.E. (2012). Impact of galvanic corrosion on lead release from aged lead service lines. *Water Research,* **46**: 5049-5060.

White, C., Tancos, M. and Lytles, D.A. (2011). Microbial community profile of a lead service line removed from a drinking water distribution system. *Applied and Environmental Microbiology,* **77(15)**: 5557-5561.

Willison, H. and Boyer, T.H. (2012). Secondary effects of anion exchange on chloride, sulfate, and lead release: Systems approach to corrosion control. *Water Research,* **46**: 2385-2394.

Woollam, J.A. (2013). Ellipsometry measurements (Tutorial). Retrieved from: http://www.jawoollam.com/tutorial_4.html.

Xie, Y. and Giammar, D.E. (2011). Effects of flow and water chemistry on lease release rates from pipe scales. *Water Research,* **45**: 6525-6534.

Zidouh, H. (2009). Velocity profiles and wall shear stress in turbulent transient pipe flow. *International Journal of Dynamics of Fluids,* **5(1)**: 61-83.

APPENDIX A – SUPPLEMENTARY DATA

Table A.1 – Average bulk water turbidity for all water conditions tested

Sample	Average Turbidity (NTU)	Total Pb (µg/L)	NAD Pb (µg/L)	Average % increase	Lower Tailed Paired T test
pH7.4/DIC(3)	0.61	1349.6	1438.4	12.5	0
pH7.4/DIC(3)/Cl$_2$	0.37	1447.9	1510.6	5.6	0
ZOP(20)/pH7.4/DIC(3)	7.74	759	819.4	10.1	0.001
ZOP(20)/pH7.4/DIC(3)/Cl$_2$	10.88	748.1	814.3	11.4	0.005
pH9.2/DIC(3)	0.28	702.3	763.4	10.7	0
pH9.2/DIC(3)/Cl$_2$	0.31	747.8	814	21.6	0
ZOP(20)/pH9.2/DIC(3)	5.57	1045.7	1121.4	9.2	0.006
ZOP(20)/pH9.2/DIC(3)/Cl$_2$	4.91	436.3	519.5	18.4	0.047
pH7.4/DIC(7)	0.39	616.5	751	16.2	0.047
pH7.4/DIC(17)	0.29	353	357	1.8	0.258
pH8.3/DIC(7)	0.16	375.3	400.5	8.3	0.003
pH8.3/DIC(17)	0.13	182.6	189.4	2.5	0.142
pH9.2/DIC(7)	0.17	341.8	317.4	2.9	0.291
pH9.2/DIC(17)	0.12	173.6	177.6	5.2	0.064
OP(10)/pH7.4/DIC(7)	1.62	350.3	378.4	5.1	0.064
OP(10)/pH7.4/DIC(17)	0.84	211.4	214	6.6	0.298
OP(10)/pH8.3/DIC(7)	2.31	581.1	504.6	27.1	0.102
OP(10)/pH8.3/DIC(17)	0.62	199.5	186.3	-8.9	0.163
OP(10)/pH9.2/DIC(7)	3.26	498	486.8	16.6	0.389
OP(10)/pH9.2/DIC(17)	0.69	293.6	222.6	22.5	0.206
OP(20)/pH7.4/DIC(7)	2.68	863.9	975.7	0.1	0.414
OP(20)/pH7.4/DIC(17)	1.51	702.8	465.1	-6	0.026
OP(20)/pH8.3/DIC(7)	1.86	611	542.4	13.1	0.127
OP(20)/pH8.3/DIC(17)	0.7	244.1	257.8	3.1	0.403
OP(20)/pH9.2/DIC(7)	1.48	784.2	668.7	-2.9	0.091
OP(20)/pH9.2/DIC(17)	0.34	113.3	103.8	6.1	0.349

Table A.2 – Average lead and copper release after 1, 2, and 4-day stagnation for all water conditions tested in this study.

	Average Pb Release (µg/L)			Average Cu Release (µg/L)		
	1-Day	2-Day	4-Day	1-Day	2-Day	4-Day
pH7.4/DIC(3)	912	1234	2094	12	14	16
pH7.4/DIC(3)/Cl$_2$	1012	1359	1803	11	13	13
ZOP(20)/pH7.4/DIC(3)	605	927	592	4	4	4
ZOP(20)/pH7.4/DIC(3)/Cl$_2$	841	1073	762	3	5	5
pH9.2/DIC(3)	501	608	890	12	16	17
pH9.2/DIC(3)/Cl$_2$	514	751	1155	11	19	16
ZOP(20)/pH9.2/DIC(3)	334	343	356	4	4	3
ZOP(20)/pH9.2/DIC(3)/Cl$_2$	303	325	438	3	3	3
pH7.4/DIC(7)	346	627	456	53	40	64
pH7.4/DIC(17)	386	221	560	44	45	48
pH8.3/DIC(7)	178	277	329	25	27	29
pH8.3/DIC(17)	75	133	151	34	41	37
pH9.2/DIC(7)	155	270	209	34	50	62
pH9.2/DIC(17)	134	164	198	35	49	86
OP(10)/pH7.4/DIC(7)	41	28	50	38	53	63
OP(10)/pH7.4/DIC(17)	51	38	40	42	50	51
OP(10)/pH8.3/DIC(7)	286	209	371	43	37	47
OP(10)/pH8.3/DIC(17)	65	80	33	44	54	69
OP(10)/pH9.2/DIC(7)	211	95	104	27	39	49
OP(10)/pH9.2/DIC(17)	76	127	55	33	44	41
OP(20)/pH7.4/DIC(7)	467	398	356	36	47	64
OP(20)/pH7.4/DIC(17)	521	184	345	33	36	34
OP(20)/pH8.3/DIC(7)	388	564	897	20	26	25
OP(20)/pH8.3/DIC(17)	245	185	584	29	44	58
OP(20)/pH9.2/DIC(7)	412	602	673	31	41	50
OP(20)/pH9.2/DIC(17)	25	19	26	22	29	25